WEATHER CONTROL OF WHEAT PLANT WATER RELATIONS

by

Keith Leslie Bristow
B.Sc.(Hons.), Natal

submitted

in partial fulfilment of the requirements for the

degree of

Master of Science in Agriculture
in the Department of Agrometeorology

University of the Orange Free State
Bloemfontein

Promoter: Professor J.M. De Jager

1980

I declare that this thesis, submitted to the University of the Orange Free State for the degree of Master of Science in Agriculture, is the result of my own work and has not been submitted to any other University/Faculty.

K.L. BRISTOW

TO MY PARENTS

'Hallo!' said Piglet, 'what are you doing?'

'Hunting', said Pooh.

'Hunting what?'

'That's just what I ask myself. I ask myself, what?'

'What do you think you'll answer?'

'I shall have to wait until I catch up with it', said Winnie-the-Pooh.

A.A. Milne.

'To write simply is as difficult as to be good'

W. Somerset Maughn.

C O N T E N T S

INTRODUCTION

In South Africa water supply may be considered the major factor limiting agricultural production. It is thus imperative to determine the water requirements of agricultural crops. This will ensure minimal water application at the appropriate time and hence optimal response to irrigation and will result in improved usage of the limited water resources.

The aim of the work here described will be to investigate the influence of weather on plant water relations and the consequent flow of water through the wheat crop. Quantitative analyses will be adopted to develop reliable mathematical simulations of responses to plant moisture status and weather control of plant water status. These deterministic models will be structured so as to improve decision making for scheduling irrigation. In pursuance of these goals the instrumentation used in the study of plant water relations will be investigated and an attempt made to improve on existing experimental techniques. All experimentation was carried out in the field in order to eliminate confounding unrepresentative conditions induced in growth chambers and glass houses.

Basically, the physical dynamics of the soil-plant-atmosphere continuum will be investigated. Essentially, a mathematical description with control of crop transpiration by atmospheric evaporative demand is sought. The concept of crop hydraulic conductivity (ϕ) is introduced to account for the contribution of plant physiology to the process. The parameter ϕ is evaluated from measurements of leaf water potential (ψ_ℓ), soil moisture potential (ψ_s) and crop evaporation (E). The control of leaf water potential upon photosynthesis, and hence wheat crop growth rate, is reflected in the relationship between leaf diffusive resistance and leaf water potential. This relationship and the hydraulic conductivity were determined during the late vegetative and early reproductive growth stages.

Leaf water potential (ψ_ℓ) was measured using the Wescor leaf psychrometer,

J14 press and Scholander pressure chamber. A modified technique using a strip chart recorder facilitated accurate measurements with the leaf psychrometer. The J14 press is a relatively new instrument on the market. It was calibrated against the Scholander pressure chamber and the results obtained appear most encouraging.

Leaf stomatal resistance (r_s) was measured using the LI-65 Autoporometer. Calibration of this instrument was carried out in a growth chamber over a wide range of temperatures. This permitted a more accurate analysis of field data than the recommended practice of converting readings at other temperatures to the 25 °C 'standard'. Both abaxial and adaxial surface resistances were measured and used in determining r_s.

The leaf water potential - leaf diffusive resistance relationship was investigated in an attempt to determine the critical value of ψ_ℓ below which decrease in effective photosynthesis is induced. Two empirical models were obtained, both with high coefficients of determination.

In order to determine the soil water status (ψ_s), soil moisture characteristic curves were obtained for both the soil types used in the study. The standard pressure plate assembly was used for this purpose.

A new technique using micrometeorological measurements was developed to estimate crop evaporation rate (E). This technique makes use of a reiterative method to find that canopy surface temperature (T_o) which balances the surface energy budget equation. Measured and calculated T_o were used to validate the technique. This method resulted in E values of accuracy acceptable for agricultural purposes and furthermore utilises robust, simple, inexpensive equipment.

SECTION A

METHODS AND MATERIALS

CHAPTER 1

THE EXPERIMENTAL SITE

1.1 The Field Site

The meteorological station at the University of the Orange Free State was chosen as the site to carry out these field trials. This station occupies a total area of ± 2 ha. All the standard meteorological instruments are installed above a short grass surface and data collected on a routine basis. The station is situated 1 414 m above sea level at latitude 29° 07' S and longitude 26° 11' E. The site and surrounding area is essentially flat and buildings of the UOFS bound both the north-eastern and eastern limits of the station. The northern hectare of the station was used for the cultivation of the wheat crop (see Fig. 1) while the standard instrument site made up the southern section (see Fig. 2 and Fig. 3). The entire 2 ha is enclosed by a 3 m security fence.

Situated in the southern third of the experimental plot were four large bins in which soil moisture conditions could be controlled. They are embedded with their rims flush with the ground surface so that wheat growing therein may be considered part of a uniform crop.

The instrumentation used in this study was situated in the region immediately surrounding the bins. The predominent winds are north-westerly and by siting the instruments as indicated the largest fetch possible was utilised.

Fig. 1 : The wheat crop. Buildings of the Faculty of Agriculture (U.O.F.S.) appear in the background.

Fig. 2 : The standard instrument site at the U.O.F.S. meteorological station.

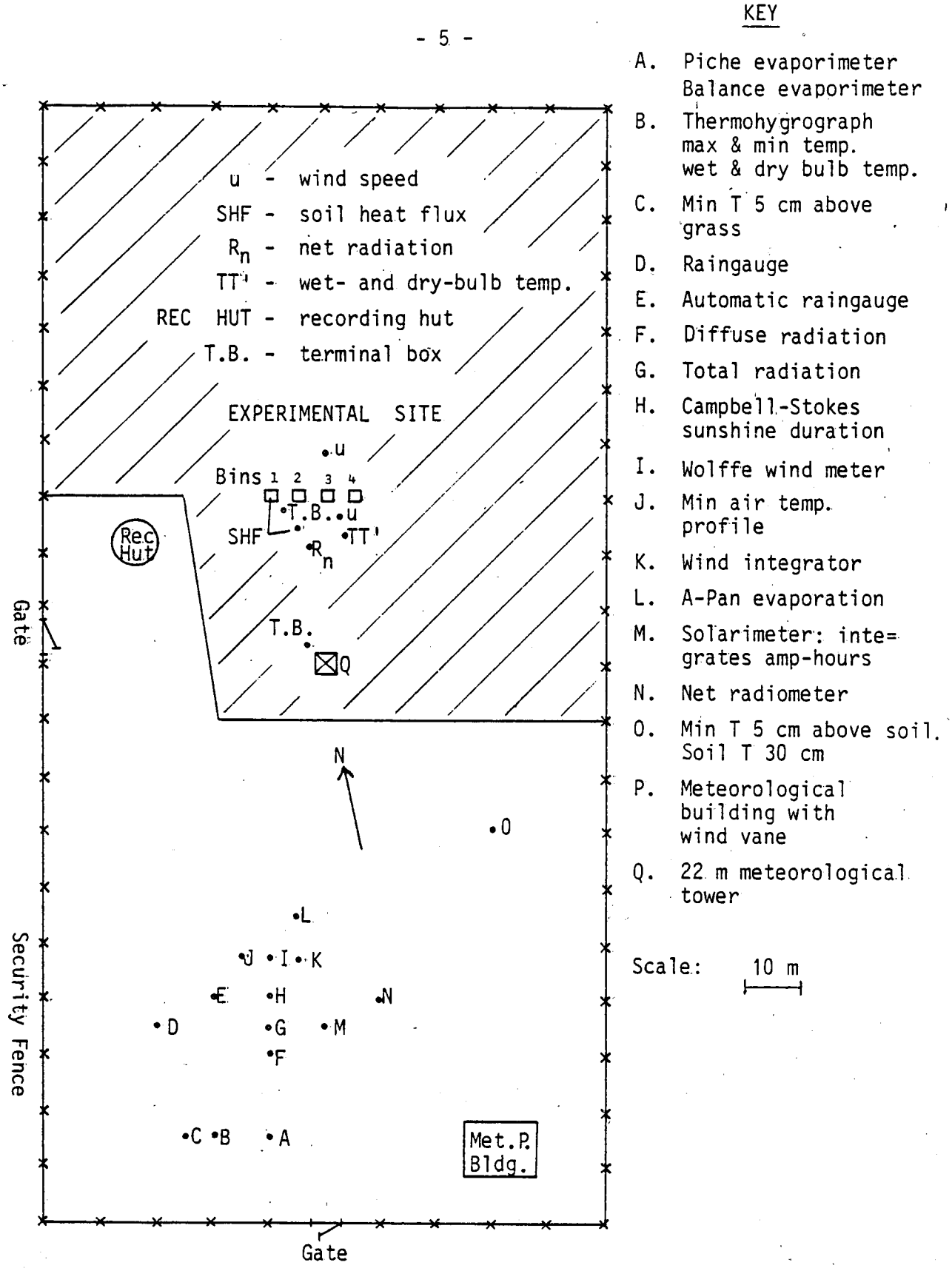

Fig. 3 : Schematic representation of the meteorological station at the University of the Orange Free State.

1.2 General Description of the Soils

1.2.1 The experimental plot

The soil of the experimental site belongs to the Skildekrans series of the Valsrivier form (Macvicar, De Villiers, Loxton, Verster, Lambrechts, Merryweather, Le Roux, van Rooyen & von M Harmse, 1977). The general description thereof is given in Table 1.

TABLE 1 : General Description of the Soil of the Experimental Site.

Horizon	Depth (m)	Description
A1	0 - 0,30	Weak sub-angular blocky structure, moist, gradual transition
B21	0,30 - 0,65	Strong angular blocky structure, gradual transition
C	0,65 +	Weathering shale

Soil characteristics are by no means uniform over the extent of the land and this was reflected in the crop development. A dense layer of clay occurs at an average depth of 0,4 - 0,5 m throughout the land. In some areas this clay layer was so shallow, that apart from impeding root development, waterlogging became a problem.

1.2.2 The soil in the bins

The bins were filled with soil belonging to the Bainsvlei series of the Bainsvlei form (Macvicar et al, 1977). Its general description is outlined in Table 2.

TABLE 2 : General Description of the Soil used in the Bins.

Horizon	Depth (m)	Description
A1	0 - 0,25	5 Yr 4/3, Reddish brown, moist, massive apedal structure, clear transition
B21	0,25 - 0,50	5 Yr 3/4, Dark reddish brown, moist, massive apedal structure, gradual transition
B22	0,50 - 0,85	5 Yr 4/6, Yellowish red, moist, massive apedal structure, clear transition
B23	0,85 - 1,00	7 - 5 Yr 5/6, Strong brown, moist, frequent yellow, grey, black mottles, frequent hard and soft concretions

This soil was obtained from the farm Bainsvlei in the Bloemfontein district. All vegetation was removed from the surface and topsoil excavated to a depth of approximately 0,15 m. The soil was then sieved and mixed to ensure an essentially uniform profile in each bin.

In the remainder of this dissertation the two soil types will be referred to as simply the site and bin soil.

1.3 The Bins

The bin dimensions are 1,82 m x 1,82 m x 1 m.

A perforated plastic pipe (20 mm diameter) was laid along the base of each bin and covered with a piece of asbestos sheeting. A 0,1 m layer of 12 mm gravel was then placed in the bin before it was filled with soil. The soil was packed to a density of $\pm$ 1 650 kg m^{-3}. The bins were then saturated with water and the soil allowed to settle in an attempt to obtain a profile of uniform density. A plastic tube was

connected to the perforated base pipe so as to extend up and out of the bin. Excess water could be removed via this pipe by means of a suction pump, thus preventing the occurrence of waterlogging.

The effective soil depth in the bins was ± 0,85 m.

1.4 Agronomic Aspects

Turpin 4 wheat cultivar was planted in both the 1978 and 1979 seasons. The dates of cultivation, planting, emergence and application of fertilisers, weed killers and insecticides are given in Table 3. In 1978 the crop was planted by means of a 0,3 m planter in east-west rows. An attempt was made to produce a denser stand in 1979 than in 1978. One-third of the seed was sown in a criss cross fashion (east-west and north-south rows) by means of the 0,3 m planter. The rest of the seed was then sown by hand with the aid of an oats sower. Although the uniformly dense stand hoped for did not materialise, no distinct rows resulted from this method of planting.

No serious problems were encountered in the 1978 season and a healthy uniform stand of wheat resulted. This, however, was not the case in the 1979 season. Severe cold experienced immediately after planting retarded the emergence of the crop and imposed severe stress on the young plants. Immediately following the apparent recovery of the crop from the cold, repeated attacks by Russian wheat lice (diuraphis noxia) resulted in further setbacks. The crop partially recovered and apart from being patchy in appearance, on average, managed to reach two-thirds of the height attained in the 1978 season. The problems en= countered during the 1979 season prevented the collection of data from the wheat in the bins. Fortunately, the areas in the immediate vicinity of the instrumentation were not the worst affected and enabled the experiment to proceed.

TABLE 3 : The Dates of Cultivation, Planting, Emergence and Application of Fertiliser, Weed Killers and Insecticides for both the 1978 and 1979 Season.

1978 Season

Julian Day	Operation
186	Entire experimental plot ripped to a depth of ± 0,4 m
191	Land rotavated - preparation of seed bed
194	Land planted and fertilised - seeding rate 90 kg/ha Fertiliser application 600 kg 2:3:2/ha
199	Bins planted and fertilised - seeding rate 30 g/bin Fertiliser application 250 g 2:3:2/bin
208	First signs of emergence of the wheat crop

1979 Season

Julian Day	Operation
143	Weeds cut - land rotavated
163	Cultivation of the land by means of a five tooth ripper
164	Land rotavated - preparation of seed bed
165	Land planted and fertilised - seeding rate 100 kg/ha Fertiliser application 550 kg 2:3:0/ha and 100 kg K.A.N./ha
173	Bins planted and fertilised - seeding rate 30 g/bin Fertiliser application 50 g K.A.N./bin and 200 g 2:3:2/bin
183	First signs of emergence of the wheat crop
197	Additional planting carried out in the bins
222	Insecticide application - metasystax
232	Insecticide application - metasystax
234	Additional planting done in the bins
248	Weed killer application - 2-4-D Ester
250	Fertiliser application - 250 kg K.A.N./ha

1.5 The Irrigation System

Irrigation of the wheat crop was carried out by means of an overhead sprinkler system. The measured rate of application capability was found to be 6,5 mm per hour which is considerably less than the 14 mm per hour claimed by the manufacturer. Since only one-sixth of the experimental site could be irrigated at any one time, it took at least two days to irrigate the whole land effectively. During the early stages of crop growth, irrigation was applied regularly to ensure healthy plant development. Thereafter irrigation was only applied as required to prevent crop death or to provide non-stressed plants for experimental purposes.

1.6 Soil Moisture Determinations

Soil sampling by the standard gravimetric method was carried out on all experimental days and produced accurate estimates of soil moisture content. The soil moisture characteristic curves for the site and bin soils (see Section 7.3) were used to determine the water status of the respective soils on all experimental days.

CHAPTER 2

METEOROLOGICAL INSTRUMENTATION

Elements of the microclimate relevant to the study were continuously measured in the plant community. Apart from explaining the diurnal variation in the plant parameters measured, these observations were used to develop a technique whereby evapotranspiration could be estimated on an hourly basis. The elements measured included net radiation (R_n), soil heat flux (G), wet- and dry-bulb temperatures (T' and T) and wind speed (u).

All recorders used for assembling the field data were housed in the recording hut situated in the south-western corner of the experimental plot (see Fig. 3). Fig. 4 illustrates some of the instrumentation installed in the recording hut. Two terminal boxes situated in the land (Fig. 3) were connected to the recording hut via underground cable and facilitated coupling of the instruments in the field to the record= ing equipment.

2.1 Net Radiation

Net radiation above the canopy was measured by means of a Beckman and Whitely (Model N 188)[1] net radiometer (see Fig. 5). The horizontal sensing element contains a ventilated thermopile whose output is pro= portional to the difference between the radiation incident upon the upper surface and that incident upon the lower surface. The net radio= meter was mounted at a height of 1,5 m above ground level with its sensing element parallel to the soil surface. The output was recorded

[1]The mention of proprietary products anywhere in this thesis is for the convenience of the reader and does not constitute endorsement or pre= ference by the author or the University of the Orange Free State.

(A) - 1979 season

(B) - 1978 season

Fig. 4 : Some of the instrumentation installed in the recording hut. (A) illustrates the improved conditions during the 1979 season as compared to those during the 1978 season (B).

Fig. 5 : The Beckman and Whitely (Model N 188) net radiometer.

continuously for the duration of the growing season on a Leeds and Northup Strip Chart Recorder (Model 5 Speedomax Type G). Calibration was carried out on a routine basis prior to its installation in the crop.

2.1.1 Calibration

The Linke Feusner actinometer, which is a substandard instrument and measures the direct component of incoming radiation, was used as the calibration standard. Calibration was carried out on cloudless days during which readings were taken every half hour. By shading the net radiometer for one minute in each half hour period, it is possible to determine the chart value equivalent to the vertical component of incoming direct radiation. This value is compared to the product of the direct radiation recorded by the Linke Feusner and the sine of the solar declination. The latter was calculated using the standard equation and accurate time. The Linke Feusner reading was corrected according to the temperature of the instrument. The calibration factor so determined was found to be 18,35 Wm^{-2} div^{-1}.

2.2 Soil Heat Flux

Soil heat flux in the bins and land were measured by means of soil heat flux disks (Thornwaite Model 610). These disks were buried approximately 5 mm below the soil surface. The output from the disk in the bin was recorded on a Thornwaite Portable microvoltmeter recorder and that from the land on a Mosely Autograf (Model 680 M) recorder. Laboratory calibration was carried out prior to installation in the field.

2.2.1 Calibration

The normal calorimetric technique was utilised. The soil heat flux disk is placed in direct contact with a copper calorimeter filled with distilled water which is cooled to below room temperature. The deflection on the chart recorder is recorded while the temperature of the water returns to room temperature. The total heat flow through the sensor is equal to the product of water mass, specific heat of water, and rise in water temperature. This heat flow divided by the relevant time period is compared to the average voltage recorded during this time period. The results obtained are given in Table 4.

TABLE 4 : Calibration Factors for the Soil Heat Flux Disks used in this Study.

Recorder	Measured Calibration Factor $Wm^{-2}\ mV^{-1}$
Thornwaite Recorder (Bins)	188
Mosely Recorder (Land)	168

2.3 Wet- and Dry-Bulb Temperatures

For the measurement of wet- and dry-bulb temperatures three ventilated psychrometers were constructed. During the 1978 season resistance type thermometers were used and the temperatures recorded continuously on a Hartmann & Braun twelve channel dotted line Polycomp Recorder. Different input resistances were used on each channel so that each thermometer record was offset by $\pm$ 2 divisions from its immediate neighbour. Calibration was effected against a mercury-in-glass thermometer and the regression equations used when analysing the data are given in Table 5.

TABLE 5 : The Regression Equations used when Analysing Temperature Data stored on the Polycomp Recorder. T = temperature in °C; R = reading recorded on Hartmann & Braun recorder in divisions.

Temperature Sensor	Regression Equations	Correlation Coefficient
1	T = -39,09 + 1,03 R	0,9992
2	T = -41,38 + 0,98 R	0,9993
3	T = -53,35 + 1,03 R	0,9990
4	T = -52,35 + 0,99 R	0,9993
5	T = -54,20 + 1,00 R	0,9997
6	T = -55,95 + 0,99 R	0,9996

During the 1979 season a temperature sensing system using integrated circuits (LN 335Z) was constructed at the UOFS Electronic Workshop. The circuit diagram of the sensors is shown in Fig. 6. The potential divider was adjusted so that at 0 °C the output from the system was 0 mV. Since sensitivity of the integrated circuit thermometer is 10 mVK^{-1}, temperature could be recorded directly on the S145 Digital Recorder (manufactured by Diel, SA) with a resolution of 0,1 °C when the latter was set on the 0 - 50 mV scale. Initially a $\pm$ 0,5 °C fluctuation or 'noise' was observed. This appeared to stem from the mains frequency and was reduced to $\pm$ 0,1 °C by placing 100 µF condensors across the data logger inputs.

These sensors were calibrated against a mercury-in-glass thermometer with the aid of a constant temperature bath. Fig. 7 shows a typical calibration curve. Table 6 gives the regression equations used when analysing the data recorded on the data logger.

Inadequate wetting of the wet-bulb thermometers was the major problem encountered in the field. Care had to be taken to change the wicks frequently in order to keep them clean and serviceable.

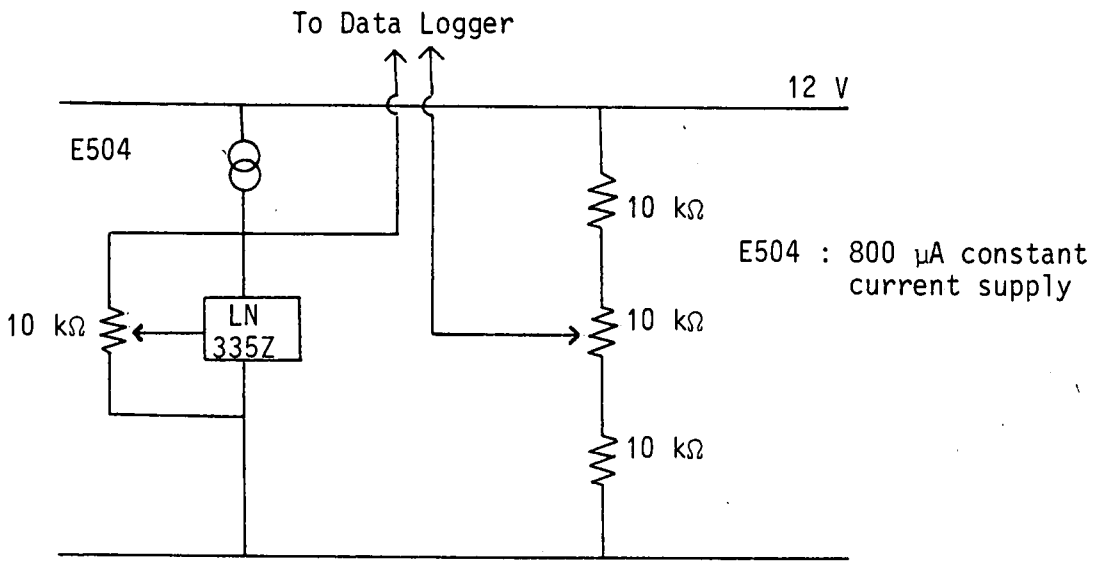

Fig. 6 : The integrated circuit temperature sensor circuit diagram (LN 335 Z).

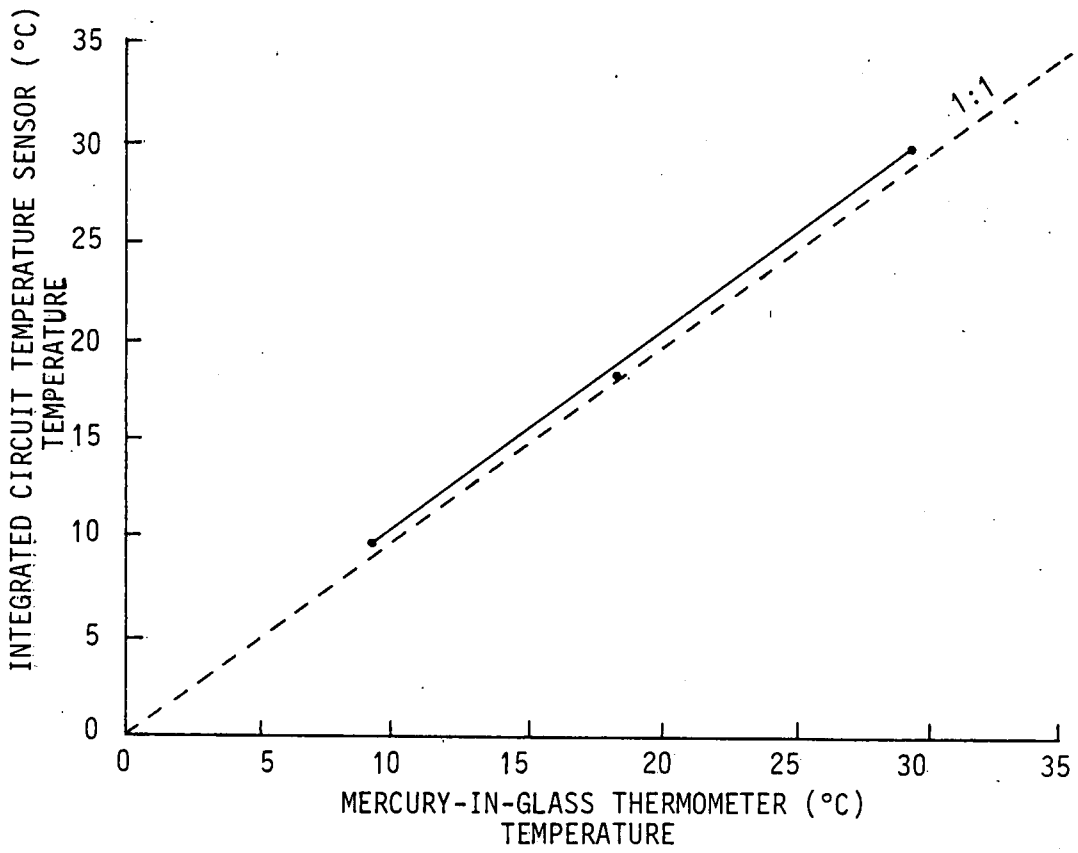

Fig. 7 : Typical calibration curve obtained for the LN 355 Z integrated circuit temperature sensor. The dotted line indicates the 1:1 relation.

TABLE 6 : The Regression Equations used when Analysing Temperature data stored on the Data Logger. T = corrected temperature in °C; R = observed reading on the data logger.

Temperature Sensor	Regression Equations	Correlation Coefficient
1	T = (R/1,0261 - 0,1984)/10	0,9997
2	T = (R/1,0405 - 0,6713)/10	0,9999
3	T = (R/1,0595 - 1,1685)/10	1,0000
4	T = (R/1,0735 - 1,1685)/10	0,9999
5	T = (R/1,0388 - 0,7736)/10	0,9999
6	T = (R/1,0357 - 0,3470)/10	0,9998

The ventilated psychrometers were installed at heights $(d + z_o)$m, where d is the zero displacement level and z_o the roughness parameter (Monteith, 1973), at $(d + z_o + 0,5)$m and at 2 m. The heights of the psychrometers at the two lower levels were adjusted as the crop developed. Over the experimental periods crop height varied between 0,5 m and 0,9 m.

2.4 Wind Speed

Wind run during the 1978 season was recorded using a Wolffe mechanical wind recorder situated with the anemometer cups 2 m above the short grass surface of the standard instrument site.

During the 1979 season, three Gill 3 Cup Anemometers (Model 12102) were installed above the wheat crop (see Fig. 8). These instruments exhibit a stopping distance of approximately 2,4 m and a threshold of 0,35 - 0,45 ms^{-1}. The open circuit voltage output of the generator is 2 000 mV $\pm$ ½ % at 1 500 rpm. The cup wheel results in a 0,3 ms^{-1} zero offset which is taken into account when analysing the recorded data. The output of the three Gill 3 Cup anemometers was coupled directly to the S145 Digital Recorder. To smooth the voltage

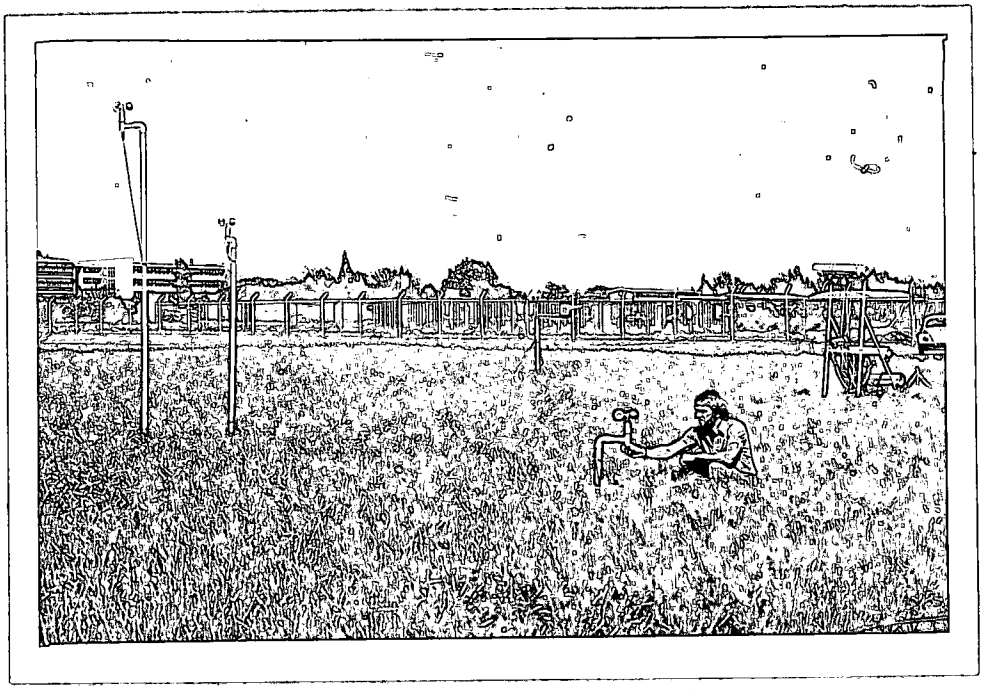

Fig. 8 : The three Gill 3 Cup Anemometers used to record wind speed during the 1979 season. They were installed at heights $(d + z_o + 0,5)$m; 2 m and 3 m above the wheat crop.

ripple produced, 470 µF condensors were placed across the logger inputs. Wind speed was recorded at the heights $(d + z_o + 0,5)$m, 2 m and 3 m.

2.5 Analysis and Storage of Field Data

The Hewlett Packard 9845 A Desktop system (see Fig. 9) was used extensively in the analysis and manipulation of field data.

Data recorded on strip chart recorders was digitised and stored directly on magnetic tapes. The programs necessary to plot and 'clean' the data were written as required. An example of a general digitising program is given in Appendix 1. The various calibration factors and regression equations were applied directly in the digi= tising programs so that only absolute data was stored on tape. In most cases the hourly mean values were used to trace the diurnal variation in the variables measured in the study. A plot program developed to assist in the display and interpretation of the results is given in Appendix 2.

All data stored on the Diel data logger was transformed and trans= ferred to the HP 9845 A magnetic tapes for ease of manipulation.

Fig. 9 : The Hewlett Packard 9845 A Desktop system used for the analysis and manipulation of field data.

CHAPTER 3

MEASUREMENT OF LEAF WATER POTENTIAL

3.1 Water Potential

The term water potential was first proposed by R.K. Schofield in 1949 (Owen, 1952) in an attempt to introduce a meaningful term with which to measure the water in any system. Water movement through the soil-plant-atmosphere continuum occurs along energy gradients since the free energy decreases from the soil, through the plant and out into the atmosphere. Thus, it is the energy status of the water and not necessarily the quantity of water which is truely significant in explaining water movement in the natural environment (van Haveren & Brown, 1972). The concept of water potential provides a thermodynamically based measure of the energy status of water in the given system.

Volumetric water potential is defined in terms of the chemical potential (partial molar Gibbs free energy) of water as

$$\psi_w = \frac{\mu_w - \mu_w^o}{V_w} \qquad \ldots\ldots\ldots\ldots\ldots\ldots \quad (1)$$

where

ψ_w = the volumetric water potential (Jm^{-3} or Pa),
μ_w = the chemical potential of water ($J\ mole^{-1}$),
μ_w^o = the chemical potential of water in the reference state ($J\ mole^{-1}$), and
V_w = the partial molar volume of water ($m^3\ mole^{-1}$).

(Slatyer, 1967)

This represents the potential energy needed to move a unit volume of water from the system under consideration to the reference position.

The choice of the reference state is arbitrary and is usually assumed to be an infinitesmally shallow pool of pure free water at atmospheric pressure and at some chosen elevation. Due to this choice of reference state the water potentials in the soil-plant-atmosphere continuum are usually negative. Although the Pascal is the standard SI unit, the bar is an accepted practical unit given to water potential (Baughn, 1974) and is used throughout this study.

Other authors (Salisbury & Ross, 1969) define water potential as

$$\psi_w = \mu_w - \mu_w^o \quad \ldots\ldots\ldots\ldots\ldots\ldots \quad (2)$$

and in this case the units are J kg^{-1}. This water potential is termed the specific water potential and is defined as the potential energy needed to move a unit mass of water from the system under consideration to the reference position.

Water potential is the sum of a number of component forces acting on water in a given system. The total water potential, ψ_w, as applied to the soil-plant-atmosphere continuum is given as

$$\psi_w = \psi_p + \psi_\pi + \psi_\tau + \psi_g \quad \ldots\ldots\ldots\ldots \quad (3)$$

where

ψ_p = the pressure component,
ψ_π = the osmotic component,
ψ_τ = the matric component, and
ψ_g = the gravitational component. (Hillel, 1971)

An interaction term (ψ_i) can also be included to emphasise that the terms in Eqn. 3 are not independent of each other, and so are not strictly additive quantities (Brown, 1972). Within living tissue, the total water potential and its components change continuously.

Thus in most cases estimates of water potential are based on the measurements of an integrated value of one or more of the indivi= dual components. It is total soil and plant water potential which relates the water status to photosynthesis and not water content. Hence, it is of utmost importance to be able to determine this quantity accurately (Jameson, 1972).

The psychrometer, Scholander pressure chamber and J14 press were used during this study to obtain leaf water potential measurements and are discussed in Chapters 3 (Section 3.2 - 3.9) and 4. The psychro= meter measures total leaf water potential and the Scholander pressure chamber and J14 press measure hydrostatic potential or $\psi_p + \psi_\tau$.

3.2 Leaf Psychrometers

A psychrometer is a device that consists essentially of a wet- and dry-bulb thermometer and measures relative humidity. There are basically two types that are used to measure the water potential in soil and plant samples. These are the Spanner psychrometer and the Richards psychrometer. Both these psychrometers consist of a thermo= couple junction in a small sealed chamber wherein the vapour is in equilibrium with the water in the leaf tissue.

The wet junction of the Richards psychrometer (Richards & Ogata, 1958) consists of a short silver cylinder. It is wetted by manually applying a water drop. The wet-bulb temperature at the steady state reached during evaporation of the manually introduced drop is measured. Rawlins (1966) develops and explains the steady state theory for the Richards technique. In contrast, the Spanner psychrometer induces a drop of water to form upon the wet thermocouple junction by a short period of cooling of the thermojunction by means of the Peltier effect. The junction temperature is measured during evaporation of this water after the cooling current is discontinued. The fluxes of heat and water vapour between the enclosed air sample and the wet junction

determine the wet junction temperature and its rate of change (Peck, 1968). The measurement of the wet-bulb depression relative to the dry-bulb temperature gives the relative humidity from which the water potential may be calculated. The dry-bulb thermojunction is embedded in the sensor block. Heat flows to the wet junction by radiation from the sample material and chamber walls, by conduction through the thermocouple wires supporting the wet junction and by con= duction and convection to and from the air in the chamber. These factors play an important role in the design and construction of thermocouple psychrometers. The design and construction is dis= cussed by Rawlins (1966) and Mohsin & Ghildyal (1972). Sample properties which affect the psychrometer output and cause errors in water potential determinations are discussed by Campbell, Campbell & Barlow (1973), Campbell & Campbell (1974), Peck (1969), Barrs & Cramer (1969), Barrs (1965) and Rawlins (1964).

Neumann & Thurtell (1972) designed a dewpoint hygrometer and used it to carry out in situ measurements. The fundamental principle of the dewpoint method is based upon the natural phenomenon that:

> If held at the dewpoint temperature, a wet thermocouple junction will neither lose water through evaporation nor gain water through condensation.
>
> (Campbell et al, 1974)

In this system the Peltier current is electronically controlled to balance all heat transfer and thus the temperature of the wet junction is forced to converge on the dewpoint temperature. This method is extremely sensitive to temperature change and abrupt changes in the external environment produce large errors by disturbing the thermal equilibrium. Equilibrium time for this method ranges from 20 minutes at low water potential to several hours at higher water potential (Neumann et al, 1972) and is one reason why this method is not readily used in field applications. However, once equilibrium is attained

and if thermal equilibrium can be maintained, this method will closely follow the water potential and is probably more accurate than the psychrometric method.

In this study the commercially available Wescor L51 leaf psychrometer[1] and the Wescor HR-33 T microvoltmeter were used for the determination of leaf water potential under field conditions. A modified form of the psychrometric method was used for all determinations.

3.3 The Psychrometric Method

The psychrometric method of water potential determination makes use of a thermocouple to measure relative humidity in a small chamber placed over the leaf and carefully sealed (Meidner & Sheriff, 1976). Physically, this involves the measurement of the output voltage produced by the instruments fine-wire thermocouple. The vapour enclosed within the minute cavity is in equilibrium with the water within the enclosed leaf tissue and the wet-bulb temperature of this ensealed air is measured. In actuality, the output voltage is a function of water potential in the chamber and chamber temperature as stipulated by the following equation given by the manufacturer:

$$\Delta V = \frac{aRT^2}{\lambda} \left[1 - \exp \left(\frac{\psi_w}{RT} \right) \right] \quad \ldots\ldots\ldots \quad (4)$$

where

ΔV = the psychrometric electromotive force (μ volts),
a = the thermoelectric power of the thermocouple (μ volts $^{\circ}C^{-1}$),
R = the universal gas constant (J mole^{-1} $^{\circ}C^{-1}$),
T = the chamber temperature ($^{\circ}C$),
λ = the latent heat of vapourisation of water (J kg^{-1}), and
ψ_w = the water potential (J kg^{-1}).

---

[1] Wescor Inc., 459 South Main Street, Logan, Utah 84321, USA.

For water potentials between 0 and -40 bar, and a temperature of 25 °C, the output voltage increases essentially linearly with wet-bulb depression. It is normal practice to correct readings obtained at other temperatures to their equivalent at the adopted arbitrary standard of 25 °C. This obviates having to calibrate the instrument at various temperatures under controlled thermal conditions. The temperature correction is affected by dividing the recorded measurement by the factor (M + N T) where M and N are empirically determined constants and T is the temperature in °C. The manufacturers quote M and N as 0,325 and 0,027 respectively.

3.4 Operating Principle of the Leaf Psychrometer

Once equilibrium is reached between the liquid and vapour phases in the sample chamber, a cooling current (Peltier effect) is passed through the thermocouple. As the temperature of the junction falls below the dewpoint temperature, condensation of water takes place on the junction. When the cooling current is now switched off, the water droplet that has formed commences heating by conduction and convection from the enclosed air. Hence, there is a difference in temperature between the thermojunction in the water droplet and its mate embedded in the aluminium block of the sensor. This temperature difference produces a measurable μV output. The temperature of the droplet gradually increases tending towards the temperature of the chamber. When, however, the wet-bulb temperature is reached, this warming rate decreases, and even for a while entirely ceases because of the latent heat liberated. Since this wet-bulb depression is directly proportional to both the potential difference across the thermocouple and to the water potential of the leaf sap leaf water potential may be determined using a suitable microvoltmeter and Eqn. 4. The major difficulties experienced with this technique arise from determining when the reduced rate of movement in the microvoltmeter needle commences. This point indicates the wet-bulb depression.

3.5 Modified Technique

In the modified procedure adopted in this study, the output of the microvoltmeter is connected to a strip chart recorder. Now during the cooling of the junction, the deflection of the recorder pointer, and hence the trace, increases. Once the cooling current ceases, heating commences and the trace decreases towards zero. When evaporation of the water droplet starts, the temperature of the junction tends to remain approximately constant with time; and a levelling off or plateau is observed in the output trace. When the droplet has completely evaporated, heating of the junction resumes and the output trace returns to zero as the junction approaches chamber temperature (see Fig. 10). This rate of heating of the water droplet is a function of drop size and hence cooling time. Thus, the accurate determination of the wet-bulb depression is a compromise between cooling time and chart speed. When the needle was allowed to deflect to full scale on the 10 microvolt range of the measuring instrument, a cooling time of approximately 5 s had elapsed. The chart speed that provided the most acceptable trace was found to be 20 s cm^{-1}. A typical trace of the microvoltmeter output recorded during a typical determination on a strip chart recorder (CR 100 by JJ Lloyd Instruments, U.K.) is given in Fig. 10.

To extract the true reading a ruler is placed along heating trace I (Fig. 10) which decreases from its maximum position towards zero. The microvoltage corresponding to the wet-bulb depression is defined as the point at which the trace first deflects appreciably from the ruler. A deflection of 1 mm is deemed significant. This point should be independent of the slope or duration of the plateau and is thus independent of cooling time. The zero offset is defined as the number of divisions between the chart zero and the value to which the trace returns after the cooling/heating cycle and is subtracted from the recorded reading before applying the temperature correction. Experience taught that inaccurate readings result if the zero offset differs appreciably from the instrument zero as this indicates thermal instability in the

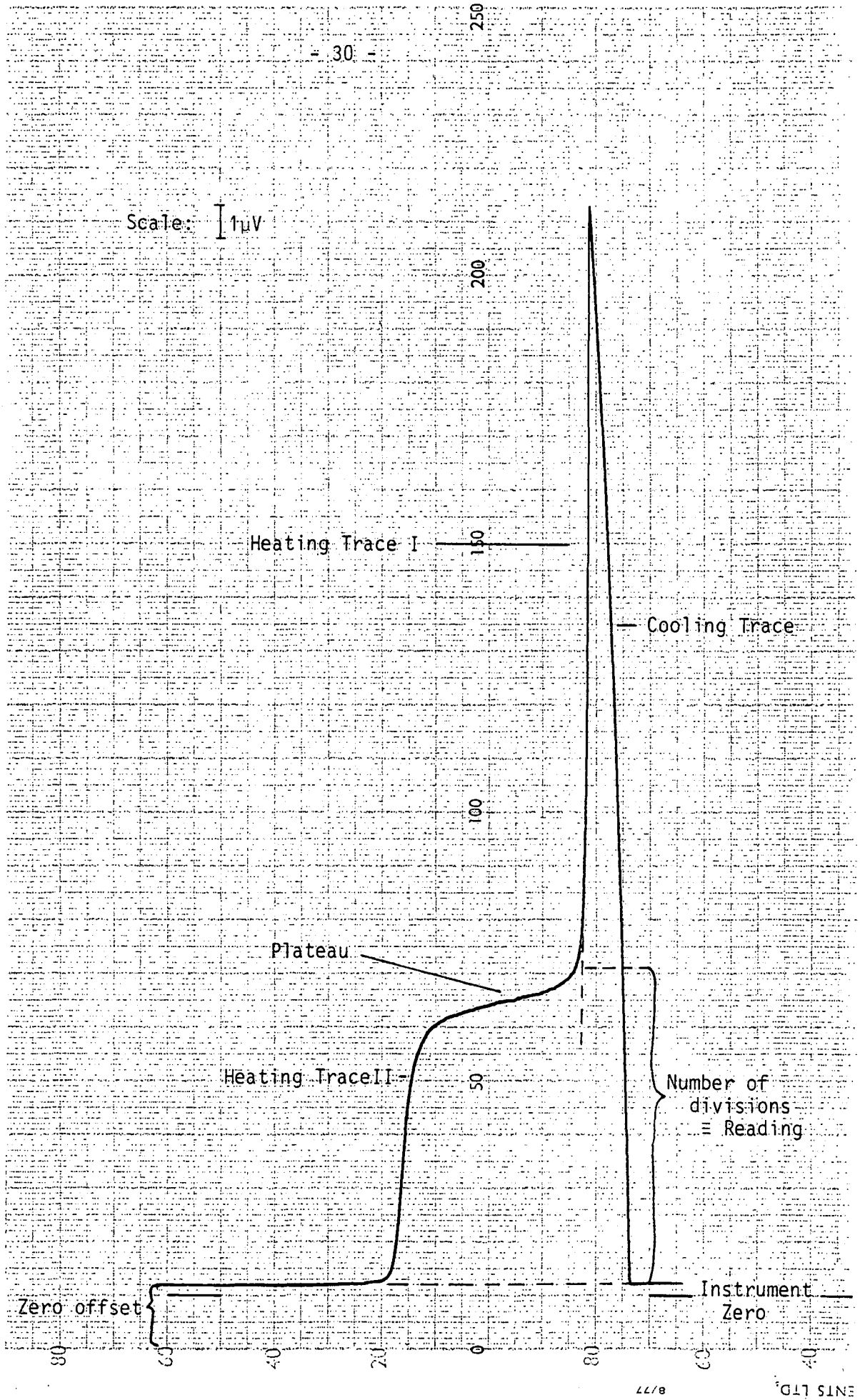

Fig. 10 : A typical actual trace recorded on the strip chart recorder during the determination of leaf water potential.

aluminium sensor block. The instrument zero reading is obtained with the control switch in the Wescor microvoltmeter set at SHORT.

It should be noted that it is not possible to measure block tem= perature (i.e. chamber temperature) and the thermocouple output voltage simultaneously on the HR-33T microvoltmeter. Thus, the temperature sensor leads were first attached to the microvoltmeter and the temperature recorded. These leads were then removed and the thermocouple leads attached. With the output of the microvolt= meter connected to the strip chart recorder, the wet-bulb temperature reading was taken. Directly following this the temperature was again recorded and if it varied by more than 0,3 °C from the initial temperature, the reading was scrapped and a new measure= ment made (see Meidner et al, 1976).

Apart from the maintenance of a constant temperature during measure= ment, it is the determination of the decrease in heating rate that causes most difficulty in field applications. It was found that the duration of the plateau depends amongst other factors, upon cooling time. Increased cooling time causes a large water droplet to be formed on the junction and this results in an extended hori= zontal plateau. The slope of this plateau relative to the zero line of the chart is a function of cooling time. When measurements are being carried out by eye using the instruments microvoltmeter, utilisation of a constant cooling time should reduce the error in measurement. However, with a strip chart recorder, the wet-bulb temperature can be determined precisely as discussed above and is independent of cooling time.

As is seen from the above discussion, the effective use of the leaf psychrometer for field observations was a result of adhering strictly to the experimental procedure. The main features of the method applied in this study include:

1) The use of a suitable strip chart recorder to accurately determine wet-bulb depression according to the technique described above. This had the added advantage of providing a permanent record of the water potential measurements;

2) exercising care to ensure that the thermocouple junction was cooled to below dewpoint;

3) defining the required reading on the chart as the point at which the plateau first deflects 1 mm off-line from the heating trace;

4) defining the thermocouple zero as the value to which the output settles after passing through the plateau region. This zero offset was subtracted from the reading before carrying out temperature corrections;

5) refusing to take observations when the zero offset differs by more than 0,5 μV from the instrument zero;

6) the use of a chart speed of 20 scm^{-1} for cooling times of approximately 5 - 15 seconds.

The method of leaf water potential determination described above was used in calibrating the L51 leaf psychrometer and in field determinations during the 1978 season.

3.6 Calibration of the L51 Leaf Psychrometer

3.6.1 Calibration procedure

Standard sodium chloride solutions of various molatities were prepared using distilled water and reagent grade NaCl. The table provided by the manufacturer makes it possible to convert a given molality at a given temperature to water potential.

Molality is defined as the concentration of a solution in moles of solute per kilogram of solution. Thus, a one molal solution is made up of 58,44 g of NaCl and 1 000 g of H_2O.

Molal solutions of 0,0; 0,1; 0,2; 0,3; 0,4; 0,7; 1,0 and 1,2 were used to calibrate the instrument on the 10 and 30 microvolt ranges. These standard solutions provided water potentials in the psychrometer chamber ranging between 0,0 bar and -56,8 bar. The water potential of distilled water equals zero.

For the calibration, a leaf simulator was constructed by enclosing a filter paper disc in an aluminium foil envelope. The aluminium envelope had a hole punched in one side where 3 or 4 drops of the particular standard solution were administered to the filter paper. This imitation leaf was inserted into the leaf slit of the psychrometer and the aluminium cylinder pressed onto the envelope with the thermocouple cavity directly above the filter paper. The aluminium cylinder was then fixed in this position using the lock nut provided. The edge of the sensor cylinder was coated with a thin film of petroleum jelly to ensure an air tight seal.

As no constant temperature enclosure was available, the psychrometer was placed in a large box lined with foam rubber to dampen temperature fluctuations. The sensor was allowed to reach thermal equilibrium before a reading was taken. It was assumed that no temperature gradients existed in the sensor block when less than 0,5 µV deflection is registered when switching the microvoltmeter from the SHORT to the READ setting. Under these circumstances the dry thermojunction and the aluminium block are at the same temperature. It is important to switch directly between READ and SHORT and to avoid any heating or cooling of the psychrometer. Note that a large spike is often observed when switching from READ to SHORT. This is caused by the switching action itself and has no effect on the existing equilibrium conditions.

After each measurement the thermocouple end of the cylinder was cleaned with acetone and rinsed in distilled water. The wet junction was then blown dry with dichlorodifluoromethane to prevent a salt deposit forming on the thermocouple and thus influencing the calibration.

The psychrometer was calibrated three times for both the 10 and 30 microvolt range. A summary of all raw data, together with linear regressions obtained using the HP97 calculator is given in Tables 7 and 8. Graphical representations of the calibration curves referred to a temperature of 25 °C for both the 10 and 30 microvolt range are given in Fig. 11. The graphs were drawn using the regression equations for the lumped data.

TABLE 7 : Calibration Data for the 10 Microvolt Range.

Molality	Net Recorder Deflection (div.)	Chamber Temperature (°C)	x Net Corrected Deflection (div.)	y Water Potential (bar)	Linear Regression Analysis y = a + bx
Run 1					
0,1	35	21,0	39	- 4,5	
0,2	64	21,1	71	- 9,0	r^2 = 0,9940
0,3	92	20,4	105	-13,4	a = -0,2388
0,4	122	20,0	141	-18,0	b = -0,1217
0,5	156	19,4	184	-22,0	
Run 2					
0,1	38	26,5	37	- 4,6	
0,2	73	28,5	67	- 9,3	r^2 = 1,0000
0,3	104	28,0	97	-13,8	a = 1,1415
0,4	136	28,3	125	-18,4	b = -0.1557
0,5	172	28,9	156	-23,1	
Run 3					
0,1	43	26,0	42	- 4,6	
0,2	80	27,3	75	- 9,2	r^2 = 0,9824
0,3	108	25,9	105	-13,7	a = 0,5392
0,4	165	25,5	158	-18,3	b = -0,1286
0,5	182	26,5	175	-22,9	

Linear regression analysis for all 10 microvolt data lumped together:
r^2 = 0,9594; a = 0,0390; b = -0,1303

TABLE 8 : Calibration Data for the 30 Microvolt Range.

Molality	Net Recorder Deflection (div.)	Chamber Temperature (°C)	x Net Corrected Deflection (div.)	y Water Potential (bar)	Linear Regression Analysis y = a + bx
Run 1					
Distilled H_2O	7	26,3	7	0	
0,1	16	28,1	15	- 4,7	r^2 = 0,9977
0,2	22	27,5	21	- 7,2	a = 3,8824
0,3	33	26,8	31	-13,8	b = -0,5540
0,4	43	27,2	41	-18,4	
0,5	50	26,5	48	-22,9	
Run 2					
0,1	13	26,5	12	- 4,6	
0,2	26	28,5	24	- 9,3	r^2 = 0,9988
0,3	36	28,0	33	-13,8	a = 0,9458
0,4	48	28,3	44	-18,4	b = -0,4427
0,5	60	28,9	54	-23,1	
Run 3					
0,1	18	26,0	18	- 4,6	
0,2	30	27,3	28	- 9,2	r^2 = 0,9990
0,3	41	25,9	40	-13,7	a = 3,4163
0,4	53	25,5	52	-18,3	b = -0,4297
0,5	64	26,5	62	-22,9	
0,7	87	26,6	83	-32,3	
1,0	128	27,8	119	-46,9	
1,2	148	27,8	138	-56,8	

Linear regression analysis for all 30 microvolt data lumped together:
r^2 = 0,9851; a = 1,0246; b = -0,4142

3.6.2 The effect of cooling time

Cooling time affects the shape and duration of the plateau, but when using the above described experimental technique, cooling time was found to have no effect on the water potential determinations.

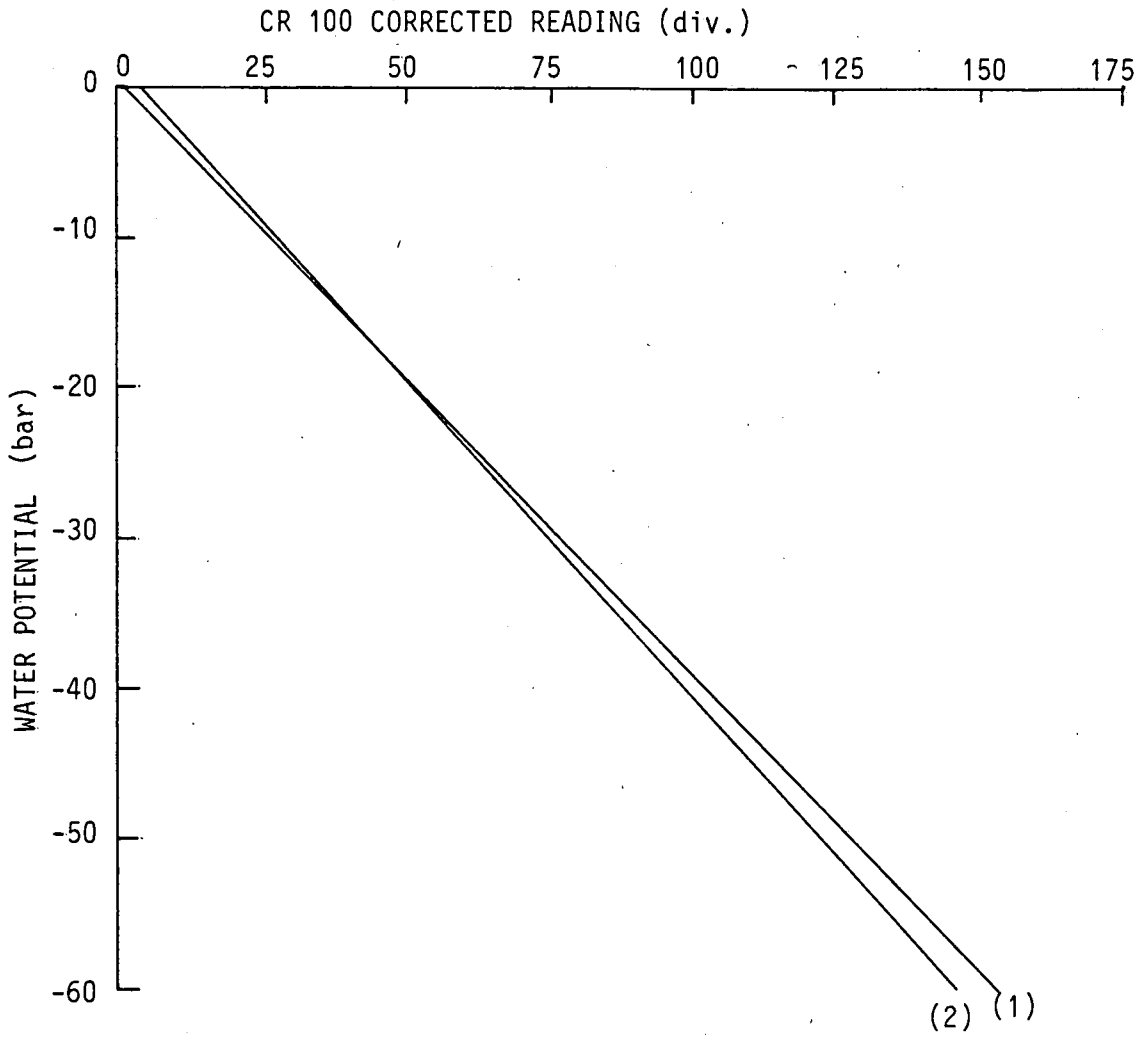

Fig. 11 : Comparison of Standard Calibration curves obtained for the 10 and 30 microvolt ranges. The regression equations for the lumped data are plotted.

x = CR100 deflection in divisions

y = water potential in bar

(1) 10 microvolt range : $y = 3(0{,}0390 - 0{,}1303\ x)$

(2) 30 microvolt range : $y = 1{,}0246 - 0{,}4142\ x$.

This is indicated in Table 9 where the effect of cooling time on the microvoltmeter deflection corresponding to the water potential measurement of a 1 molal solution at a temperature of 28,5 ± 0,2 °C is given. When using the naked eye to read the meter needle deflection directly, the use of a constant cooling time will improve the accuracy of the results obtained.

TABLE 9 : The Effect of Cooling Time on the Microvoltmeter Deflection corresponding to the Water Potential Measurement of a One Molal Solution at a Temperature of 28,5 ± 0,2 °C.

Cooling Time (s)	Net Corrected Deflection (div)	Water Potential (bar)
10	30	-47,0
15	30	-47,0
20	30	-47,0
25	30	-47,0
30	30	-47,0
40	30	-47,0
50	30	-47,0
60	30	-47,0

3.6.3 Thermal equilibration time

Meidner et al (1976) claim that it is often necessary to allow samples to equilibrate for several hours before taking water potential measurements. This, however, is not practical for field work. The effect of equilibration time was tested in the laboratory and the results obtained are given in Tables 10 and 11.

The zero offset and instrument zero were found to coincide with one another within 60 s of the sample being sealed in the psychrometer unit. This probably indicates that thermal equilibration of the sensor block required less than 60 s and hence the uniformity of the

TABLE 10 : Effect of Equilibration Time on Water Potential Measurements of a 1,0 Molal Solution : 30 microvolt range.

Equilibration Time (minutes)	Temperature (°C)	Net Corrected Divisions (div)	Water Potential (bar)
0	29,5	87,4	-47,20
2	29,4	87,6	-47,18
5	29,3	87,8	-47,17
9	29,2	88,9	-47,15
13	29,0	92,1	-47,11
17	29,3	91,4	-47,17
20	29,3	91,4	-47,17
25	29,1	91,8	-47,13
30	29,1	90,9	-47,13
40	28,9	87,8	-47,09

TABLE 11 : Effect of Equilibration Time on Water Potential Measurements of a 0,2 Molal Solution : 10 microvolt range.

Equilibration Time (minutes)	Temperature (°C)	Net Corrected Divisions (div)	Water Potential (bar)
0	29,4	67,0	- 9,28
3	29,3	66,3	- 9,28
5	29,2	65,6	- 9,28
8	29,0	65,9	- 9,27
12	29,0	65,0	- 9,27
15	29,0	64,1	- 9,27
33	28,6	61,1	- 9,26
37	28,6	60,2	- 9,26

results quoted in Tables 10 and 11. In the field, however, reliable results can only be obtained when zero offset equals instrument zero

± 0,5 μV, which could take some considerable time to be achieved. This further emphasises the need for meticulous care when testing the zero of the instrument in the field. The lengthy time which may be required for thermal equilibrium to be achieved in the field limits the effectiveness of the psychrometer when regular measurements of leaf water potential are required.

3.7 Field Determination of Leaf Water Potential using the L51 Leaf Psychrometer

The previously described technique (Section 3.5) was used to obtain leaf water potential measurements in the field during the 1978 season. The leaf psychrometer was attached to the leaf and allowed to equilibrate before commencing with the readings. In some cases the sensor was attached to the leaf in the evening and the experimental run commenced the following morning. Extreme care was taken to clean the thermojunction before it was positioned above the leaf. The psychrometer remained attached to the same leaf for the duration of each experimental run. A thin film of petroleum jelly (or a wax-petroleum jelly mixture) was used on the base of the thermocouple chamber to perfect the seal between the leaf and chamber. Occasionally on hot days, this petroleum jelly would melt and cover the section of leaf in the cavity making all further water potential determinations meaningless. This condition was easily detected in the meter needle movement of the microvoltmeter and necessitated the termination of that particular experimental run.

The youngest mature leaf was used in all cases for the determination of leaf water potential. Measurements were made on an hourly or half hourly basis throughout each experimental run. The mean values quoted are the arithmetic mean of three successive water potential determinations.

In order to test the measuring technique, the values of water potential obtained using the initial temperature and the first water

potential trace were compared to the water potentials obtained using the mean values from three determinations. Though not presented graphically, no significant difference was observed between these two procedures. It is thus concluded that several sensors could be used and that only one cooling/heating cycle be carried out on each sensor at any given time. The mean value so found would give a measure of the leaf water potential which would closely represent the value for the crop as a whole.

3.8 The Scholander Pressure Chamber

During the 1979 season leaf water potential was measured in the field by means of the pressure chamber technique (Scholander, Hammel, Bradstreet & Hemmingsen, 1965; Waring & Cleary, 1967).

This method involves sealing the leaf in a pressure chamber with the cut edge extending through an air tight seal. Air pressure is then applied until cell sap just oozes out of the cut edge. The pressure at which the sap is first observed at the cut edge is taken to reflect the endpoint reading. This balancing pressure, with a negative sign, is considered equal to the hydrostatic pressure existing in the water of the leaf xylem vessels before excission (Scholander et al, 1965). Slavik (1974) claims this reading gives a good estimate of leaf water potential. Certain authors (Baughn, 1974; Campbell et al, 1974) have compared leaf water potential measurements obtained by the pressure chamber technique and in situ hygrometer method and found that the pressure chamber technique tends to underestimate leaf water potential by approximately 1 bar. These comparisons and their interpretation are difficult to make because of the difficulty in measuring the temperature of pressurisation in the pressure chamber.

To obtain a value of leaf water potential in the field, a leaf was selected and wrapped in a damp cheesecloth. The youngest mature

leaf was used for all determinations. It was cut approximately 10 mm from the stem of the plant and placed in the pressure chamber in the conventional manner. Care was taken to cut the leaf only once and not to trim the cut edge. The first cut causes the sap in the xylem vessels to retract from the cut edge. This results in a rise in turgor in the leaf and further cutting could thus upset the reading.

Once the leaf was in the chamber, air pressure was increased at approximately 0,5 bar s^{-1} and airflow stopped immediately the endpoint was reached. The pressure at which this occurred was taken to reflect the suction with which the cell walls retain water. For practical reasons the leaf water potential is expressed in bars.

3.9 The J14 Press

In an attempt to obtain reliable field measurements of leaf water potential, the J14 press[1] (see Fig. 12) was used extensively in conjunction with the Scholander pressure chamber during the 1979 season.

The J14 press, a new instrument on the market, offers certain advantages over both the psychrometer and the Scholander pressure chamber. These include mechanical and operational simplicity, ruggedness, rapid measurements and low cost. The initial results obtained with this instrument appear encouraging and it may prove to be the ideal instrument for use in irrigation scheduling. A detailed description of the use and accuracy of the J14 press and the results of initial field work are given in Chapter 4.

---

[1] Campbell Scientific Inc., 750 West 2nd North. P.O. Box 551, Logan, Utah 84321, USA.

Fig. 12 : The J14 press used to obtain measurements of leaf water potential during the 1979 season.

CHAPTER 4

CALIBRATION OF THE J14 PRESS

4.1 Introduction

In order to use the J14 press effectively it is necessary to relate it to leaf water potential measurements obtained by means of an accepted standard instrument. For this study the Scholander pressure chamber was adopted as the calibration standard. The relationship between J14 press measurements and Scholander pressure chamber measurements was established. The results obtained appear encouraging and the J14 may yet prove a useful instrument for leaf water potential measurements.

4.2 Experimental Procedure

Hourly mean values of leaf water potential were obtained using the J14 press and Scholander pressure chamber on a series of days during both the vegetative and reproductive growth stages of the wheat crop. On each day during which measurements were made, an area approximately 3 m x 3 m was selected and all leaf samples obtained within these confines. It was assumed that all plants were subjected to equivalent environmental and soil moisture conditions. Eight and sixteen readings per hour were obtained with the Scholander pressure chamber and the J14 press respectively. The method used to obtain leaf water potential measurements by means of the Scholander pressure chamber is discussed in Section 3.8.

For the J14 press determination, a leaf was selected and a 20 - 30 mm portion removed from the end closest to the stem. This segment was then placed in the press and the pressure increased mechanically by means of the rubber diaphragm over its entire length. The pressure reading when the sap first flowed freely from the cut edges was taken as representative of leaf water potential. For the particular

J14 press used in this study the measurements were expressed in arbitrary units on a scale of 0 - 600. It is interesting to note that the manufacturer distinguishes three different end points. It is the second of these, which the manufacturer claims correlates well with Scholander chamber readings, that was used. It was found in a series of preliminary experiments to be the most repeatable measurement. The other two endpoints are extremely difficult to define and the identification of these points was found to differ from person to person.

Hourly mean values of leaf water potential, standard deviations and the coefficient of variation for the data obtained from both instruments were determined and compared.

4.3 Results and Discussion

Figs. 13 and 14 show the diurnal variation of leaf water potential for four days (28/9/79; 4/10/79; 11/10/79 and 15/10/79) as observed by means of the Scholander pressure chamber and J14 press respectively. The four days were characterised by different climatic and soil moisture conditions. Soil water contents (expressed as percentage on a mass basis) for the depths 0,1; 0,2; 0,3 and 0,4 m respectively as well as the mean values through the entire profile are presented in Table 12. The daily mean value of leaf water potential (ψ_ℓ) as measured by both instruments is also given in Table 12.

It is interesting to note that although higher soil moisture contents existed on day 2 as compared to day 1, the value of leaf water potential for day 2 fell well below the minimum value experienced on day 1. Day 1 was characterised by mild cloudy conditions while the other three days were characterised by sunny clear skies and intermittent mild north westerly winds.

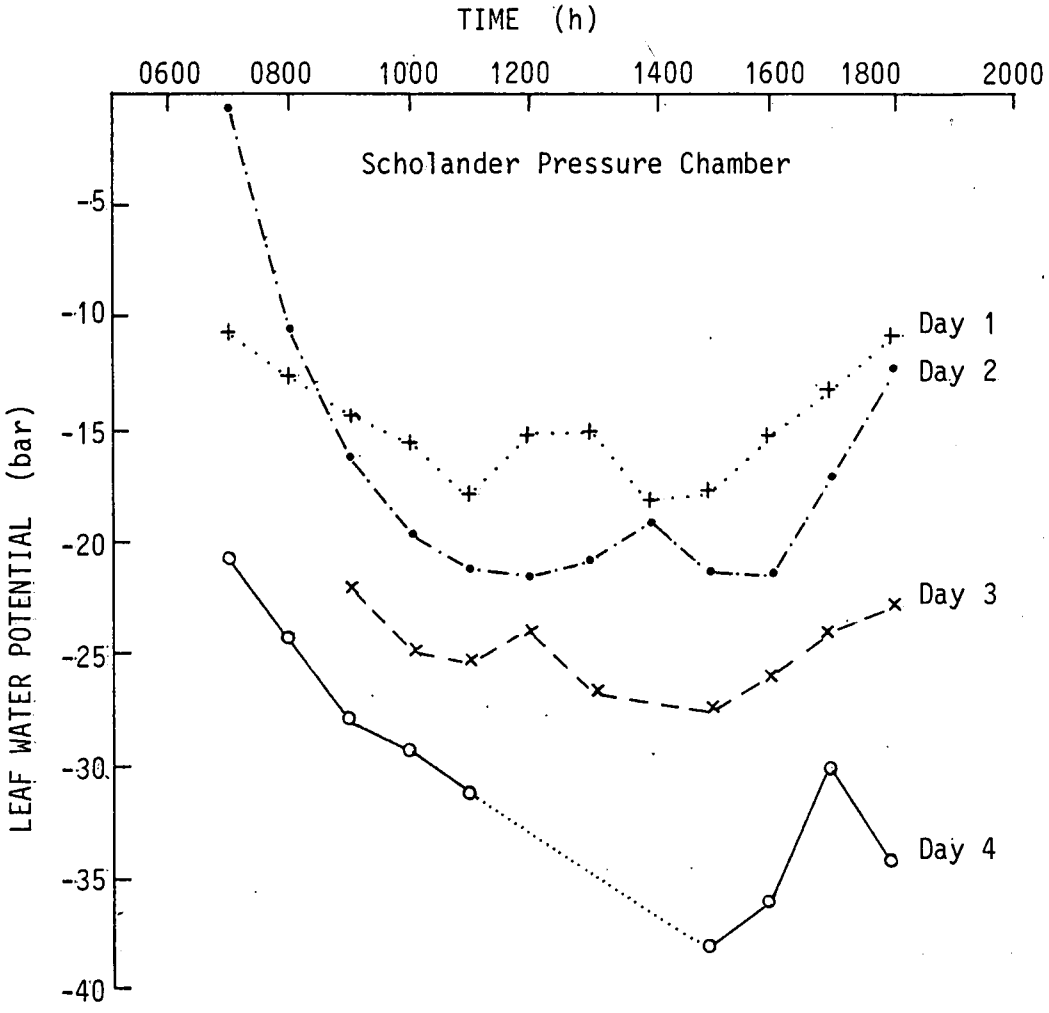

Fig. 13 : Diurnal variation in hourly mean values of leaf water potential for four days characterised by different climatic and soil moisture conditions. Measurements were made by means of the Scholander Pressure Chamber. (..... indicates missing data).

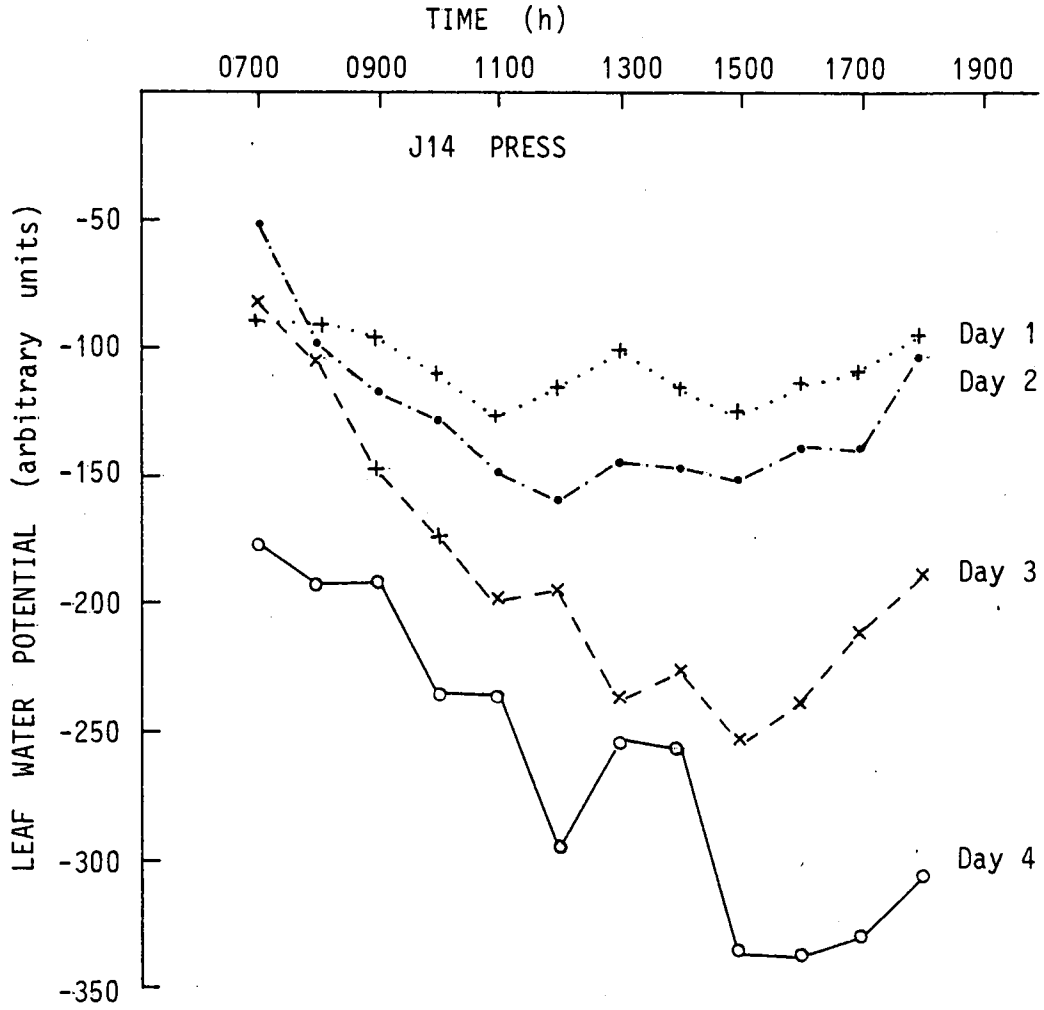

Fig. 14 : Diurnal variation in hourly mean values of leaf water potential for four days characterised by different climatic and soil moisture conditions. Measurements were obtained by means of the J14 Press.

TABLE 12 : Soil Moisture Contents (%) and Mean Daily Leaf Water Potential (ψ_ℓ) for the Four Days.

Day	Soil Moisture Content at Depths of:				Mean Water Content (%)	Mean ψ_ℓ J14 Press (div)	Mean ψ_ℓ Scholander Pressure Chamber (bar)
	0,1 m (%)	0,2 m (%)	0,3 m (%)	0,4 m (%)			
1(28/9/79)	12,1	12,7	16,4	19,3	15,1	-108	-14,8
2(4/10/79)	17,2	14,7	17,4	21,8	17,8	-127	-16,8
3(11/10/79)	8,3	10,2	13,1	15,7	11,8	-189	-24,8
4(15/10/79)	5,1	6,9	9,4	10,9	8,1	-262	-30,3

Fig. 15 displays the diurnal variation in hourly mean values of leaf water potential on day 2 as measured by the Scholander pressure chamber and J14 press. The coefficient of variation for the hourly mean values as obtained by the two instruments are depicted graphically in the lower half of the figure. It is apparent from this figure that the Scholander pressure chamber is more sensitive to variation in climatic conditions than the J14 press.

To test the ability of the two instruments to detect hourly and daily differences in leaf water potential, a one way analysis of variance (Steel & Torrie, 1960) was carried out with the aid of a HP 97 calculator. Due to different prevailing climatic and soil moisture conditions day 1 and 3 where chosen and analysed to test for hourly differences. The F statistics obtained are given in Table 13. From these results it is evident that most hourly means differed significantly from one another. All tests were carried out at the 1 % level of significance.

The test was also carried out for all four days to determine whether there is a significant difference between daily mean values of leaf water potential. The F statistics obtained are given in Table 13.

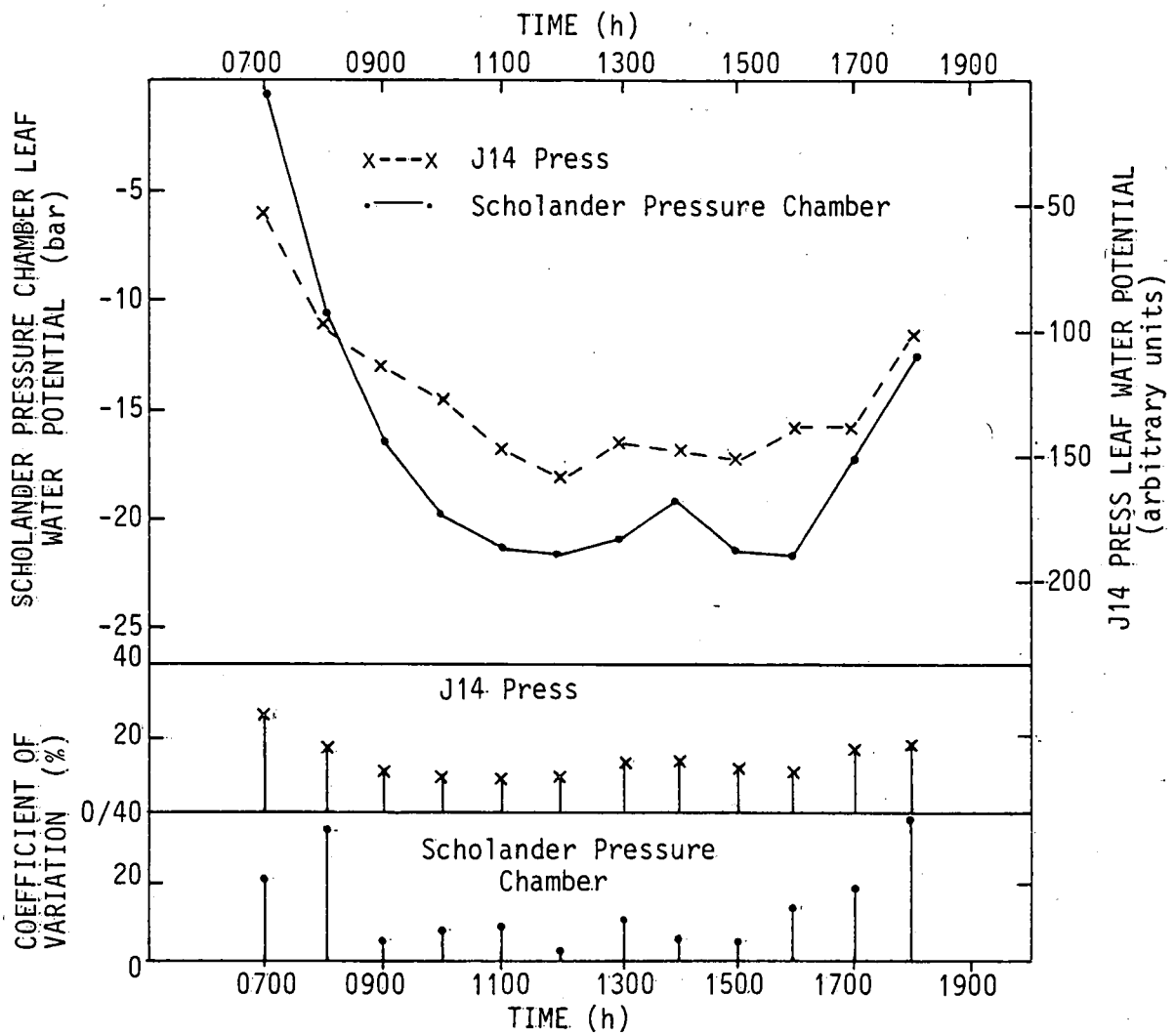

Fig. 15 : Diurnal variation in hourly mean values of leaf water potential on day 2 as measured by the Scholander pressure chamber and the J14 press.
Coefficients of variation for the two instruments are depicted in the lower half of the Figure.

Table 13 : The F Statistics obtained when Testing the Ability of the J14 Press and Scholander Pressure Chamber to detect Hourly and Daily Variations in Leaf Water Potential. The F-Distribution points are quoted for comparative purposes.

INSTRUMENT	The F statistic obtained when testing for hourly differences		The F statistic obtained when testing for daily differences
	DAY 1	DAY 2	
J14 Press	$F_{11,156} = 16,54$	$F_{11,179} = 57,27$	$F_{3,44} = 31,30$
Scholander Pressure Chamber	$F_{11,76} = 19,15$	$F_{8,61} = 3,39$	$F_{3,38} = 25,66$

The F-Distribution points for comparative purposes are:

$F_{0,01,11,156} = 2,3$ $F_{0,01,11,179} = 2,3$ $F_{0,01,3,44} = 4,3$

$F_{0,01,11,76} = 2,6$ $F_{0,01,8,61} = 2,8$ $F_{0,01,3,38} = 4,5$

From these tests one can conclude that both instruments will detect differences in leaf water potential provided eight and sixteen measurements are made with the Scholander pressure chamber and J14 press respectively. This means that either instrument can be used with confidence to follow hourly and daily variations in leaf water potential.

Fig. 16 shows the diurnal variation in the hourly mean coefficient of variation in observations made with the two instruments over six days during the vegetative growth stage. The same variation existed for measurements carried out during the reproductive growth stage. For the Scholander pressure chamber the highest coefficients of variation were obtained in the early morning and late afternoon. No irregularities could be found in the measuring technique and the presence or absence of dew in the morning had no effect on the results. Although it was assumed that the plants were subjected to the same environmental conditions, the occurrence of this large variation suggests that the response of individual plants to the prevailing microclimate is significant. This emphasizes the need to obtain as large a sample

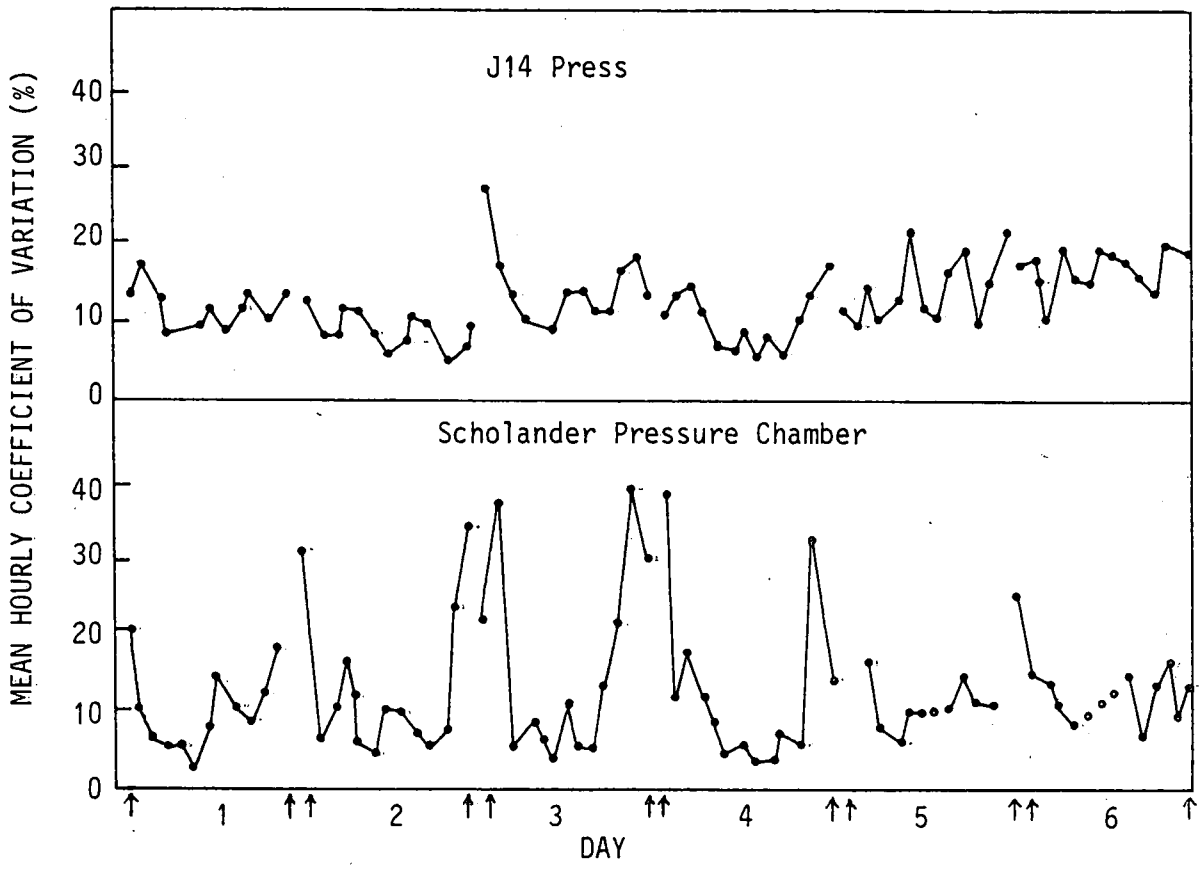

Fig. 16 : Diurnal variation in the coefficients of variation for the Scholander Pressure Chamber and J14 Press for six days during the vegetative growth stage. (◦ indicates missing data).

as is practically possible when attempting to obtain values represen= tative of the crop as a whole. The coefficients of variation from the J14 press remain more constant and do not exhibit the diurnal variation found for the Scholander pressure chamber (see Fig. 16).

The relationship between the J14 press measurements and those obtained by means of the Scholander pressure chamber for all the measurements carried out during the season is presented graphically in Fig. 17. An exponential relationship ($y = 59{,}64\ e^{0{,}049x}$) was found to give the best fit to these data. The coefficient of determination is $r^2 = 0{,}81$. The same relationship was found when the data for the vegetative and reproductive growth stages were analysed separately, suggesting that the stage of crop development has no effect on the relationship.

It is difficult to explain the non-linearity between the two techni= ques. When using the J14 press to apply pressure to the leaf, the structural unevenness of the leaf and the nylon gauze used must be overcome before all parts of the leaf are subjected to the same pressure. Thus during the initial stages the xylem vessels may not be responding to the pressure indicated by the pressure gauge. It is only once the structural resistance due to the unevenness of the leaf and gauze is overcome that the whole leaf, including the xylem ves= sels, will respond directly to the measured pressure and a "true" reading can be obtained.

On the application of air pressure, as in the case of the Scholander pressure chamber, there is no structural resistance to overcome as all parts of the leaf in the chamber are subjected to uniform pressure. This tends to suggest that a realistic reading will be obtained. However, the effect of the rubber stopper used to seal the leaf section into the pressure chamber is not known. At low pressures the situation could arise where the pressure exerted on the leaf by the rubber stopper is greater than the internal applied air pressure. In this case a higher pressure than that needed to cause the sap to exude from the cut edge would have to be applied, resulting in an overestimate. Depending on the elasticity of the stopper used,

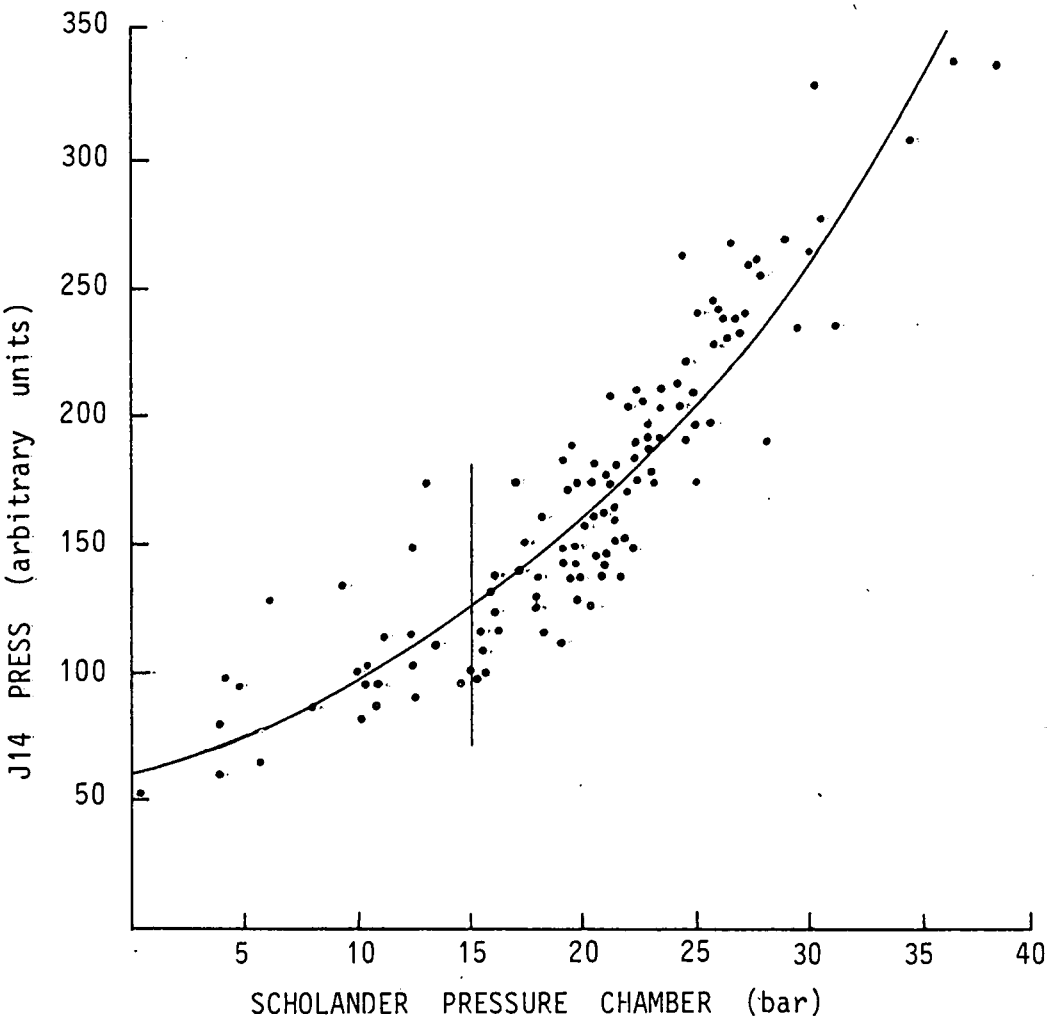

Fig. 17 : The relationship between the J14 Press and Scholander Pressure Chamber for all the data lumped together. The exponential curve which gives the best fit is plotted. It is divided into two regions to illustrate apparent variability in sensitivity of one or both instruments.

mechanical damage to the xylem vessels could also influence the reading obtained. At high pressures above 30 bar, the rubber stopper was found to break or damage the leaf where it entered the stopper. In this case, the xylem vessels obviously could not respond directly to the applied pressure and few reliable results could be obtained. Thus, it appears that at high external pressures greater than 30 bar, the xylem walls are damaged or deflated and the observations could be a function of the pressure induced by the rubber stopper. Similarly, the reliability of the J14 press at high pressures is questioned. A thorough investigation should be made of the effect mechanical pressure has on the leaf structure and the resulting flow of sap.

In Fig. 17 the exponential relation is divided into two regions to illustrate the apparent changed sensitivity of one or both instruments. There appears to be increased sensitivity in the high pressure region above 15 bar while low insensitivity is apparent in the low pressure region. The least scatter in data is exhibited in the region from 15 to 25 bar. The important critical value of leaf water potential that separates stressed plants from non-stressed plants generally falls within this region. Hence, the accuracy of the J14 technique here suggests the instrument should be an efficient tool for irrigation scheduling as well as in the many research projects currently being conducted in the field of plant water relations. A linear curve ($y = -55{,}21 + 10{,}74x$) was fitted to the data above 15 bar. It yielded a coefficient of determination of $r^2 = 0{,}84$. This suggests the J14 press will be reliable when used to measure low leaf water potentials, i.e. stressed plants.

The leaf samples prepared for these two instruments differed. For the Scholander pressure chamber, the sample had only one cut edge whereas for the J14 press it had two cut edges. When the vessel elements of the leaf are cut for the first time, the sap withdraws from the cut edge and produces a rise in turgor in the leaf. When the leaf is used in the Scholander pressure chamber a certain minimum pressure, equal in magnitude to the leaf water potential, is required to force the sap back to the cut edge (Scholander et al, 1965). For

the J14 press, however, the leaf is cut at both ends and so sap retracts from both cut edges as shown in Fig. 18. The effect this has on the value obtained for leaf water potential is not known. The effect of cutting either one or both edges of the leaf used in the J14 press deserves to be investigated. It will possibly be more accurate to use a segment of leaf taken from the leaf tip and having only one cut edge rather than a segment taken from near the stem and having two cut edges. From the above discussion it is intuitively felt that the combined effect of mechanical pressure and the two cut edges are important factors resulting in the exponential rather than a linear relationship between J14 press and Scholander pressure chamber readings.

Certain precautions must be observed when using either method to determine leaf water potential. The loss of water due to evaporation must be kept to a minimum. Thus, when preparing leaves for either pressure chamber, care must be taken to ensure they are covered with a damp cloth. This is not easy when preparing a sample for the J14 press as the leaf is exposed to the atmosphere while placing it in the press. It is important to limit this exposure to the absolute minimum. Scholander et al (1965) state that trimming is not an important consideration in monocotyledons. However, it is suggested that only one clean cut be made to reduce any errors that may arise from this source.

4.4 Conclusions

It is apparent from Fig. 14 and the analysis of variance test that the J14 press is capable of following hourly variations in leaf water potential provided sixteen leaves per sample are used.

The occurrence of high values of coefficients of variation in the early morning and late afternoon emphasizes between - leaf variation due to differing microclimate and individual plant conditions. Thus, as large a sample as is practically possible is needed when

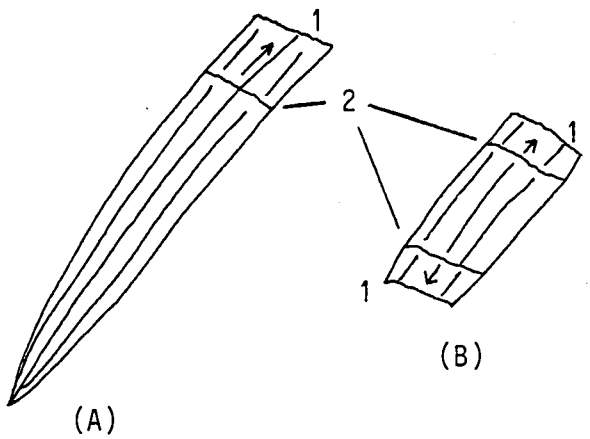

Fig. 18 : Leaf samples prepared for the determination of leaf water potential. The cut edges (1) and points to which the sap recedes (2) are illustrated. The arrows indicate the movement of sap on application of pressure to the leaf as a whole.

(A) Illustrates a sample as used in the Scholander Pressure Chamber.

(B) Illustrates a sample as used in the J14 Press.

plant parameters representative of the crop as a whole are required, particularly when measurements are carried out in the early morning or late afternoon.

Although the two instruments operate on the same principle of increasing pressure on a leaf sample, the existence of an exponential rather than a linear relationship between the two techniques suggests that the leaf responds differently to air and mechanical pressure. Furthermore, the J14 appears to exhibit improved sensitivity to change in leaf water potential at pressures in excess of 15 bar.

Due to its relatively low cost and simple operation, the J14 press could be a useful aid to irrigation farmers. Given the critical leaf water potential for a particular crop, the J14 press can be used routinely to distinguish between stressed and non-stressed plants and so assist irrigation decision making.

Furhter investigation into the peculiarities of the J14 press is needed before it be permitted to compete with the Scholander pressure chamber as an experimental tool in research projects.

CHAPTER 5

MEASUREMENT OF LEAF DIFFUSIVE RESISTANCE

5.1 Operating Principle of the LI-65 Autoporometer[1]

The LI-65 autoporometer is of the type originally designed by Van Bavel, Nakayama & Ehrler (1965) and later modified by Kanemasu, Thurtell & Tanner (1969).

When the sensor cup is placed on a leaf or calibration plate (see Section 5.2), the electrical conductivity of the lithium chloride sensor increases as water vapour diffuses into the cup. The increasing conductivity causes the meter needle to move across the scale at a rate which is directly proportional to diffusion rate. This diffusion rate is inversely proportional to the leaf diffusive resistance to water vapour transfer. The time for the meter needle to move between two preselected points is recorded automatically and displayed by means of a high output LED display with a 1/100 second resolution.

After each reading the sensor is dehydrated with dry air. This is an automatic process which proceeds to the same degree of dehydration during each cycle. Ensuring this is important to obtain reliable results (Morrow & Slatyer, 1971a).

The diffusion process is temperature dependent and so leaf temperature is measured by a thermistor bead able to read temperature accurate to within ± 0,5 °C. The sensors thermistor can be adjusted by a screw action so that it is brought into contact with the leaf.

It is common practice to account for temperature by normalising all resistance determinations to an arbitrary standard of 25 °C. This is done by making use of the relevant correction factor curve supplied by the manufacturer. This procedure obviates having to calibrate the

---

[1] LI-COR Ltd, 4421 Superior Street, Lincoln, Nebraska 68504, USA.

instrument at a number of different temperatures, each under well controlled thermal and humidity conditions. It was found that this method is not as accurate as the method used by Morrow et al (1971a) and adopted in this study.

Due to the fact that wheat has a narrow leaf a narrow aperture sensor was used in this study.

5.2 Calibration Procedure

The LI-65 autoporometer was calibrated to the resistance plate assembly supplied with the instrument. This assembly comprises an acrylic base plate and an aluminium upper plate which is fastened to the base plate during calibration. The upper plate contains a series of pores (drilled holes) to simulate leaf diffusive resistance. The resistance of each bank of holes is calculated from the equation

$$r = 4A\,(Lo + \frac{\pi d}{8}) / \alpha n \pi d^2 \quad \ldots\ldots\ldots\ldots\ldots \quad (5)$$

where

r = the diffusive resistance ($s\ cm^{-1}$),
A = the aperture area of the vapour cup (mm^2),
Lo = the actual length of each hole (mm),
d = the diameter of the holes (mm),
α = the diffusivity of water vapour in the air at a given temperature ($cm\ s^{-1}$), and
n = the number of holes.

During calibration, filter paper is placed between the two plates. It is kept saturated by filter paper wicks which are immersed in beakers of distilled water. The saturated filter paper represents substomatal conditions where the relative humidity is 100 % (Slatyer, 1967). Care must be taken to ensure that free water does not rise into the holes.

Due to the fact that the diffusion process is highly sensitive to temperature fluctuations calibration was carried out in a growth chamber. Here the temperature and high humidity conditions could be accurately controlled. Five separate calibration runs were carried out at temperatures of 14,2; 19,5; 23,5; 28,0 and 36,1 °C. This range was found to enclose the major portion of temperature conditions experienced in the field.

Calibration started with the lowest temperature and proceeded in increasing temperature steps. Care was taken to ensure that the calibration plate temperature did not fall below dewpoint temperature (McCree & van Bavel, 1977), thus preventing condensation taking place on the plate or in the pores. The occurrence of water condensation in these areas will affect the results obtained. On changing the temperature of the growth chamber a minimum of 18 hours was allowed for thermal equilibrium to be reached before the next set of readings was undertaken.

To carry out the calibration the sensor was placed above each bank of pores and the time, Δt, recorded for the meter needle to move between two preselected points. The temperature during each measurement was recorded. A minimum of 5 readings per bank of pores was obtained. The mean values of Δt obtained at a constant temperature were plotted against the appropriate r value calculated using Eqn. 5. Straight lines were fitted to this data and the resultant calibration curves for the five different temperatures are depicted in Fig. 19. The regression data and x-intercept for these linear fits is given in Table 14.

The value of Δt obtained reflects the total diffusive resistance encountered by the water vapour molecules. This total resistance (r) comprises the calibration plate resistance (which is analogous to leaf resistance, r_ℓ say) and the resistance in the sensor cup (r_o). r_o is a function of cup and sensor geometry and its value can be obtained from the negative intercept on the resistance axis of the calibration curve. Thus, when measurements are made on actual

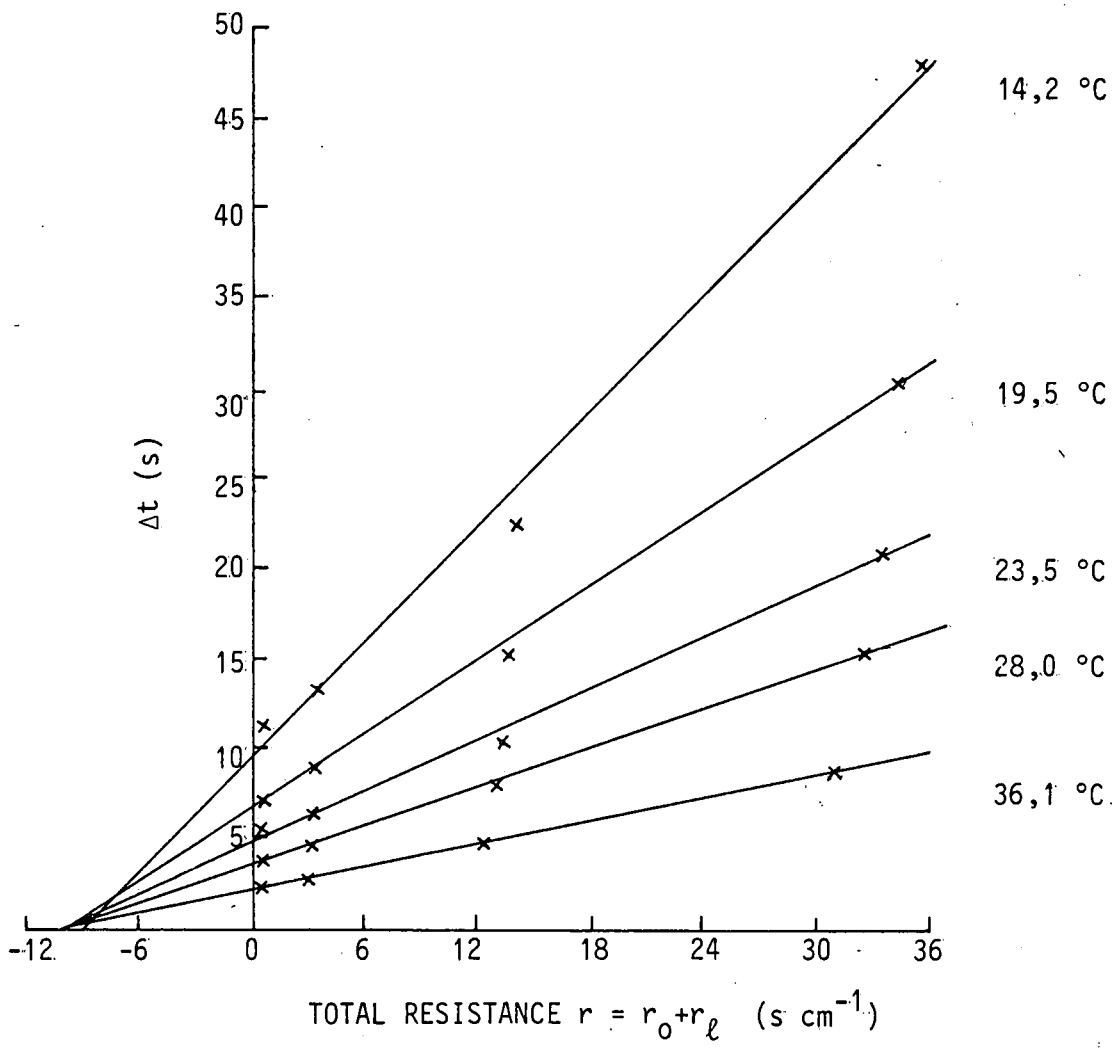

Fig. 19 : The LI-65 Autoporometer calibration curves obtained over a range of temperatures under well controlled thermal conditions.

Table 14 : Linear Regression Data used to Plot the Diffusive Resistance Calibration Curves. The x-intercept is also given.

Calibration temperature (°C)	Intercept a	Slope $b = \frac{\Delta t}{r}$	x-intercept	Coefficient of determination r^2
14,2	9,46	1,07	- 8,8	0,9923
19,5	6,49	0,69	- 9,4	0,9969
23,5	4,80	0,47	-10,2	0,9955
28,0	3,49	0,36	- 9,7	0,9986
36,1	2,14	0,21	-10,2	0,9996

leaves, estimates of r_ℓ can be made from the relationship

$$r_\ell = \frac{\Delta t}{(\Delta t/r)} - r_o \quad \ldots\ldots\ldots\ldots\ldots\ldots \quad (6)$$

where

$\frac{\Delta t}{r}$ = the slope of the calibration curve, and

$r = r_\ell + r_o$.

(Morrow et al, 1971a)

The slope of the calibration curve is temperature dependent and to accommodate all temperatures encountered in the field the $\frac{\Delta t}{r}$ vs T relationship was developed. This relationship is depicted graphically in Fig. 20. A power curve $\frac{\Delta t}{r} = a\ T^b$ was fitted to the data and the regression data obtained was:

$a = 115,80$

$b = -1,75$

$r^2 = 0,9927.$

Combining this regression data with Eqn. 6 yielded the equation

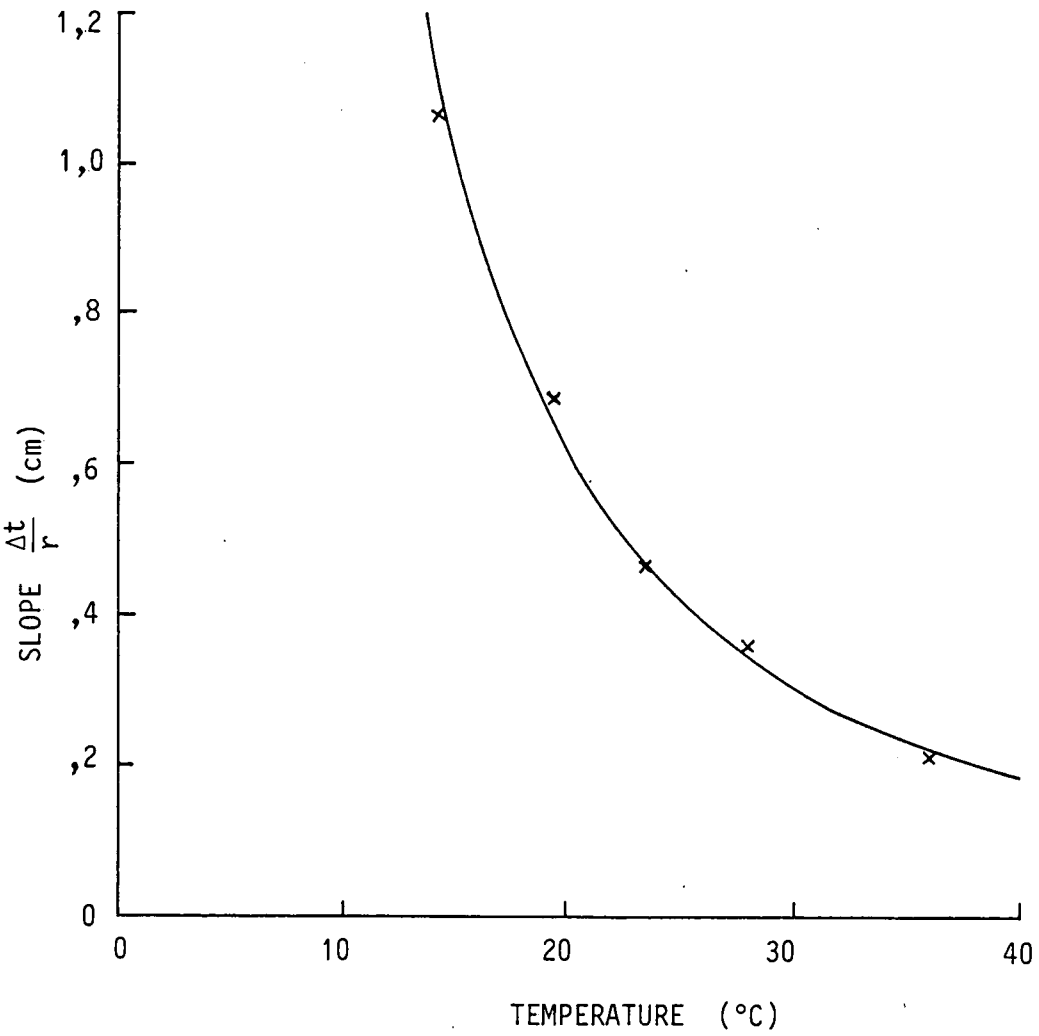

Fig. 20 : The $\frac{\Delta t}{r}$ vs T relationship developed for the LI-65 Autoporometer used in this study.

$$r_\ell = \frac{\Delta t}{115,80} T^{1,75} - r_o \quad \ldots\ldots\ldots\ldots \quad (7)$$

This meant that the field data collected could be quickly and easily converted to actual leaf diffusive resistance. The mean r_o value determined was 9,7 s cm^{-1}. Other authors (McCree et al, 1977) prefer to plot r against Δt since when $\frac{r}{\Delta t}$ is plotted at different temperatures, the curves are almost linear.

Although the diffusion process is temperature dependent, it is common practice to calibrate the porometer in the laboratory and to account for temperature by normalising all resistance determinations to an arbitrary standard of 25 °C. This is done by making use of the relevant correction factor curve which is supplied with the instrument. This obviates having to calibrate the instrument at a number of different controlled temperatures. Once the standard curve is obtained, field data may be corrected for temperature and the required resistance read off the standard curve. This method, developed by Kanemasu et al (1969), serves its purpose if no constant temperature facilities are available, but is not as accurate as the method described above and adopted in this study.

The correction factors supplied with the instrument were applied to the calibration data obtained in this study and the "standard" curves obtained are plotted in Fig. 21. At the temperatures 23,5; 28,0 and 36,1 °C the data yielded "standard" curves extremely close to one another and are represented by one curve in Fig. 21. The two lower temperatures of 14,2 and 19,5 °C however, yielded "standard" curves that differ markedly from one another and from the high temperature "standard" curves.

These results emphasize the importance of calibrating the autoporometer in the range of temperatures likely to be encountered in the field. From the present results it appears that the standard temperature approach may be valid when working in the high temperature region from 25 - 35 °C.

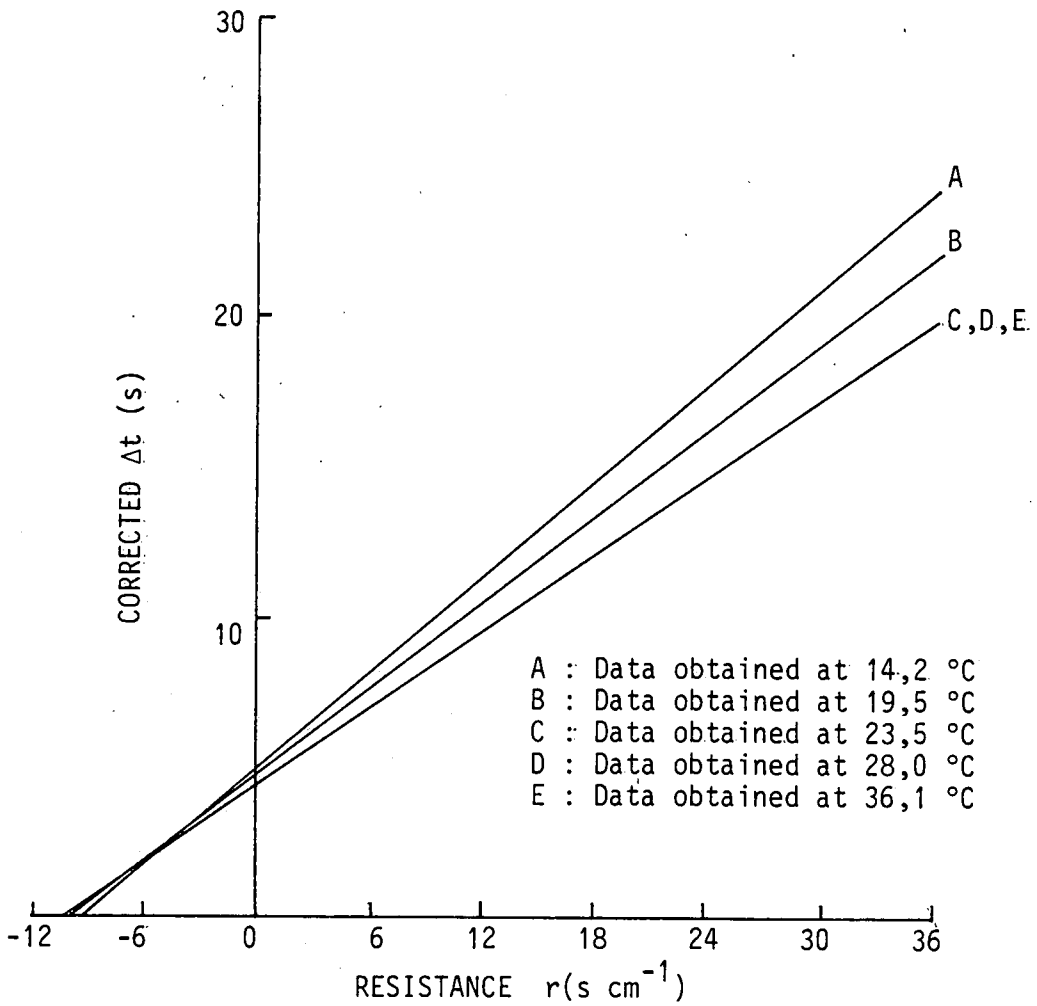

Fig. 21 : The different standard calibration curves obtained depending on the temperature conditions prevailing during calibration.

In plotting the calibration curve it is imperative to use the temperature of the diffusion process. Some authors (Bower, 1978) use the calibration beaker water temperature to obtain their standard calibration curves. Fig. 22 shows data obtained from the present study and the effect temperature has on the standard curve. (A) shows the plot obtained using the diffusion process temperature while (B) shows the plot obtained using the temperature of the water in the beakers. It is obvious that use of the incorrect temperature will cause errors in the resistance value obtained.

5.3 Determination of Leaf Diffusive Resistance in the Field

The youngest mature leaf was used for all stomatal resistance measurements. During the 1978 season only the adaxial surface resistance was measured. Since wheat has an amphystomatous leaf both the adaxial and abaxial surface resistances were measured during the 1979 season. The total resistance was then determined from the relationship:

$$\frac{1}{r_T} = \frac{1}{r_{adaxial}} + \frac{1}{r_{abaxial}} \quad \ldots\ldots\ldots\ldots \quad (8)$$

(Monteith, 1973)

Leaf diffusive resistance measurements were normally made on an hourly basis. The instrument was subjected to several wet/dry cycles before starting each set of resistance determinations, and again whenever it was switched off while carrying out a set of measurements. The arithmetic mean of between eight and twelve observations was taken as the value representative of the hourly period under observation.

Only fully exposed sunlit leaves were used for diffusive measurements. Oke (1978) states that despite transpirative and convective losses, a sunlit leaf is commonly 5 - 10 °C warmer than the surrounding air. Morrow & Slatyer (1971b) indicate that shading of the leaf for

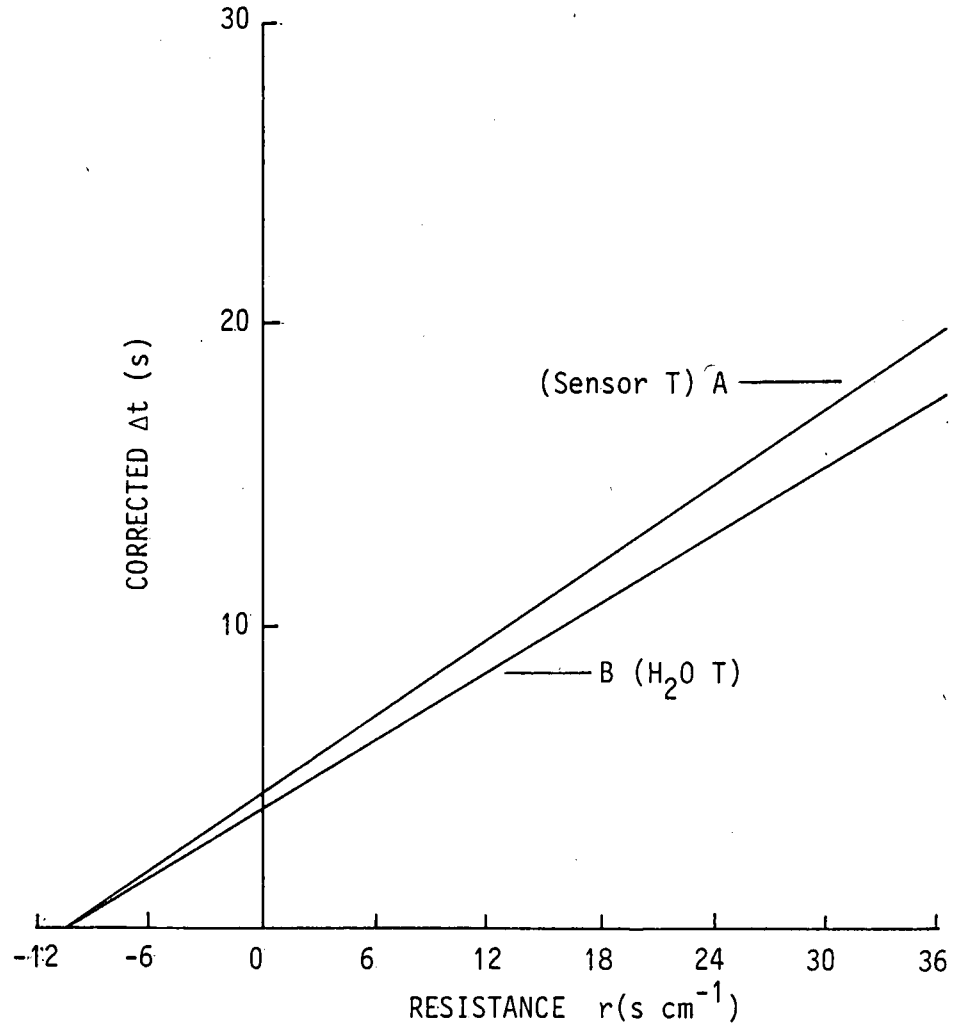

Fig. 22 : The different standard calibration curves obtained depending on whether the temperature of the diffusion process or water temperature is used to normalise Δt.

± 30 s is necessary before carrying out diffusive resistance measurements. This enables the leaf temperature to adjust to within ± 1 °C of ambient temperature and so increases the accuracy of the measurement. The reaction rate of stomates to external stimuli range from a few minutes to several hours (Bidwell, 1974) and often do not respond fully to light and dark conditions because of the endogenous rhythms (Meidner & Mansfield, 1968). Thus shading and the placing of the sensor on the leaf for the short time required to make a measurement should not affect the diffusion process and hence the reliability of the results.

In this study the direct method of shading was not adopted. The manufacturer claims that the thermistor measures the diffusion process temperature and not the pre-measurement leaf temperature. This is due to the heat sink capacity of the sensor which is higher than that of the leaf segment involved. Temperature was, however, measured just prior to the removal of the sensor. This meant the leaf had been shaded for the maximum length of time possible other than having individual shading as part of the measuring technique.

Although no radiation shield (McCree et al, 1977) was consutrcted for the porometer sensor, great care was taken at all times to keep it shaded. Between each set of measurements the sensor was stored in a dehydrated plastic case away from any direct radiation.

CHAPTER 6

ESTIMATION OF EVAPOTRANSPIRATION USING AN ENERGY BUDGET METHOD

6.1 INTRODUCTION

Evapotranspiration is the composite loss of water to the air from all sources (Oke, 1978). This includes evaporation from open water surfaces, the soil, and the transpiration of vegetation. When soil and plant factors are non-limiting, evapotranspiration is a purely energy transforming process. It is then determined entirely by meteorological factors such as radiation, wind, temperature and humidity.

There are a number of different methods employed to estimate the water loss from crops through evapotranspiration. These include the water balance or hydrological method, the energy budget technique, the aerodynamic technique and the many empirical methods that have been developed. These methods, together with a larger number of references, are discussed by Du Pisani (1974).

The equipment required by present day techniques to estimate evapotranspiration is either extremely expensive (lysimeters), or intricate and susceptible to breakage (aerodynamic sensors). One of the aims of this study was to develop a technique which makes use of equipment that is durable, foolproof and which can be installed and maintained by unskilled labour. Such a technique would be of great value to the large irrigation schemes provided measurements of evapotranspiration of accuracy acceptable for agricultural purposes could be achieved.

The theory for the new technique used in this study is derived from the balance of radiative, momentum, mass and heat energy in plant communities. This budget provides a complete accounting of how solar energy is partitioned at a surface and hence makes possible an accurate analysis of the environment at the surface. It could be usefully employed in explaining the interaction between the physical

driving forces and the growth and behaviour of the biological system.

The energy budget at any natural surface can be described by the implicit energy balance equation of six terms, namely, net radiation (R_N), latent heat flux (λE), sensible heat flux (C), soil heat flux (G), photosynthetic flux (P) and heat storage (J). The latter two terms are omitted as they are usually negligibly small when compared to the other terms (Monteith, 1973; Thom, 1975).

The energy budget can thus be expressed as

$$R_N = G + C + \lambda E \; . \quad \ldots\ldots\ldots\ldots\ldots\ldots \quad (9)$$

Fig. 23 shows the canopy surface of a plant community and the radiative and soil heat flux directions for day and night time conditions.

The net radiation and soil heat flux terms in Eqn. 9 can be measured directly, or estimated using any of the widely accepted empirically determined ratios. To estimate these two terms by the latter method, standard macroclimatic observations and sunshine duration are required. These observations are easily obtained and the equipment required is inexpensive and durable, thus offering decided advantages for agricultural research. In this, the development of the technique, the soil heat flux and net radiation were measured directly. However, it is felt that reliable empirical methods could be substituted when this technique is applied in practice.

The evaporative and convective terms of the energy budget equation are solved by recording wet- and dry-bulb temperatures and wind speed at the momentum exchange surface in the canopy and at some distance above the canopy surface.

Use of the appropriate theory and the input data described above, enables the energy budget equation to be evaluated by the reiterative technique described by De Jager & Harrison (1979). The reiterative technique is a self-correcting, repeated trial and error method of

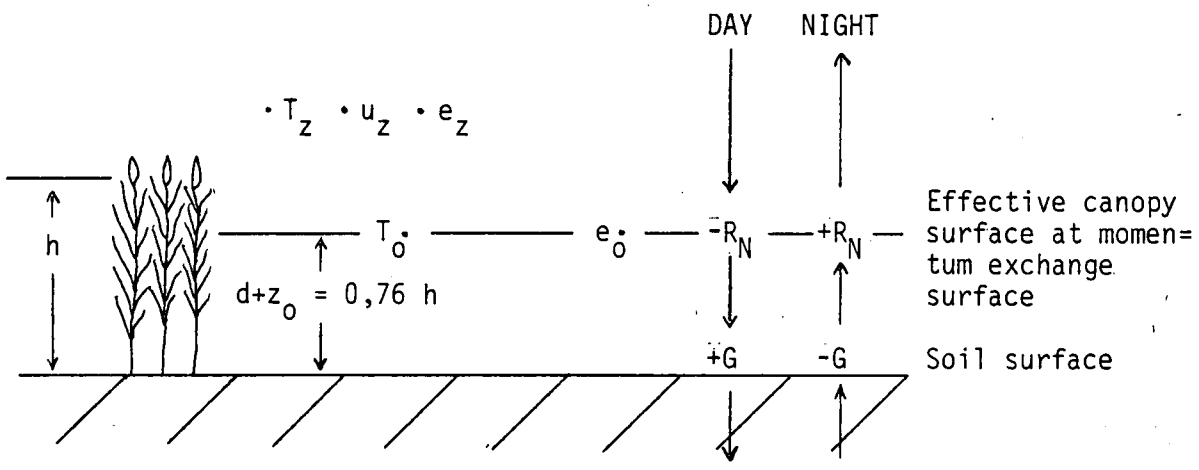

Fig. 23 : The plant community showing the canopy surface, the various measuring positions and the adopted sign convention.

numerical solution that is used to find the canopy surface tempera= ture which ensures that the energy budget equation (Eqn. 9) balances to within $\pm$ 1 Wm^{-2}.

Hourly mean values of the weather elements were used to follow daily variations in the driving forces. The closeness of agreement between the measured and computed surface temperature was used as a test of the accuracy of the technique. The basic principle of the technique depends on several major assumptions, namely:

(1) the canopy surface is assumed to occur at the height at which wind speed is theoretically zero. This height is given by $d + z_o$ where d is the zero displacement level and z_o the roughness parameter. ($d = 0{,}63\ h$ and $z_o = 0{,}13\ h$ (see Monteith, 1973) where h is the crop height),

(2) the relative humidity measured at this height is assumed to indicate the magnitude of the source or sink of the vapour from which exchange with the atmosphere is taking place,

(3) the similarity hypothesis is valid in the case of the crop under observation, and

(4) a "conglomerate mass" hypothesis is applied to the crop. By this one assumes the crop to behave as a conglomerate mass of uniform temperature and relative humidity.

6.2 General Theory

The energy budget equation may be written as

$$R_N = C + \lambda E + G \qquad \ldots\ldots\ldots\ldots\ldots\ldots \qquad (9)$$

where

R_N = the net radiation reaching the canopy surface (Wm^{-2}),
C = the sensible heat flux (Wm^{-2}),
λ = the latent heat of vapourisation ($J\ kg^{-1}$),
E = the evaporation ($kg\ m^{-2}s^{-1}$),
λE = the latent heat flux (Wm^{-2}), and
G = the soil heat flux (Wm^{-2}).

In this study R_N and G are measured quantities and C and λE are unknowns. To solve this single equation for two unknowns a reiterative method (De Jager et al, 1979) is used to compute the canopy surface temperature T_o which balances the equation. To express the latent heat flux, λE, and sensible heat flux, C, as functions of T_o, an aerodynamic treatment of momentum, mass and heat exchange is followed. This theory is adapted from Thom (1975).

For conditions over vegetation, where λE and C are independent of height, equations expressing aerodynamic resistance to the flow of these entities in terms of the change of vapour pressure, e, and temperature, T, at two levels only can be derived from the definition of aerodynamic resistance (aerodynamic resistance = $\frac{\text{concentration difference}}{\text{flux}}$). These equations can be written as

$$r_{aV} = \frac{\rho C_p}{\gamma} \frac{(e_o - e_z)}{\lambda E} \quad \ldots\ldots\ldots\ldots \quad (10)$$

and

$$r_{aH} = \rho C_p \frac{(T_o - T_z)}{C}, \quad \ldots\ldots\ldots\ldots \quad (11)$$

where

r_{aV} = the aerodynamic resistance to the transfer of water vapour ($s\ m^{-1}$),
r_{aH} = the aerodynamic resistance to the transfer of heat ($s\ m^{-1}$),
ρ = the density of air ($kg\ m^{-3}$),
C_p = the specific heat of air ($J\ kg^{-1}\ °C^{-1}$),

γ = the psychrometric constant (mbar $°C^{-1}$),
e_o = the surface vapour pressure (mbar),
e_z = the vapour pressure at the reference height z (mbar),
T_o = the surface temperature (°C), and
T_z = the temperature at the reference height z (°C).

Use of the similarity hypothesis for fully forced convection yields

$$r_{aM} = r_{aV} = r_{aH} = \frac{\left[\ell n(\frac{z-d}{z_o})\right]^2}{k^2 u(z)} \quad . \quad \ldots\ldots\ldots \quad (12)$$

This relationship permits latent heat flux (λE) and sensible heat flux (C) terms of the energy budget equation to be written as

$$\lambda E = \frac{\rho C_p \, k^2 \, u(z)}{\gamma} \quad \frac{(e_o - e_z)}{\left[\ell n(\frac{z-d}{z_o})\right]^2} \quad , \quad \ldots\ldots\ldots\ldots \quad (13)$$

and

$$C = \rho C_p \, k^2 \, u(z) \quad \frac{(T_o - T_z)}{\left[\ell n(\frac{z-d}{z_o})\right]^2} \quad , \quad \ldots\ldots\ldots \quad (14)$$

where

r_{aM} = the aerodynamic resistance to the transfer of momentum (s m^{-1}),
k = von Karman's constant (= 0,41),
u(z) = the wind speed at height z (m s^{-1}),
z = the reference height at which measurements are made (m),
d = the zero plane displacement level (m), and
z_o = the roughness parameter.

The mean value of the vapour pressure at the effective surface, e_o, can be expressed as $RH_o \, e_s \, (T_o)/100$ where RH_o is the mean value of relative humidity and $e_s(T_o)$ is the saturation vapour pressure at this surface. $e_s(T_o)$ can be expressed as a function of T_o via an integrated form of the Classius-Claperyon equation, namely:

$$e_s(T_o) = 6{,}11 \exp\left[5347{,}61\left(\frac{1}{273{,}16} - \frac{1}{273{,}26 + T_o}\right)\right] \text{ (mbar) . .... (15)}$$

This means that if RH_o is measured using the wet- and dry-buld thermometers, then λE can be expressed as a function of T_o.

It should be noted that both the evaporative and convective flux terms given here apply to neutral conditions, in which the effect of temperature gradients are ignored. To allow for the effects of instability and stability on the basic neutral profiles, the flux terms of λE and C for neutral conditions are corrected by multiplying by the stability factor F, where

$$F = (1 - 5R_i)^2 \quad \text{if } R_i \text{ is positive,}$$

and $$F = (1 - 16R_i)^{3/4} \quad \text{if } R_i \text{ is negative.}$$

R_i is the prevailing Richardson number and is easily calculated from the recorded temperature and wind data.

The energy budget equation,

$$R_N = \lambda E + C + G \quad \text{.....} \quad (9)$$

can now be written in an expanded form as

$$R_N = G + \rho C_p\, k^2\, u(z)\, \frac{(RH_o\, e_s(T_o)/100 - e_z)}{\gamma \left[\ell n\left(\frac{z-d}{z_o}\right)\right]^2} + \rho C_p\, k^2\, \frac{u(z)(T_o - T_z)}{\left[\ell n\left(\frac{z-d}{z_o}\right)\right]^2} \quad \text{.....} \quad (16)$$

It is evident from this equation that should R_N, G, z, u(z), RH_o, e_z and T_z be given, then the equation is solely a function of T_o and unique physical constants and is therefore solvable for T_o by reiteration.

To follow the daily variations in the atmospheric driving forces hourly mean values of the weather elements are inserted into the equation and an initial T_o value selected. Once the energy budget equation balances, it is assumed that the resulting T_o is the "effective" surface temperature and required values such as R_N, λE, E, C and G may be computed.

In this study the sign convention adopted is negative for fluxes reaching the surface and positive for those fluxes leaving the surface (see Fig. 23).

6.3 Experimental Procedure

The instrumentation used for this study has been discussed in the section on meteorological instrumentation (Chapter 2). Net radiation, soil heat flux, wet- and dry-bulb temperatures and wind speed were recorded continuously. One psychrometer was situated at the zero momentum exchange surface, i.e. a height of $d + z_o = 0{,}76\ h$, to monitor conditions at the canopy surface. The other psychrometers monitored conditions at the reference levels above the canopy surface at heights $z = (d+z_o + 0{,}5)$ m and $z = 2$ m.

The hourly mean values which had been stored on magnetic tape (HP 9845 A system) were used as inputs in the computer program (see Appendix 3) which balanced the surface energy budget equation by a reiterative method. For the results quoted in Section 6.4, the wind data recorded by means of the Wolffe mechanical wind recorder situated at a height of 2 m was used. Before these data were used in the program, they were corrected to their equivalent value at the reference level by means of the logarithmic wind profile equation (Monteith, 1973). Since the experimental site suffered from having too small a fetch the low reference level ($z = (d+z_o+0{,}5)$) was adopted. Once the energy budget equation balanced to within $\pm$ 1 Wm^{-2}, the hourly evaporation was calculated.

6.4 Results and Discussion

In order to test this technique experimentally, the results of a six day period were selected and analysed in detail. Table 15 is an example of the HP 9845 A printout which gives the hourly mean values once the energy budget equation has been balanced by the reiterative method. In Table 15 R_N is the net radiation reaching the canopy surface (Wm^{-2}), G is the soil heat flux (Wm^{-2}), C is the sensible heat flux (Wm^{-2}), Le is the latent heat flux (Wm^{-2}) computed by the reiterative method, Leq is the equilibrium latent heat flux (Wm^{-2}), Lep is the potential latent heat flux (Wm^{-2}) calculated using the Penman type equation, F is the stability factor, T_o is the computed surface temperature (°C), TM is the measured surface temperature (°C), Tair is the air temperature at the reference level (°C), B is the Bowen ratio ($B = \frac{C}{Le}$) and E is the evapotranspiration ($mm\ h^{-1}$).

The agreement between the measured and computed surface temperature may be used to test the validity of the technique and Fig. 24 shows a graphical representation of the hourly mean surface temperature versus the temperature measured at the momentum exchange level over the six days. The straight line illustrates the 1:1 relation. These data fit a linear relationship with a coefficient of determination of 0,92.

The computed and measured surface temperature for the six days were subjected to the students t test for paired observations (Steel et al, 1960). The analysis yielded $t = 0,44$ for 63 df ($\rho < 0,05$), implying no significant difference between the computed and measured surface temperature and an indication of the validity of the technique.

The computed daily evaporation (E_T) was compared to the class A pan evaporation (E_p) and $\frac{E_T}{E_p}$ ratios for the six days were found to be 0,76; 0,97; 0,72; 0,72; 1,05 and 1,03 respectively.

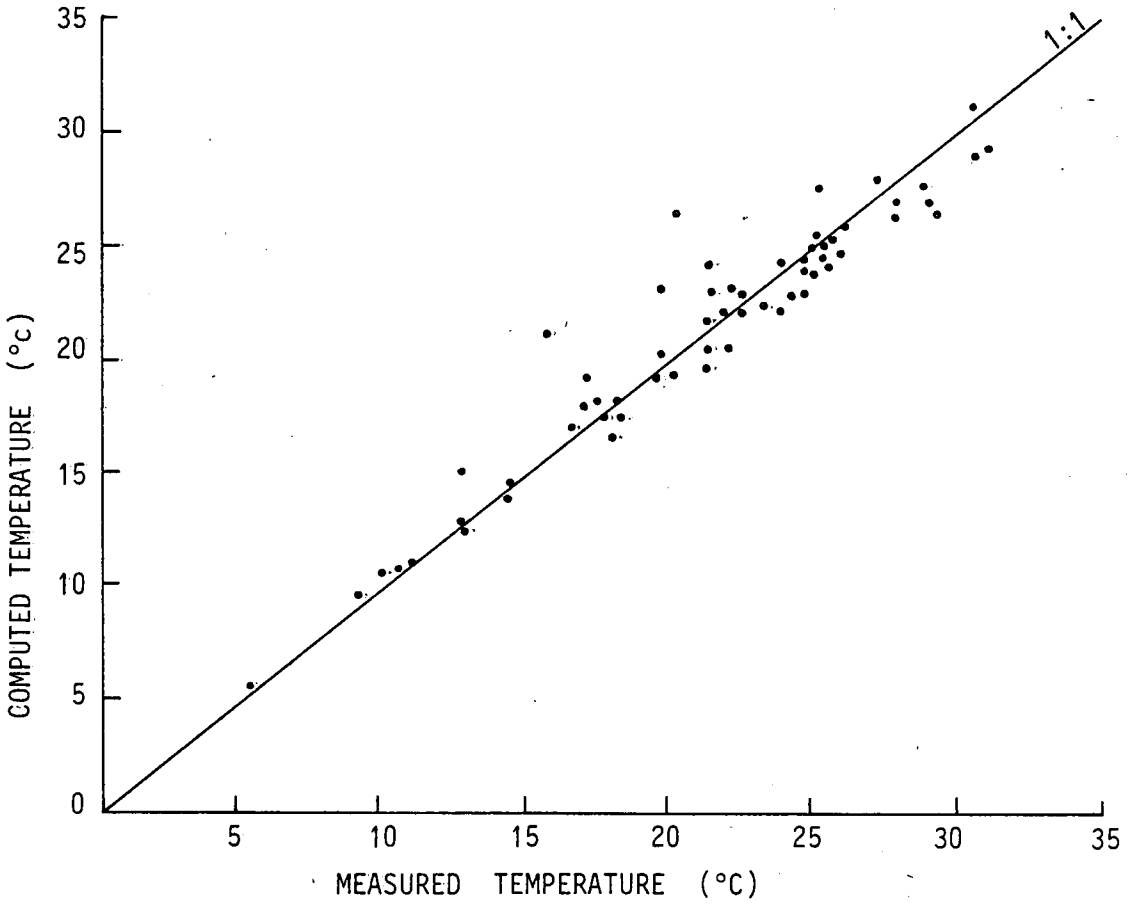

Fig. 24 : Computed hourly mean surface temperatures versus the hourly mean temperature measured at the momentum ex= change level for the six day period.

Table 15 : An example of the HP 9845 computer printout showing the hourly mean values of the various terms used to estimate crop evaporation. See text for explanation of the symbols used.

CROP HEIGHT : 0,49 m

Time	Rn	G	C	Le	Leq	Lep	F	To	TM	Tair	B	E
09h00	-335	012	53	270	193	466	1.12	12.7	13.0	11.9	0.2	0.40
10h00	-587	018	170	398	370	655	1.18	19.4	17.2	16.2	0.4	0.58
11h00	-717	062	239	425	453	687	1.38	23.3	19.7	18.4	0.6	0.62
12h00	-782	018	228	536	537	970	1.20	23.1	21.4	19.7	0.4	0.79
13h00	-782	029	141	613	534	1207	1.09	22.3	22.0	20.6	0.2	0.90
14h00	-713	040	141	531	477	1213	1.07	22.3	22.0	20.7	0.3	0.78
15h00	-587	073	130	383	360	1179	1.04	21.9	21.3	20.5	0.3	0.56
16h00	-433	040	95	299	269	1025	1.03	20.4	19.8	19.3	0.3	0.44
17h00	-251	054	16	288	198	730	0.95	17.9	17.1	17.6	0.1	0.42
18h00	-084	059	34	108	85	460	0.79	15.3	12.9	14.3	0.3	0.16

COMPUTED DAILY EVAPORATION (mm) 5.65

MEASURED A-PAN EVAPORATION (mm) 7.43

E_T/E_p = 0.76

These ratios lie well within the range for wheat quoted by Streutker (1978) and Meyer, Walker & Green (1979), providing further verification of the method. It is interesting, and in agreement with Meyer et al (1979), that for the prevalent stage of crop development, it is possible during times of high atmospheric demand for the crop to transfer more water to the atmosphere than will evaporate from an open pan.

In addition to the latent heat flux (λE), the equilibrium (λE_q) and the potential latent heat flux (λE_p) were computed and compared. The equilibrium latent heat flux, or the latent heat flux from an infinitely large, freely transpiring vegetated surface where the air is saturated, and the potential latent heat flux were computed using the equations

$$\lambda E_e = \frac{H\Delta}{\Delta+\gamma} \quad \ldots\ldots\ldots\ldots\ldots\ldots\ldots \quad (17)$$

and

$$\lambda E_p = \frac{H\Delta + \rho C_p + \delta_e / r_a}{\Delta+\gamma} . \quad \ldots\ldots\ldots\ldots \quad (18)$$

In these equations

$H = R_N - G \quad (Wm^{-2})$,

Δ = the slope of the saturated vapour pressure curve at the temperature of the system (mbar $°C^{-1}$),

r_a = the aerodynamic resistance (s cm^{-1}), and

δ_e = the saturation deficit of the atmosphere at the reference level (mbar).

Fig. 25 shows the temporal variation in the mean hourly values of the computed equilibrium and potential latent heat flux for the six days. The evaporation corresponding to the total heat fluxes represented under the λE, λE_e and λE_p curves are 7,3; 4,9 and 17,9 mm respectively. The mean A-pan evaporation for the six days was 8,2 mm.

An exact evaluation of the new technique such as a comparison with measurements made in a lysimeter is desirable. Unfortunately a lysimeter with the required sensitivity was not available. However, taking into account the close agreement between equilibrium and potential evapotranspiration reported by Meyer et al (1979), and the correspondence between equilibrium evaporation and evaporation calculated using the reiterative method; it seems that the latter offers a reliable estimate of hourly evapotranspiration. Of interest is the high Penman evapotranspiration computed, which at this stage remains unexplained.

It is also felt that, apart from the advantages of the new technique summarised in Section 6.5; the fact that a measurement is actually made within the canopy itself and that all terms of the surface energy budget are involved in the calculation of evapotranspiration, tend to make this a reliable technique for estimating evapotranspiration. Hence, this technique was adopted for the determination of

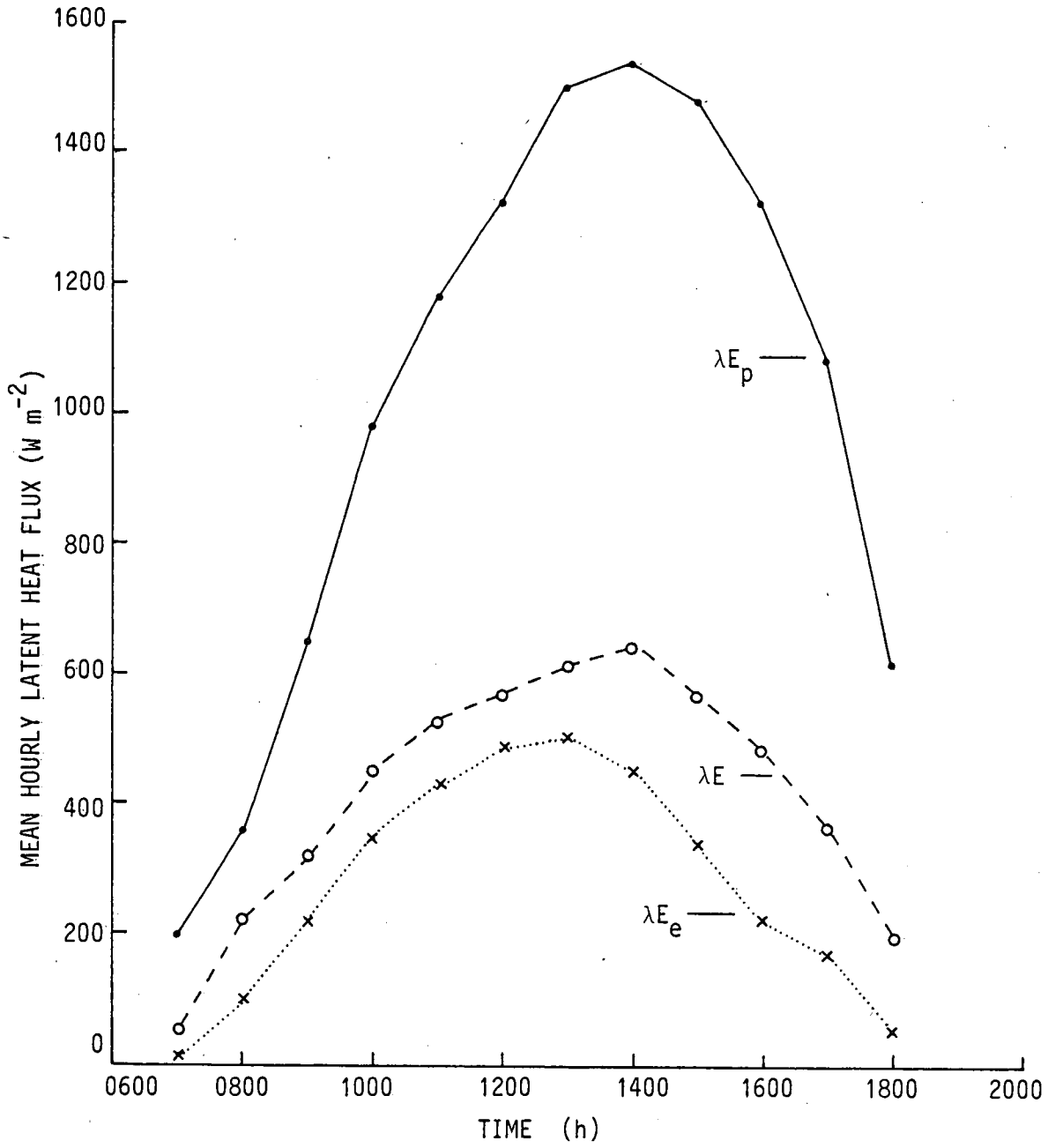

Fig. 25 : Mean hourly values of computed latent heat flux (λE), equilibrium latent heat flux (λE_e) and potential latent heat flux (λE_p) for the six day period.

hydraulic conductivity (see Chapter 11).

6.5 Conclusions

The main advantages of the new reiterative energy budget technique used to estimate evapotranspiration include:

(1) Large gradients are measured and thus less sensitive and cheaper equipment is required. For experimental purposes when small plots are used, the reference level (z) can be relatively low to satisfy the fetch restrictions (Thom, 1975) and yet large gradients of temperature and vapour pressure will be obtained, thus reducing the required precision of the measuring equipment.

(2) The technique provides measurements of crop evaporation of accuracy acceptable for agricultural purposes.

(3) The equipment required is durable, foolproof and can be installed and maintained by unskilled labour.

(4) The aerodynamic exchange coefficients may be calculated using a single anemometer as the surface value is assumed to be zero.

(5) A reasonably small calculator such as the HP 97 can be used for all computations.

(6) The results obtained describe in detail the surface energy budget, and thus the true micro-environment at the canopy surface.

S E C T I O N B

RESULTS AND DISCUSSION

C H A P T E R 7

SOIL PROPERTIES

7.1 Chemical Analysis

The pH was measured in a 1:25 soil:distilled water suspension. The basic cations were determined from an extract of 5 g of soil with 100 ml of 1 N ammonium acetate. The Zn determination was carried out from an extract of 10 g of soil with 100 ml of 0,1 N HCl. The remaining cation contents of the samples were determined by atomic absorption spectrophotometric methods. The phosphorous content of the samples were determined colorimetrically (Fogg & Wilkinson, 1958) in a 0,5 M sodium bicarbonate extract as described by Olsen, Cole, Watanabe & Dean (1954). The results of the chemical analysis are given in Table 16.

Table 16 : Chemical Analysis of the two Soil Types.

Horizon		pH(H_2O)	Exchangeable Plus Water Soluble Cations				Zn (ppm)	P (ppm)	Electric conductivity (ms m^{-1})
			Ca (ppm)	Mg (ppm)	K (ppm)	Na (ppm)			
Skildekrans Series	A1	6,6	1091	353	330	13,8	3,3	1,15	82
	B21	7,7	1923	445	290	5,9	3,7	4,02	164
Bainsvlei Series	A1	5,9	633	173	180	2,5	2,4	17,58	61

7.2 Particle Size Analysis

The particle size distribution of the site and bin soil was determined by means of the hydrometer method as described by Loveday (1974). The results are given in Table 17.

Table 17 : Particle Size Distribution of the Site and Bin Soil.

Class	Skildekrans Series (Site)		Bainsvlei Series (Bin)
	A1 (%)	B21 (%)	A1 (%)
Coarse sand (2 - 0,5 mm)	1,56	0,75	5,70
Medium sand (0,5 - 0,2 mm)	5,86	5,70	16,38
Fine sand (0,2 - 0,05 mm)	55,86	52,79	65,46
Coarse silt (0,05 - 0,02 mm)	5,43	5,76	3,46
Fine silt (0,02 - 0,002 mm)	5,00	4,00	2,00
Clay (< 0,002 mm)	26,29	31,00	10,00

7.3 Soil Moisture Characteristics

The functional relationship between soil moisture content and its energy status is described by the soil-moisture characteristic curve. This curve which is affected by hysteresis, expresses the influence of structure, porosity, pore-size distribution (tortuosity) and adsorption on the state of soil water. This state and how it varies in profile, determines the direction and influences the rate of soil moisture movement and uptake by plants (Hillel, 1971).

Soil moisture characteristic curves were prepared for both soil types used in this study. Duplicate undisturbed soil cores were taken

from the topsoil of each soil type by means of a core sampler. The samples were saturated and equilibrated at different pressures on a pressure plate. The standard pressure plate apparatus and method described by Richards (1954) was used. The dry mass of the samples and the volume of the cylinders were used to calculate the bulk densities. These are given in Table 18.

Table 18 : Bulk Densities of the Site and Bin Soils.

Soil Type	Bulk Density ($kg\ m^{-3}$)
Site soil	1 340
Bin soil	1 580

The results of this experiment are given in Tables 19 and 20. The linear regression analysis of various combinations of water content versus water potential is given. It was found that for both soil types a logarithmic/logarithmic relationship fitted the data best. The regression analyses yielded the following equations for the bin and site soil respectively:

$$\ell n\ \psi_s = -8{,}7559 - 3{,}1367\ \ell n\ \Theta_m \quad \ldots\ldots\ldots\ldots \quad (19)$$

and

$$\ell n\ \psi_s = -9{,}7986 - 4{,}9661\ \ell n\ \Theta_m\ , \quad \ldots\ldots\ldots \quad (20)$$

where

ψ_s = soil moisture potential (bar), and
Θ_m = gravimetric water content (ratio).

The experimental soil moisture characteristics for both the bin and site soils are presented in Fig. 26. A predicted curve (after Bennie, 1979) is presented for the sand for comparative purposes. It is obtained by using the bulk density and (silt(0,05 mm) + clay) % as inputs in a series of multiple linear regression equations. These

equations have been developed for (silt (0,05 mm) + clay) % of less than 20 % and thus could not be used as a comparison for the site soil.

Eqns. 19 and 20 were used to determine the water status of the bin and site soils from the gravimetric samples obtained through the course of the season. The water potential values determined in this way were used when determining the hydraulic conductivity of the wheat crop (see Chapter 11).

Table 19 : Matric potential (ψ_s), gravimetric water content (Θ_m) and linear regression data obtained for the bin soil: Bainsvlei Series.

ψ_s (bar)	Θ_m (ratio)	$\ell n\ \Theta_m$	$\ell n\ \psi_s$
0,10	0,122	-2,10	-2,30
0,33	0,093	-2,38	-1,11
0,66	0,073	-2,62	-0,42
1,00	0,058	-2,85	0,00
15,00	0,026	-3,65	2,71

Linear regression data :

$y = a + bx$

A. $\ell n\ \Theta_m$ (y) vs ψ_s (x)

r^2 = 0,8185
a = -23,6296
b = -9,9438

B. Θ_m (y) vs $\ell n\ \psi_s$ (x)

r^2 = 0,9431
a = 3,4881
b = -49,8932

C. $\ell n\ \Theta_m$ (y) vs $\ell n\ \psi_s$ (x)

r^2 = 0,9929
a = -8,7559
b = -3,1367

Table 20 : Matric potential (ψ_s), gravimetric water content (Θ_m) and linear regression data obtained for the site soil: Skildekrans Series.

ψ_s (bar)	Θ_m (ratio)	$\ell n \Theta_m$	$\ell n \psi_s$
0,10	0,217	-1,53	-2,30
0,33	0,176	-1,74	-1,11
0,66	0,151	-1,89	-0,42
1,00	0,142	-1,95	0,00
15,00	0,080	-2,53	2,71

Linear regression data :

$y = a + bx$

A. $\ell n\ \Theta_m(y)$ vs ψ_s (x)

r^2 = 0,8488
a = -27,4155
b = -15,9925

B. Θ_m (y) vs $\ell n\ \psi_s$ (x)

r^2 = 0,9822
a = 5,3924
b = -36,6607

C. $\ell n\ \Theta_m$ (y) vs $\ell n\ \psi_s$ (x)

r^2 = 0,9979
a = -9,7986
b = -4,9661

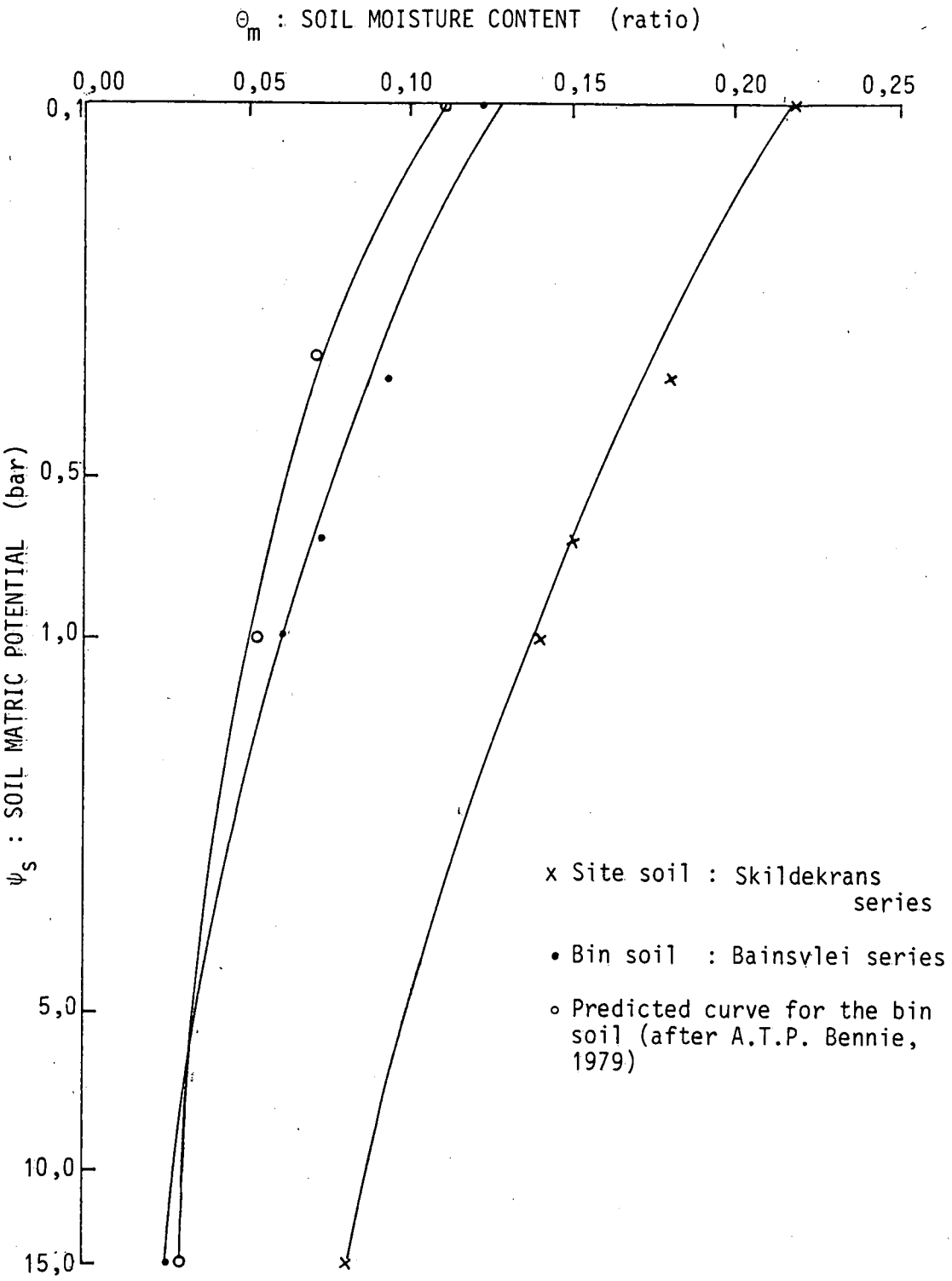

Fig. 26 : Soil moisture characteristic curves for the site and bin soil.

CHAPTER 8

LEAF MORPHOLOGY

8.1 Introduction

Monteith (1973) states that the resistance of stomatal pores depends on the geometry, size and spacing of the pores and on the associated anatomical features. In an attempt to gain information on stomatal characteristics of the Turpin 4 wheat leaf, a series of photographs of both the adaxial and abaxial surface were obtained using scanning electron microscopy. The ISI 100 scanning electron microscope was used for this purpose. From the photographs obtained it was possible to estimate stomatal density.

Stomata are formed before a leaf has completed most of its enlargement and since the number of stomata per leaf does not change significantly during leaf expansion, they are closer together in a young plant than in a mature plant (Sutcliffe, 1979). Thus, in order to obtain representative stomatal density counts, the leaf samples used in this study were collected after flowering when plant development was complete. Each sample consisted of a small leaf segment a few square millimetres in size which was removed from the area adjacent to the leaf midrib. A total of twelve samples were prepared from twelve different flag leaves selected in a random fashion throughout the experimental site.

Preparation of the samples (Hayat, 1978 and Glauert, 1974) involved fixation in a 3 % Gluteraldehyde solution in a phosphate buffer of pH 7. The samples were then dehydrated in an alcohol series (30 - 100 %) and dried according to the critical point drying method using CO_2. To complete the preparation procedure the samples were coated with a 30 nm layer of gold by means of the sputter technique.

8.2 Results and Discussion

The results of the density counts are given in Table 21. Wheat stomatal densities determined by Teare, Peterson & Law (1971) and Sutcliffe (1979) are presented for comparative purposes. Sutcliffe (1979) states that stomatal density can vary according to the stress conditions experienced. Thus, differences in the histories experienced by the crops could explain the difference in the stomatal densities given in Table 21.

Table 21 : Results of the Stomatal Counts carried out by means of the ISI 100 Scanning Electron Microscope. The results quoted by Teare et al (1971) and Sutcliffe (1979) are presented for comparative purposes.

	Stomatal Count (no/mm²)		Abaxial frequency / Adaxial frequency (ratio)
	Adaxial surface	Abaxial surface	
Present study	39 ± 3,5	29 ± 4,17	0,74 ± 0,14
Sutcliffe (1979)	33	14	0,42
Teare et al (1971)	-	-	0,75

Figures 27, 28 and 29 show photographs of the adaxial surface, abaxial surface and a close up of a single stomate respectively. It is interesting to note that trigomes are present on the adaxial surface only.

8.3 Conclusion

The number of stomates on the abaxial and adaxial surface differ in the ratio abaxial to adaxial of 0,74 ± 0,14. Hence, autoporometer readings were recorded on both surfaces of the leaf during the 1979 season. This was an attempt to improve on the results obtained during the 1978 season when only adaxial surface diffusive resistance measurements were made.

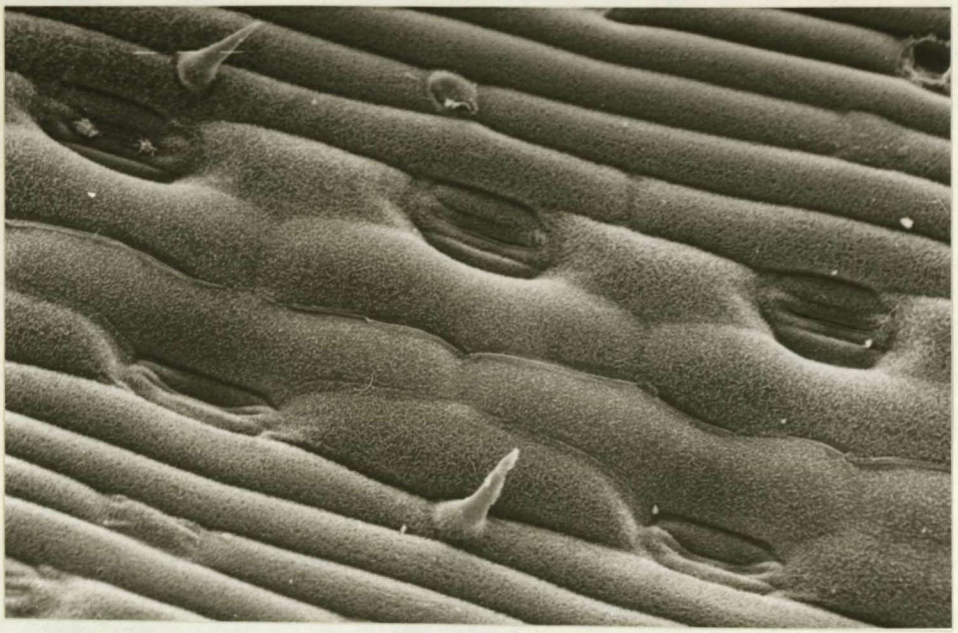

Fig. 27 : Adaxial surface stomates of the Turpin 4 wheat leaf (300 x).

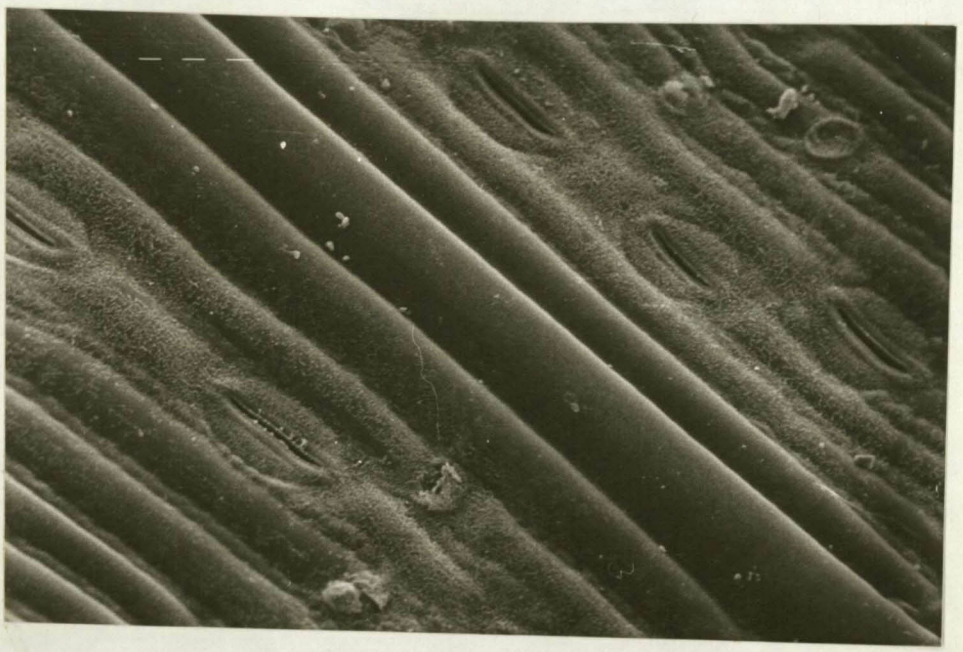

Fig. 28 : Abaxial surface stomates of the Turpin 4 wheat leaf (310 x).

Fig. 29 : Partially open stomate of Turpin 4 wheat - abaxial surface (2100 x).

CHAPTER 9

DIURNAL VARIATION IN LEAF WATER POTENTIAL AND LEAF DIFFUSIVE RESISTANCE

9.1 Leaf Water Potential (ψ_ℓ)

In this study the Wescor psychrometer, Scholander pressure chamber and J14 press were used to follow hourly variations in leaf water potential. Results of the Scholander pressure chamber and J14 press are discussed in Chapter 4. The field results of the Wescor psychrometer are discussed in this section.

Fig. 30 depicts the diurnal variation in leaf water potential for three days characterised by different soil and climatic conditions. These curves tend to follow the normal expected diurnal variation in atmospheric demand but flatten about midday. Figs. 13 and 14 obtained with the Scholander pressure chamber and J14 press reflect the same tendency. It is evident that as evening approached, atmospheric demand decreased and the plant water potential recovered tending towards a steady night time value. This night time value of leaf water potential reflects the soil water status as the whole soil-plant-atmosphere continuum tends towards a state of moisture equilibrium (cf. Rawlins, Gardner & Dalton, 1968) dictated by the soil conditions. It is interesting to note that in most cases the steady night value was reached relatively late at approximately 22h00. For each experimental run depicted in Fig. 30, the second leaf water potential reading is more positive than the initial reading. This peculiarity was found to exist in 90 % of all experimental runs undertaken, irrespective of the time of commencement of the measurements or the prevailing weather conditions. No explanation can be offered for this behaviour.

Fig. 31 depicts the variation in leaf water potential, psychrometer chamber temperature and microclimate data obtained during a typical experimental run. The daily variation in plant water status is closely

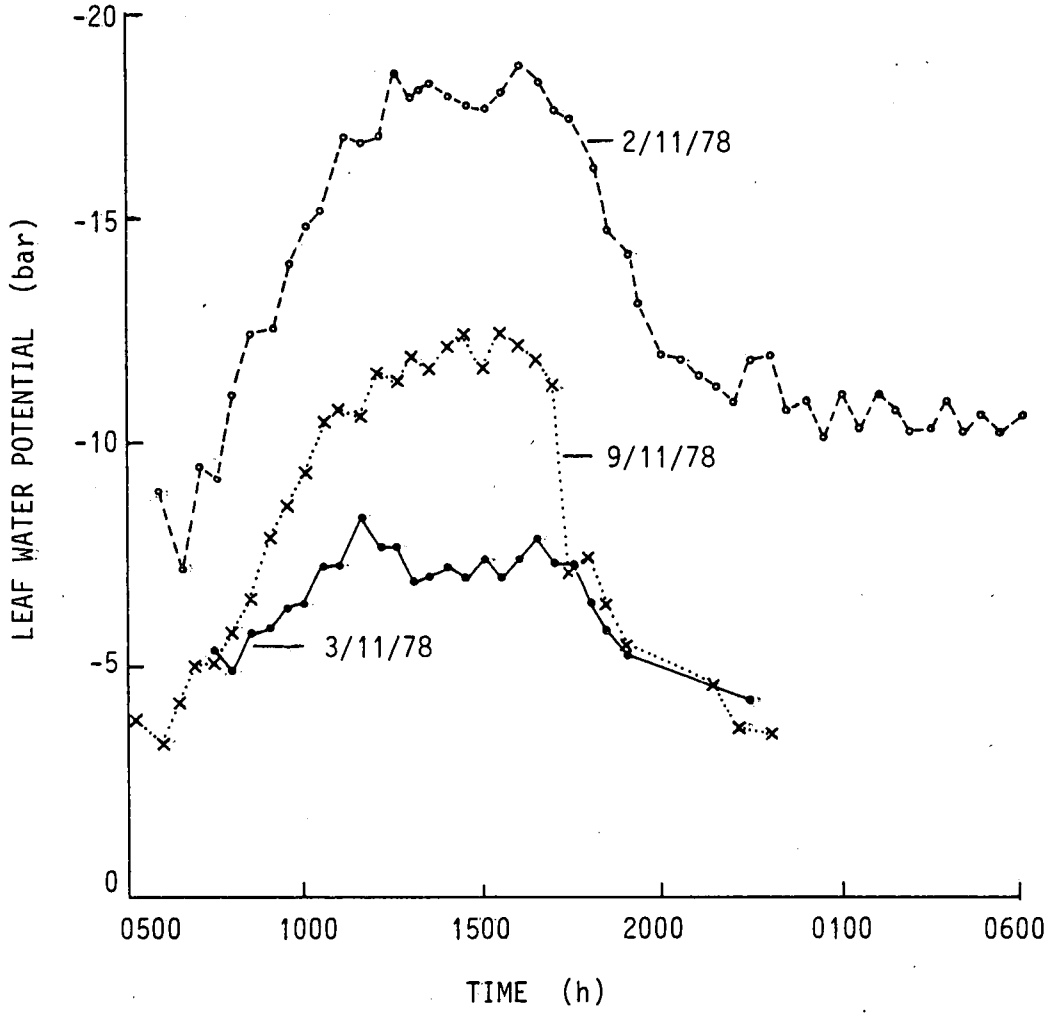

Fig. 30 : Diurnal variation in leaf water potential for three experimental runs on days with different soil and climatic conditions. Measurements were obtained by means of the Wescor psychrometer.

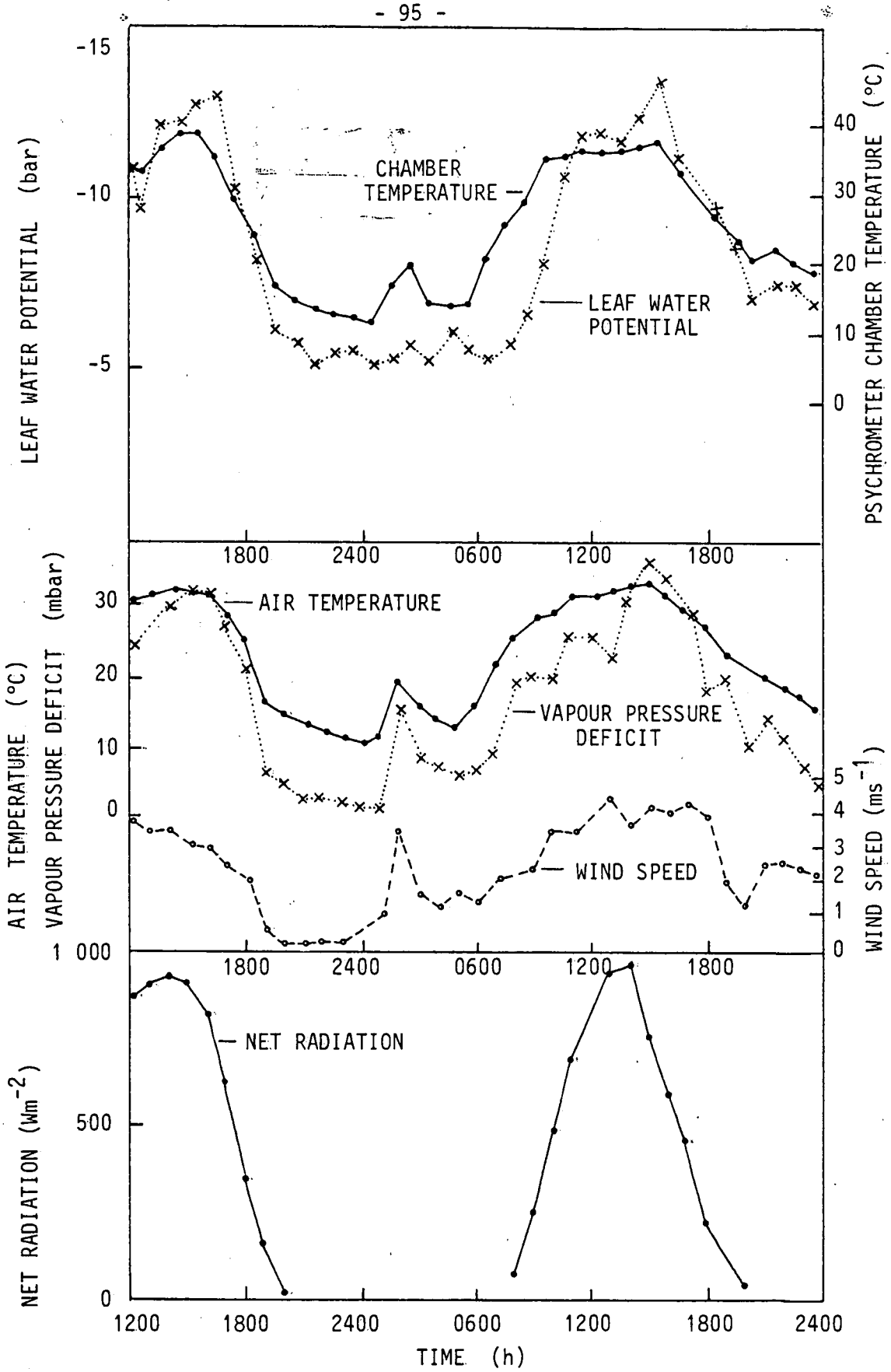

Fig. 31 : Hourly variation in leaf water potential, psychrometer chamber temperature and microclimate data obtained during a typical experimental run (16/17 November 1979).

related to radiative load (Klepper, 1968) and thus transpiration rate (Denmead & Shaw, 1962) as well as soil water potential (Thomas & Weigand, 1970) and microclimate conditions (Reicosky, Campbell & Doty, 1975). The curves presented in Fig. 31 support this statement.

Reicosky et al (1975) found that leaf water potential of well watered plants responded to energy changes within 5 to 15 minutes. The relation between leaf water potential and wind, vapour pressure deficit and temperature is evident in the cases here reported (Fig. 31) and suggests that there is little lag between changed environmental conditions and the change in leaf water potential. Waring et al (1967) found that microclimate conditions can cause the plant water status to fluctuate by as much as 5 bar per hour.

Water potential did not follow chamber temperature precisely (Fig. 31) and may be taken as an indication that the actual leaf water potential was being monitored and not the effect of temperature upon the per= formance of the instrument (see also Rawlins & Dalton, 1967).

9.2 Leaf Diffusive Resistance (r_s)

The change in leaf diffusive resistance in response to the range of environmental factors may be described by the generalised expression

$$r_s = f(Q, \psi_w, e, T, u, N, CO_2 \ldots) \quad \ldots\ldots \quad (21)$$

where

Q, ψ_w, etc. represent specific functions relating r_s to light flux density, leaf water potential, humidity, temperature, wind speed, mineral nutrition, carbon dioxide concentration, etc. (Burrows & Milthorpe, 1976). These climatic elements are highly interactive under field conditions and it is virtually impossible to analyse the individual effect of each factor on the diurnal fluctuation in leaf diffusive resistance.

However, from the present field study it was apparent that stomatal opening began soon after dawn as the light conditions and radiant flux density increased. This is illustrated in Fig. 32 where total, adaxial surface and abaxial surface resistance is plotted for a single day - 11 October 1979. Stomatal opening occurred at 08h00 and closed at 18h00 when the net radiation flux density was 91 and 20 Wm^{-2} respectively. It is interesting to note that in most cases the first observation where stomates could be considered fully open yielded the lowest resistance value obtained for the day. Resistance appeared to increase gradually from this point until rapid stomatal closure took place in the late afternoon. The time of day at which stomatal closure occurred varied and is discussed below.

The abaxial surface with its significantly fewer stomates, experiences highly variable resistance values and is generally more than double the value of the adaxial surface resistance. It is seldom that these two resistances approach equality. The total resistance and its trends are accurately reflected by the adaxial surface resistance and it is suggested that the measurement of this adaxial surface resistance might be adequate to reflect stomatal diffusion trends in wheat field data.

Adaxial surface diffusive resistance for one day typified by wet soil conditions (Soil ψ_w = -0,2 bar) and another by dry soil conditions (Soil ψ_w = -7,0 bar) are plotted in Fig. 33. The points through which these stomatal resistance curves pass are the mean values of several measurements made each hour. The scatter about these mean values is illustrated for the case of the wet day by plotting the individual diffusive resistance readings obtained. The between leaf variation and response of each leaf to the prevailing plant microclimate is emphasised by this scatter. These deviations stress the need to find the mean of as large a number of readings as is practically possible when studying the response of the crop as a whole. Excessively high or low readings recorded in a given time period were ignored when calculating the mean values through which the curves were drawn.

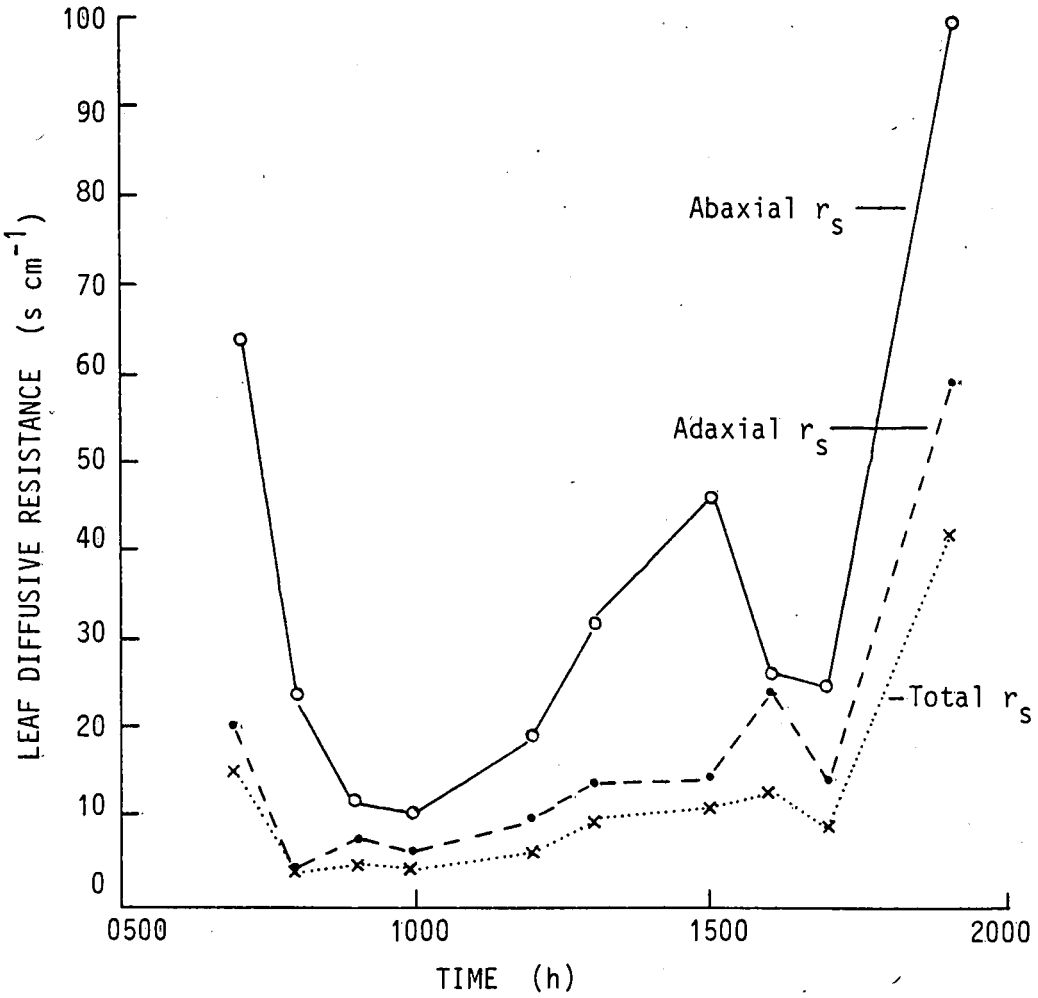

Fig. 32 : Diurnal variation in total, adaxial surface and abaxial surface diffusive resistance on the 11/10/79 (soil moisture status ψ_s = -7,36 bar).

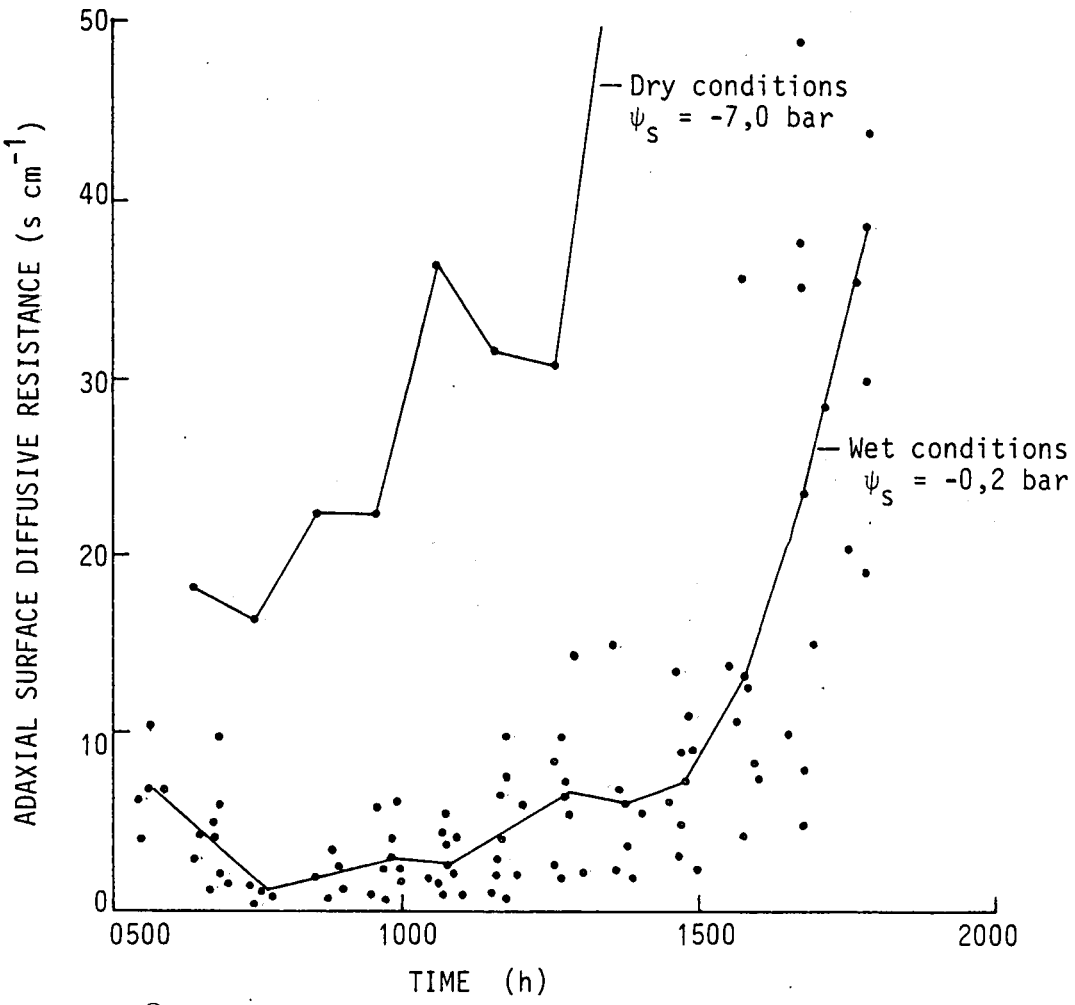

Fig. 33 : Individual and hourly mean values of adaxial surface diffusive resistance obtained for one day typified by wet soil conditions and another by dry soil conditions.

Adaxial diffusive resistance values on the dry day were approximately 20 s cm^{-1} higher than on the wet day. Although the stomates could be considered semi-closed throughout the course of the dry day, a rapid increase in diffusive resistance did occur at 13h00. Closure occurred at 16h00 on the wet day. These times differ markedly from the case depicted in Fig. 32 where closure occurred at 18h00. From these results it appears that the cummulative combined effect of soil water status, leaf water potential, light conditions and incoming radiant flux energy will determine the time of day at which stomatal closure occurs under field conditions.

CHAPTER 10

THE LEAF WATER POTENTIAL - LEAF DIFFUSIVE RESISTANCE RELATIONSHIP

The relationship between leaf diffusive resistance and leaf water potential was examined with a view to obtaining a mathematical ex= pression reliable enough for incorporation in a simulation of crop behaviour given weather input data. Such a model could be applied to irrigation scheduling.

This relationship has been studied by many investigators in recent years. It is generally accepted that leaf water potential together with certain other factors controls stomatal closure. This process is initiated when plant water deficits develop and the leaves lose turgor. Stomatal pores act as the exchange pathway for CO_2 and H_2O between the atmosphere and the plant growth cells. Thus at stomatal closure, transpiration and photosynthesis are detrimentally affected. This results in a modification of the growth process and a general lowering in yield. The relationship between diffusive resistance and leaf water potential appears to be complex, with particularly antecedent leaf moisture status conditions influencing the relation= ship on a given day. Such dependence has been reported in soyabeans by Hammel & De Jager (1980). For modelling purposes, however, such as for example determining the daily water budget, a fairly rough approximation of the situation is adequate. This was the main objective of the work here described.

During the 1978 season a preliminary investigation was carried out. The Wescor psychrometer was used to measure leaf water potential and only adaxial diffusive resistance measurements were obtained by means of the autoporometer. The crop in the bins was used as the soil conditions could be easily monitored. By withholding irrigation and allowing the bins to dry through evapotranspiration, stress conditions were induced in the crop. Once visual signs of moisture

stress were obvious, a series of dry day observations were undertaken. On completion of these measurements the bins and surrounds were ir= rigated. A series of measurements under moist conditions were then made one day later after excess water had drained from the bins.

The hourly mean adaxial diffusive resistance versus hourly mean leaf water potential for the two days on which measurements were made in 1978 are plotted in Fig. 34. Despite the scatter in points it is apparent that when the leaf water potential dropped to between -12 and -14 bar, stomatal closure commenced with a concommittant reduction in transpiration rate.

The rapid increase in stomatal resistance as leaf water potential decreases below a certain critical value has been reported for snap beans (Kanemasu & Tanner, 1969), maize and sorghum (Beadle, Stevenson, Neumann, Thurtell & King, 1973), spring wheat (Frank, Power & Willis, 1973), Italian ryegrass (Hansen, 1974a), grain sorghum (McCree, 1974), potatoes (Rutherford & De Jager, 1975), wheat (Denmead & Miller, 1976) and soyabeans (Hammel et al, 1980). Hansen (1974a) states that the critical potential is species de= pendent. Frank et al (1973) found that the critical potential varied with both leaf position and age of the wheat crop but that temperature had no effect. The latter study was undertaken in growth chambers and care must be taken when extrapolating these results to field conditions. Kanemasu et al (1969) observed a difference in the relationship obtained for field grown plants and chamber grown plants. The difference may result from exposure to different water regime histories. The effect of temperature under field conditions still needs to be investigated.

The leaf water potential - leaf diffusive resistance relationship was again investigated during the 1979 season. Leaf water potential was measured by means of the Scholander pressure chamber (see Section 3.8 for method). All measurements were obtained on the experimental site during the course of the growing season. More

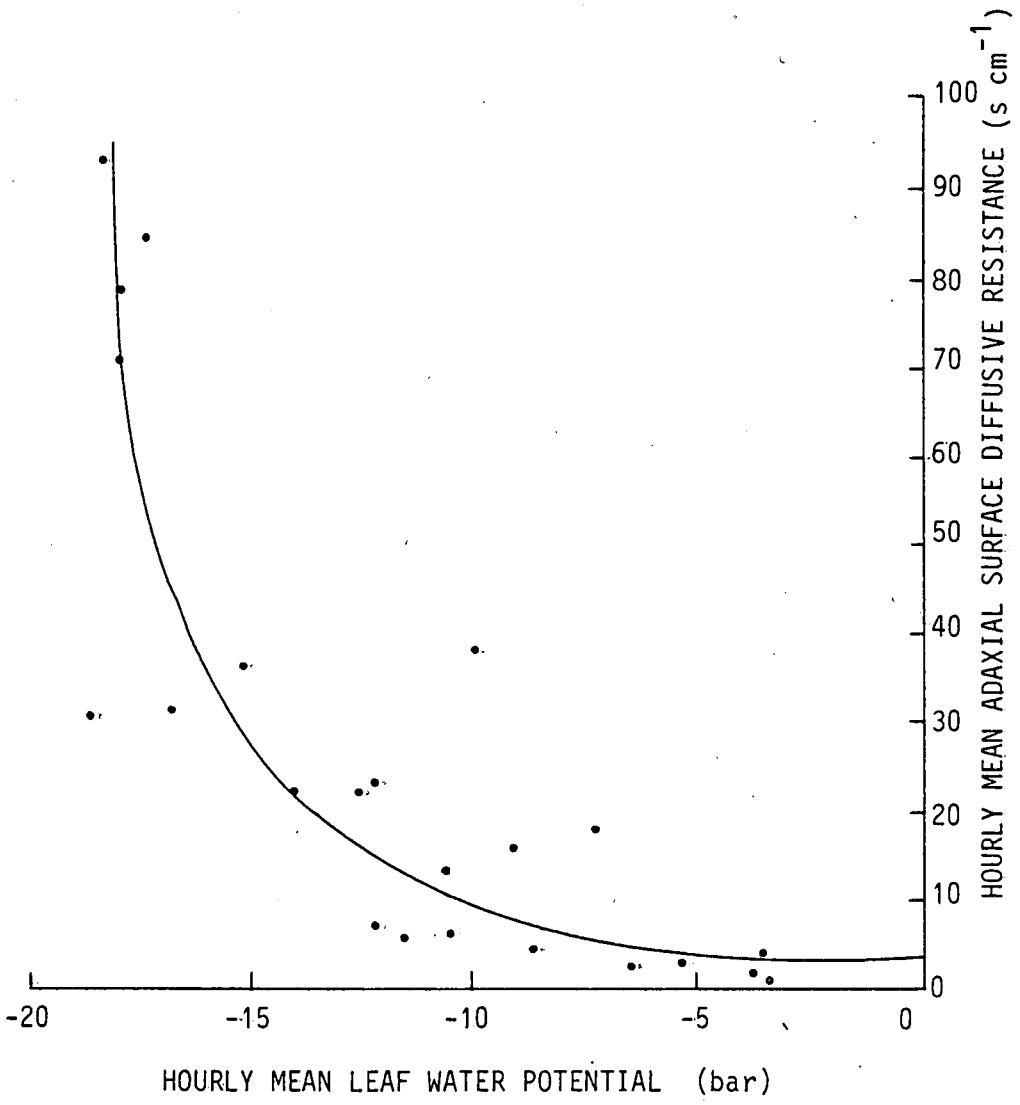

Fig. 34 : The relationship between hourly mean leaf water potential and hourly mean adaxial surface diffusive resistance (ψ_ℓ was measured by means of the Wescor psychrometer).

than 1 000 individual observations of both leaf water potential and leaf stomatal resistance were obtained. The readings were not made on the same leaf therefore some form of graphing necessary to obtain representative values was needed. The hourly mean values of leaf water potential were plotted against the hourly mean total diffusive resistance. The average resistance value over 2 bar intervals was used to enable the manipulation of the large number of data points. Due to the paucity of observations in the high potential range as compared to the low potential range, the average point of the 0 to -16 bar interval is plotted. This averaging of data points permits the achievement of a reasonably good fit but could mark a drift in the critical leaf water potential (Hammel et al, 1980).

For modelling purposes it is necessary to describe this relationship mathematically and an equation for this purpose has been proposed by Hammel et al (1980). It has the form

$$r_s = r_{min}\left[1 + e^{-\alpha(\psi_c - \psi_w)}\right] \quad \ldots\ldots\ldots \quad (22)$$

where

r_{min} = the minimum stomatal resistance under non-stress conditions ($s\ cm^{-1}$),
ψ_w = the leaf water potential (bar),
ψ_c = the critical leaf water potential (bar), and
α = a dimensionless constant which governs the rapidity with which r_s approaches infinity.

The expression is based upon the definition of ψ_c which was defined as that value at which stomatal resistance is twice the normal minimum value observed for non-stressed plants.

Applying this approach to the data of the present study yielded the relationship:

$$r_s = 3\left[1 + e^{0,15(-20-\psi_w)}\right], \quad r^2 = 0,81. \quad \ldots \quad (23)$$

This describes the curvilinear curve depicted in Fig. 35 and also suggests that leaf water potential explains 80 % of the variation in diffusive resistance. The ψ_c value of -20 bar obtained using Eqn. 23 agrees well with the value of -19 bar obtained for wheat by Millar & Denmead (1976). These authors also found that the top leaf, which is the main supplier of photosynthate for the ear, had the lowest critical water potential value. This implies that stomatal closure occurs first in the lower leaves.

The method of grouping data within 2 bar intervals might be open to criticism. It must, however, be stressed that the objective here has been the determination of an overall mathematical description of stomatal behaviour for the crop as a whole. Eqn. 23 does appear to reflect the general crop situation albeit with a wide scatter. When mathematically simulating photosynthetic activity and water consumption it is just this total crop action which is required.

Minor empirical improvements on the leaf water potential - leaf diffusive resistance relationship are possible since the points in Fig. 35 could be described by two straight lines as shown. The empirical mathematical expression thereof takes the form:

$$r_s = r_{min} + \frac{\alpha(\psi_w - \psi_c)}{1 + e^{-\beta(\psi_w - \psi_c)}} \quad \ldots\ldots\ldots \quad (24)$$

This relation in effect describes an on-off process. r_s takes on the defined r_{min} value until water potential reaches its critical value. After this point leaf water potential and r_s are linearly related, α being the slope of the linear relation. The rate constant β simply determines the rapidity with which proportionate increase in r_s becomes effective. The present data is fitted by the relationship:

$$r_s = 3 - \frac{0{,}65(\psi_w+12)}{1 + e^{5(\psi_w+12)}}, \quad r^2 = 0{,}90 \quad \ldots \quad (25)$$

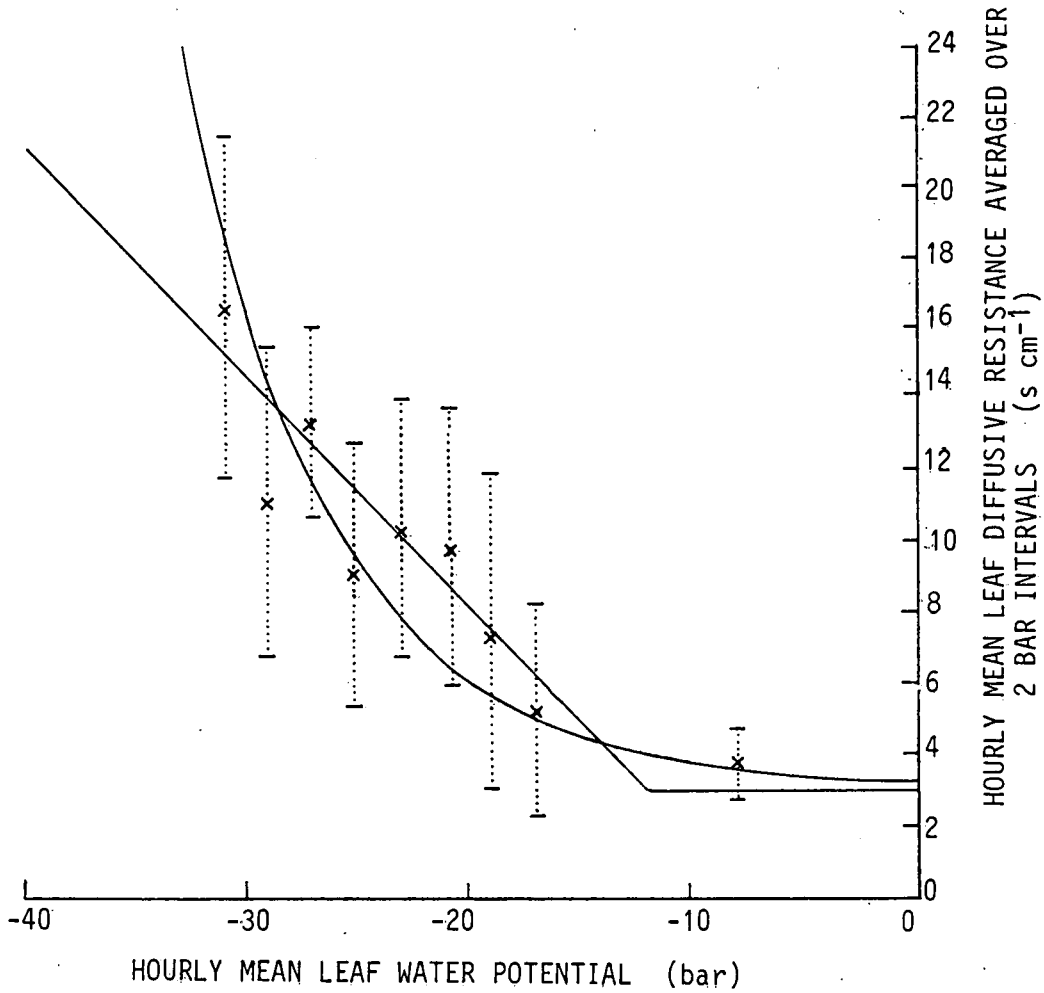

Fig. 35 : The relationship between hourly mean leaf water potential and hourly mean leaf diffusive resistance averaged over 2 bar intervals (ψ_ℓ measured by means of the Scholander Pressure Chamber).

This relationship is depicted graphically by the two straight lines in Fig. 35.

The value of ψ_c used in the two expressions differ widely, but it must be stressed that they by definition represent two entirely dif= ferent concepts. Because Eqn. 23 reflects a more rapid initial increase in r_s with increased ψ_ℓ than Eqn. 25, and thus would indi= cate stress conditions earlier than Eqn. 25, it is suggested that Eqn. 25 might be preferable for irrigation scheduling. In the range of leaf water potentials -12 bar to -24 bar it seems to fit the data here reported more accurately than the curvilinear expres= sion. Emphasis must, however, be placed on the fact that both equations are empirical approaches to the problem at hand.

This relationship was obtained for all the data collected during the 1979 season without considering stress histories or any other factors which may be involved. Leaf water potential varied between -0,5 and -38 bar and stress periods greater than 14 days were experienced. McCree (1974), Thomas, Brown & Jordan (1976) and Denmead et al (1976) found that stomates of plants pre-conditioned to stress remained open at water potential lower than those required to close the stomates of well-watered plants. This conditioning effect was found to be caused only as a result of stress induced by soil moisture and not when atmospheric conditions induced stress (McCree, 1974). The present analysis could possibly be improved upon if antecedent soil moisture were included in the investigation. Such a model would adjust ψ_c according to the intensity and duration of stress conditions experienced previously. The present analysis with its high coef= ficients of determination, however, should permit reliable irrigation scheduling and crop growth modelling.

CHAPTER 11

HYDRAULIC CONDUCTIVITY OF THE WHEAT CROP

11.1 Introduction

The continuous movement of water from the roots to the leaves of a plant is essential for its survival. In order to maintain a balance between transpiration and absorption the water column in the conducting system must be continuous. As atmospheric demand increases the transpiration will increase and a decrease in water potential takes place in the xylem sap. Water now flows from the high potential areas of the soil and roots to the leaves which are low potential areas. Under excessive transpiration water becomes limiting and the flow may not be able to meet the evaporative demand. The plant endeavours to overcome this strain by closing stomates, thus reducing transpiration. The plant is now under stress which is detrimental to the plant and lowers its yield.

During recent years an Ohms law analogy between the flow of electricity through a conductor and the flow of water through the soil-plant-atmosphere continuum has been used to explain the water transfer process (De Jager & Kaiser, 1977; Hansen, 1974a; Hansen, 1974b and Lawlor & Lake, 1976). This analogy requires water to move along gradients of decreasing water potential. One complicating factor in the biological system is the change in state of water from liquid to vapour. This takes place at evaporating surfaces such as the leaf and soil surface. For this reason water movement through the soil-plant-atmosphere continuum is generally treated stage by stage. In soils and plants the movement of water is in the liquid phase. From the evaporating surfaces to the bulk air, water transfer is in the form of vapour diffusion. The driving forces and resistances to flow in the liquid and vapour phases are quite different.

Vapour diffusion can be expressed by Ficks Law, which in its integrated form is:

$$E = -\left(\frac{\rho_{vs} - \rho_{va}}{r_v}\right) \quad \ldots\ldots\ldots\ldots\ldots \quad (26)$$

where

E = the water vapour flux density (kg m^{-2} s^{-1}),
ρ_{vs} = the vapour density at the evaporating surface (kg m^{-3}),
ρ_{va} = the vapour density of the air (kg m^{-3}), and
r_v = the resistance to vapour diffusion (s m^{-1}).

Here the driving force for evaporation is the difference between the vapour density at the evaporating surface and that of the surrounding air. The vapour diffusion resistance depends upon the structure of the exchange surface and the air flow (Campbell, 1977).

The movement of liquid phase water can be expressed by a modified form of Darcy's Law which describes one dimensional liquid flux. This can be written in equation form as

$$E = -\phi \frac{d\psi}{dz} \quad \ldots\ldots\ldots\ldots\ldots\ldots \quad (27)$$

where

E = the water flux density (kg m^{-2} s^{-1}),
ϕ = the hydraulic conductivity (kg^2 m^{-1} s^{-1} J^{-1}), and
ψ = the water potential (J kg^{-1}).

(Campbell, 1977)

The driving force for water movement in the liquid phase is the gradient of water potential $(\frac{d\psi}{dz})$.

It is obvious from the above discussion that liquid flow is directly proportional to the gradient in water potential while vapour flow is proportional to the vapour density gradient. In the soil-plant-atmosphere continuum the interface where the liquid and vapour phase meet is mainly in the leaf. It is possible to determine the water potential at an evaporating surface from the relative humidity of the air in equilibrium with the liquid phase. This can be done by means of the equation derived from the first Law of thermodynamics

for an adiabatic system. The equation is:

$$\psi_w = \frac{RT\ \ell n(e/e_o)}{M} \quad \ldots\ldots\ldots\ldots\ldots\ldots \quad (28)$$

where

ψ_w = the water potential (J kg^{-1}),
R = the universal gas constant (J K^{-1} $mole^{-1}$),
T = the temperature of the system (K),
e = the vapour pressure of the air in equilibrium with the liquid (Pa),
e_o = the saturation vapour pressure at the reference state (Pa), and
M = the molecular weight of water (kg $mole^{-1}$).

Care must be taken not to succumb to the pitfall of calculating an "atmospheric water potential" using atmospheric relative humidity.

11.2 Hydraulic Conductivity

11.2.1 Objective

The objective of this study has been

(1) to evaluate the hydraulic conductivity of a complete cover of wheat crop, and

(2) to establish its relationship to leaf water status, soil water status and atmospheric conditions.

11.2.2 Method

In order to achieve the objective the following assumptions were made:

(1) The crop approximates a three-dimensional conduit with water flowing in the bottom horizontal plane surface (roots) and evaporating from the top horizontal plane surface (leaves).

(2) The bottom surface of concern is situated 0,2 m below the soil surface. This is the level at which the roots were predominantly concentrated. It shall hence forward be referred to as the effective rooting depth.

(3) The length of the conduit is taken to be equal to the distance between the momentum exchange surface and the effective rooting depth.

(4) There is no lateral loss of vapour.

(5) A continuous mass flow of water exists from the soil through the roots, stems, leaves and out into the atmosphere, i.e. the liquid flow rate through the plant equals the rate of evapotranspiration at any given time.

(6) The crop is considered to be an inert conduit. The various interfaces between soil and root and leaf and air are not treated separately and all leaves effectively operate at the top plane surface.

(7) Soil evaporation is considered negligible for a crop with full canopy cover.

(8) The resistance to flow from soil to root is negligible.

Hence, for a complete vegetative surface, the mass flow equation (Eqn. 27) can be expressed in integrated form as

$$E = -0,28\phi \frac{(\psi_\ell - \psi_s)}{(z_\ell - z_s)} \quad \ldots\ldots\ldots\ldots \quad (29)$$

where, for the units used in this study,

E = the crop evaporation rate (mm h^{-1}),
ϕ = the hydraulic conductivity (ns),
ψ_ℓ = the leaf water potential (bar),
ψ_s = the soil water potential (bar),

z_ℓ = the height of the momentum exchange surface (m), and
z_s = the height at which ψ_s is measured (m).

The constant 0,28 is used to normalise the system of units adopted in this study. Care must be taken to express z_s as a negative value as ψ_s is measured below the soil surface.

ϕ was evaluated from Eqn. 29 under the numerous sets of soil and atmospheric demand conditions occurring in the field on the days 11/10/79; 15/10/79; 22/10/79; 29/10/79; 1/11/79 and 5/11/79. Water flux density measurements were obtained from the micrometeorologically based reiterative estimate of crop evaporation described in Chapter 6. Water flux density was set equal to evapotranspiration rate. Leaf water potential was determined by means of the Scholander pressure chamber or J14 press observations converted in accordance with Fig. 17. The measuring techniques have been described in Chapters 3 and 4. Soil water potential was determined at a depth of 0,2 m using the gravimetric technique and soil moisture characteristic curves as described in Section 7.3. From these measurements ϕ could be calculated for 62 sets of different conditions within the soil-plant-atmosphere continuum.

11.2.3 Results and discussion

The observations covered a full range of climatic conditions as indicated in Table 22.

In Fig. 36 the relation between driving force, defined as $\frac{d\psi}{dz}$, and flux density is shown. In the electrical case the relation between potential difference and current is linear, the slope of the curve being equal to resistance. Although there is a large scatter in points in Fig. 36 it appears that an approximately constant driving force ($\frac{d\psi}{dz}$) equal to roughly 33 bar m^{-1} exists during the central part of the day. Under conditions of zero transpiration rate, as is

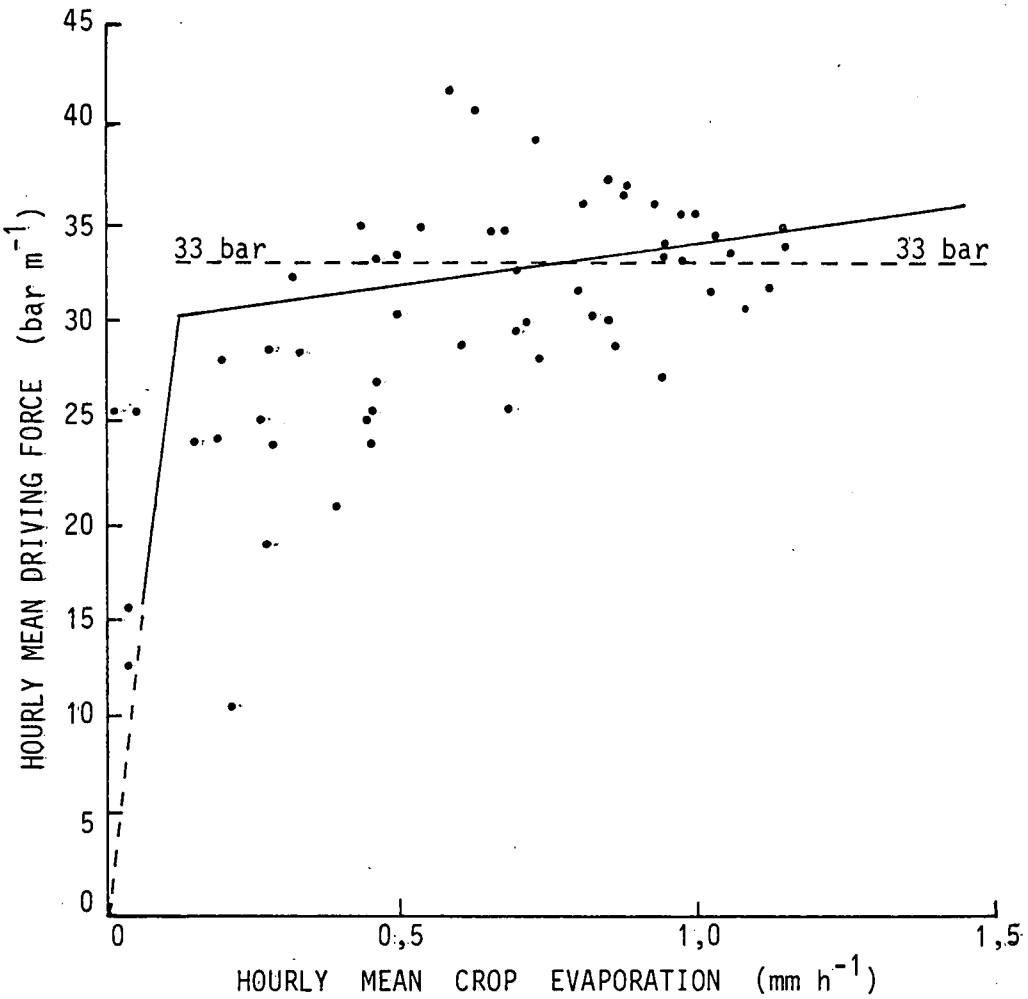

Fig. 36 : The relationship between water flux driving force $\frac{d\psi}{dz}$ (potential difference) and crop evaporation rate (current).

Table 22 : The soil moisture status (ψ_s) and open pan evaporation (E_o) conditions prevailing on the experimental days during which data collection for the determination of ϕ took place.

Date	ψ_s (bar)	E_o (mm)
11/10/79	- 7,36	9,6
15/10/79	-16,4	7,1
22/10/79	- 0,27	7,0
29/10/79	- 2,80	12,4
1/11/79	- 2,16	10,5
5/11/79	- 2,08	13,1

often the case at night, soil and plant water potential tend toward an equilibrium state. For this reason it is possible to extrapolate the curve in Fig. 36 to the origin. Bearing in mind that these results are influenced by inaccuracy of the reiterative method used to estimate water flux density, and the fact that soil water potential from one depth only was used when determining driving force; the scatter in Fig. 36 is not too severe.

The above hypothesis implies that hydraulic conductivity for early morning or late afternoon when evaporative demand is low, will increase with increasing crop evaporation rate. The relationship between hydraulic conductivity of the wheat crop and latent heat flux is shown in Fig. 37. A directly linear relationship is found to exist. This result implies that hydraulic conductivity is not a constant but varies with atmospheric demand and hence the weather. A linear equation $\phi = 0{,}0102 + 1{,}43 \times 10^{-4} (\lambda E)$ was found to give the best fit. The coefficient of determination is 0,91. The present curve does not pass through the origin and if this parameter ϕ is included in simulation models it is suggested that the curve be forced through the origin to give greater reliability in the region of low atmospheric demand. Considering the uncertainties in the input data mentioned above, the statistics reflect a remarkably constant

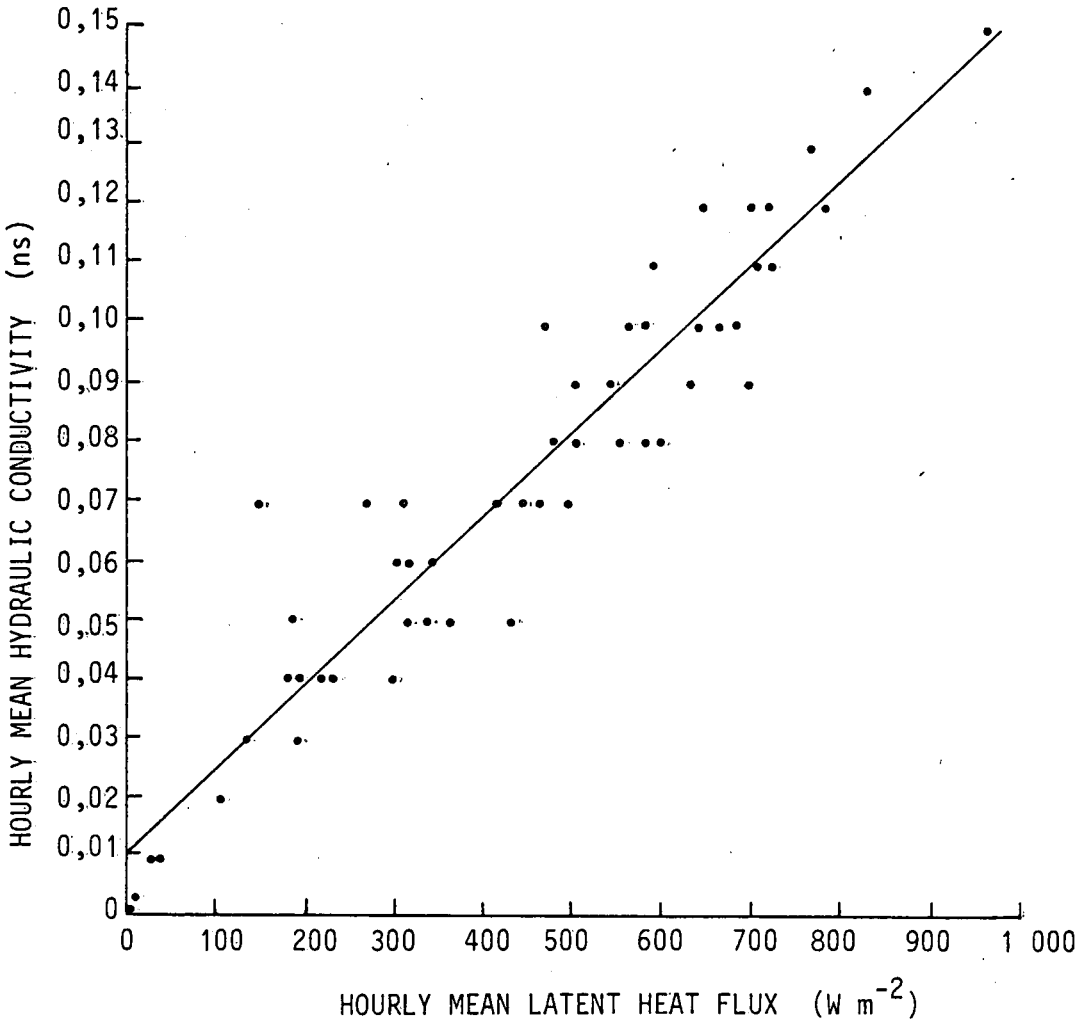

Fig. 37 : Hydraulic conductivity of the wheat crop as a function of crop evaporation.

value for $1/(\frac{d\psi}{dz})$. The inverse of the slope of the straight line in Fig. 37 is $\frac{d\psi}{dz}$ and is equivalent to 36,5 bar m^{-1}. This is $\pm$ 10 % higher than the 33 bar m^{-1} reflected in Fig. 36 because the inter= cept 0,0102 has not been taken into account.

From Fig. 37 it is apparent that the hydraulic conductivity of the wheat crop will increase as the water flux density increases. This implies that the ease with which water flows through the crop improves as the actual water flux increases. Results obtained by other authors (Stoker & Weatherly, 1971; Hansen, 1974a; Hansen, 1974b and Lawlor et al, 1976) on plant resistances confirm this result. These authors found that plant resistance diminishes as the flux increases. The assumption of a negligible resistance to water flow from soil to root is justified by the results quoted by Newman (1969) and Lawlor (1972), who claim that root resistance is generally small compared to plant resistance.

De Jager et al (1977) stated that hydraulic conductivity is analogous to electrical conductivity and that it determines the rapidity with which stressed conditions are induced. Values of between 0,2 and 0,8 ns (De Jager et al, 1977 and Neumann, 1972) were considered appropriate for the maize crop. The results of the present study indicate that the hydraulic conductivity of a crop does not appear to be constant. Evidently some feedback mechanism operates tending to improve conduc= tivity as the evaporative demand and rate increase. From Eqn. 27, hydraulic conductivity can be expressed as

$$\phi = (\frac{dz}{d\psi})\, E \,. \qquad \ldots\ldots\ldots\ldots\ldots\ldots\ldots \qquad (30)$$

This equation, and the constant slope to Fig. 37 suggests that the feedback control requires $(\frac{dz}{d\psi})$, or in fact $d\psi$, to remain constant for a given growth stage. The fundamental law now emerges predicting that as evaporative demand increases in the early morning, $d\psi$ will increase to a value which it will hold for the rest of the day until evaporative demand abates. The daily course of leaf water potential reflected in Fig. 13 and Fig. 14 (Section 4.3), and Fig. 30 (Section

9.1), support this conclusion.

Fig. 38 shows a typical trace of diurnal variation in hydraulic conductivity of the wheat crop. The data was collected on 29 October 1979. The variation in water flux density and hydraulic conductivity with time is apparent. The constancy in driving force with time from 09h00 clearly emerges.

11.3 Units, Hydraulic Conductivity and the Mass Flow Equation

Water potential as used in the literature can be expressed on a volumetric, specific or weight basis. The three different definitions can be related as follows:

$$\frac{\text{Volumetric } \psi_w}{\text{Specific } \psi_w} = \rho_w \ ,$$

$$\frac{\text{Volumetric } \psi_w}{\text{Weight } \psi_w} = \rho_w g \ , \text{ and}$$

$$\frac{\text{Specific } \psi_w}{\text{Weight } \psi_w} = g$$

where

ρ_w = the density of water ($kg\ m^{-3}$), and
g = the acceleration of gravity ($m\ s^{-2}$). (Savage, 1978)

Hence, the basic flow equation may be written in three different forms and the units of hydraulic conductivity vary according to the definition of ψ_w used. This is illustrated as follows:

For volumetric water potential (ψ_{wv}),

$$\phi = - E \frac{dz}{d\psi_{wv}}$$

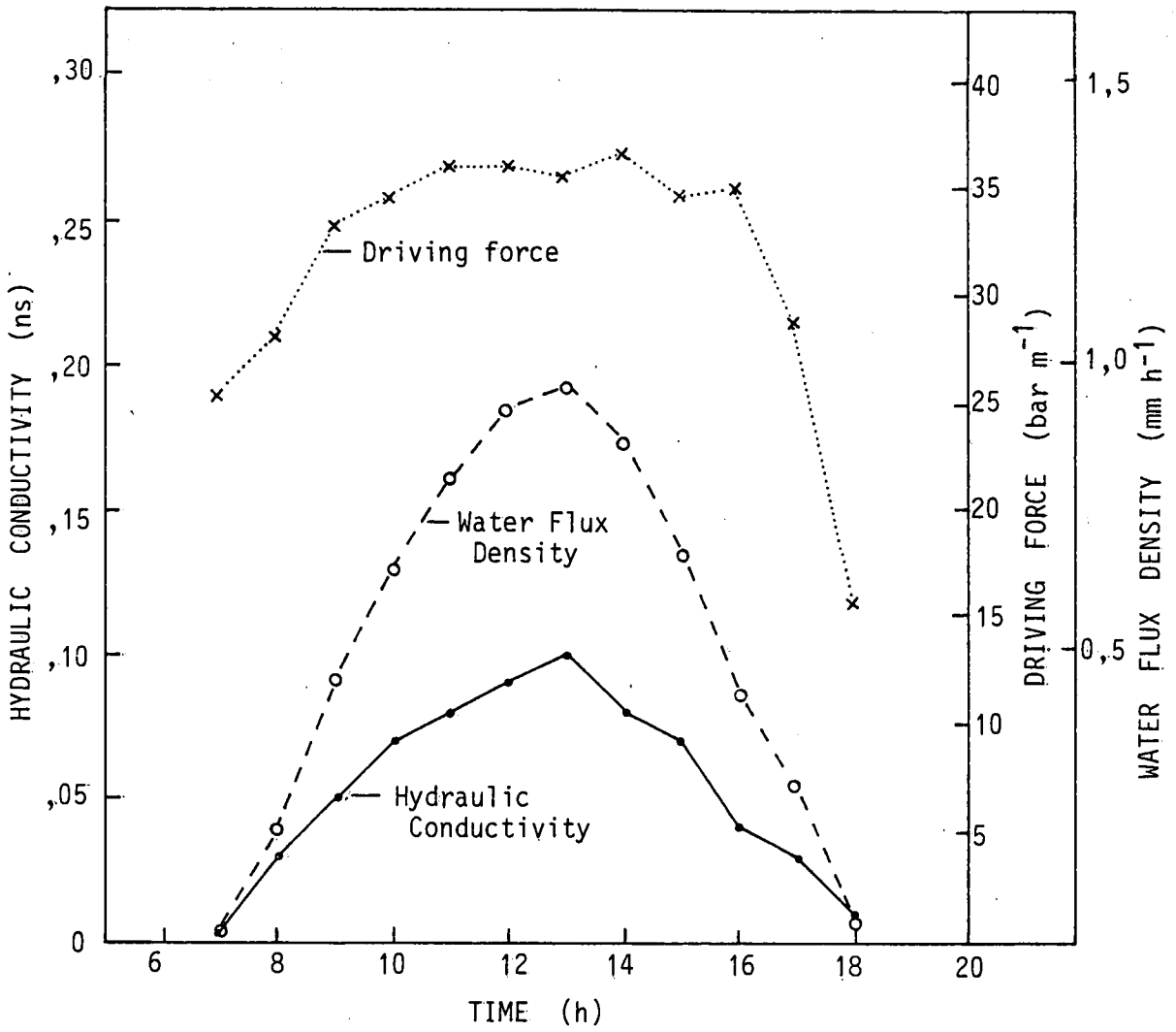

Fig. 38 : Typical trace of diurnal variation in hydraulic conductivity, water flux density and driving force (29/10/79). The respective dependence and inde= pendence of ϕ on water flux density and driving force is apparent.

where the units of ϕ are

$$\frac{(kg\ m^{-2}\ s^{-1})(m)}{(kg\ m\ s^{-2}\ m\ m^{-3})} \equiv s\ .$$

For specific water potential (ψ_{ws}),

$$\phi = - E \frac{dz}{d\psi_{ws}}$$

where the units of ϕ are

$$\frac{(kg\ m^{-2}\ s^{-1})(m)}{(kg\ m\ s^{-2}\ m\ kg^{-1})} \equiv kg\ m^{-3}\ s\ .$$

For weight water potential (ψ_{ww}),

$$\phi = - E \frac{dz}{d\psi_{ww}}$$

where the units of ϕ are

$$\frac{(kg\ m^{-2}\ s^{-1})(m)}{(m)} \equiv kg\ m^{-2}\ s^{-1}\ .$$

To facilitate comparison between values of ϕ obtained by the different methods, the 0,28 in Eqn. 29 must be replaced by appropriate dimensionless constants. These are given in Table 23.

The Scholander pressure chamber is a widely used instrument for measuring leaf water potential on a volumetric basis and hence this system has been adopted here as in Eqn. 29. Numerous other units are used in the literature to express volumetric leaf water potential and the water flow.

Table 23 : The dimensionless constant C for various combinations of units used in the generalised basic mass flow equation.

Flux density E	Water potential ψ_w	Displace= ment dx	Dimension= less constant C	Hydraulic conductivity ϕ
kg m^{-2} s^{-1}	Pa	m	10^{-9}	ns
g m^{-2} s^{-1}	Pa	m	10^{-6}	ns
mm h^{-1}	Pa	m	$0,28 \times 10^{-5}$	ns
kg m^{-2} s^{-1}	bar	m	10^{-4}	ns
g m^{-2} s^{-1}	bar	m	10^{-1}	ns
mm h^{-1}	bar	m	0,28	ns
kg m^{-2} s^{-1}	m	m	1	ns
kg m^{-2} s^{-1}	J kg^{-1}	m	10^{-1}	ns

SECTION C

SUMMARY

The object of the project has been the investigation of weather control of the plant water relations of wheat. All experimentation was carried out under field conditions with the physics of the problem receiving most emphasis. Of special interest was the determination of the hydraulic conductivity (ϕ) of the wheat crop. Defined as the rate of flow of water through the crop per unit vertical water potential difference, its evaluation required the application of special micrometeorological measuring techniques.

Leaf water potential (ψ_ℓ) was measured using the Wescor leaf psychrometer, J14 press and Scholander pressure chamber. Results from the psychrometer appear encouraging. Here a modified technique using a strip chart recorder was applied, eliminating need for a fixed cooling time and simultaneously providing a permanent record from which an accurate determination of ψ_ℓ was possible. In practice, the major source of error experienced with this technique was obtaining thermal equilibrium throughout the sensor-leaf system.

The J14 press is an inexpensive effective instrument which yielded promising results. It was calibrated against the Scholander pressure chamber. This yielded an exponential relationship

$$\psi_\ell \text{ (J14)} = 59{,}64\ e^{0{,}049\ \psi_\ell(\text{Scholander})}$$

with a coefficient of determination $r^2 = 0{,}81$. The J14 press appeared to be most accurate at pressures in excess of 15 bar, i.e. on stressed leaves. Statistical analyses showed that the J14 press and Scholander pressure chamber could be used to monitor hourly variations in ψ_ℓ. Scholander pressure chamber and adjusted J14 press measurements of ψ_ℓ were used in the determination of ϕ.

Leaf diffusive resistance (r_s) was measured using the LI-65 Autoporometer. Calibration of this instrument is critical and difficult. Instead of using the recommended approach of converting measurements to the arbitrary standard of 25 °C, calibration was carried out in a

growth chamber through a range of temperatures. The relationship

$$r_s = \frac{\Delta t}{115,80} \cdot T^{1,75} - r_o$$

was developed. Here Δt = the time interval measured by means of the autoporometer, T = the diffusion process temperature and r_o = the sensor cup resistance. This relationship facilitated quick, accurate analysis of field data.

Stomatal density counts were obtained from a series of scanning electron microscope micrographs. The ratio of the number of stomates on the abaxial to adaxial surface was found to be $0,74 \pm 0,14$. Hence diffusive resistance of both surfaces were measured and the relationship

$$\frac{1}{r_s} = \frac{1}{r_{abaxial}} + \frac{1}{r_{adaxial}}$$

used to evaluate r_s.

Leaf diffusive resistance was found to increase significantly with decreasing (more negative) ψ_ℓ for values of the latter below -20 bar. This indicates the onset of moisture stress conditions. Two empirical equations describing the leaf water potential - leaf diffusive resistance relationship were found from over 1 000 field measurements. These are:

$$(A): \quad r_s = 3\left[1 + e^{0,15(-20 - \psi_\ell)}\right], \quad r^2 = 0,81$$

and

$$(B): \quad r_s = 3 - \frac{0,65\ (\psi_\ell + 12)}{1 + e^{5(\psi_\ell + 12)}}, \quad r^2 = 0,90 \ .$$

Values of r_s exceeding 6 s cm^{-1} (at roughly -20 bar) indicate by definition approximately half the normal photosynthetic activity and the onset of moisture stress detrimental to growth. It is felt that equation (B) should promote reliable irrigation decision making and crop growth modelling.

Two soil types, the Bainsvlei and Valsrivier form, were used in this study. Standard pressure plate techniques were used to determine the soil moisture characteristics of each. Fitted curves describing soil water potential (ψ_s) in terms of gravimetric soil water content (Θ_m) were found to be:

$$\ell n\ \psi_s = -8,7559 - 3,1367\ \ell n\ \Theta_m \text{ for the Bainsvlei form,}$$

and

$$\ell n\ \psi_s = -9,7986 - 4,9661\ \ell n\ \Theta_m \text{ for the Valsrivier form.}$$

A new technique that makes use of a reiterative method to balance the surface energy budget equation was developed in order to obtain estimates of crop evaporation (E). The equipment used is durable, foolproof and easy to install. In this method the source and sink for water vapour and heat exchange between crop and atmosphere is assumed to be at the momentum exchange surface ($d + z_o$). The com= parison between calculated momentum exchange surface temperature (T_o) and the temperature measured at this level was used to validate the model. Accuracy acceptable for agricultural purposes resulted. This technique needs further verification against a lysimeter. The values of E obtained using this method were used in the determination of ϕ.

Hydraulic conductivity was determined by substituting values of the above described variables in Darcy's equation written in the form

$$\phi = \frac{E}{C(1/\frac{d\psi}{dz})}$$

where C = a constant used to normalise the system of units and z = the height at which water potential measurements are made. Contrary to expectation, ϕ was found to be a function of weather conditions. The relationship,

$$\phi = 0,0102 + 1,43 \times 10^{-4}\ (\lambda E) \quad , \quad r^2 = 0,91$$

where

λ = the latent heat of vapourisation, was obtained. This

implies that some feedback mechanism operates within the wheat crop requiring $(1/\frac{d\psi}{dz})$ to remain constant. Hence ψ_ℓ will decrease in the early morning to a certain value which it will maintain for the major part of the day. In the late afternoon ψ_ℓ will again increase tending towards the value of ψ_s as the soil-plant system reaches a state of equilibrium under night conditions.

Relatively wide scatter in the plotted points describing the control of water potential gradient $(\frac{d\psi}{dz})$ by crop evaporation rate (E) was found. This could have been due to ψ_s being measured at only one depth (20 cm).

A C K N O W L E D G E M E N T S

I wish to express my sincere gratitude to Professor James Murray De Jager, Head of the Department of Agrometeorology at the University of the Orange Free State, for his continual encouragement, guidance and inspiration during the course of these studies.

My sincere thanks are also due to:

(1) Various staff members of the U.O.F.S. for their time involved in many fruitful discussions, their encouragement and assistance. In particular:

Dr W.H. van Zyl, Mr A. van Rooyen and Mr D. Mvuya of the Department of Agrometeorology;

Dr H.F.P. Rautenbach of the Department of Biometry;

Dr A. van Rooyen and Dr A.T.P. Bennie of the Department of Soil Science;

Mr B. De Wit of the Electronic Workshop, and

Mr P. van Wyk who introduced me to the Scanning electron microscope.

(2) The Water Research Commission for permission to use the results of a research project for thesis purposes.

(3) Mrs Tillie Kloppers for her patience and endurance in typing this thesis.

(4) Mom and Dad for their financial and moral support throughout my study years.

Finally, a special word of thanks to Caryn, who not only assisted in the final preparation, but who forfeited many hours of fellowship and endured many miles of separation for extended periods in order that this thesis could be undertaken.

REFERENCES

Barrs, H.D., 1965. Psychrometric measure of leaf water potential: Lack of error attributable to leaf permeability. Science 149, 63-65.

Barrs, H.D. & Kramer, P.J., 1969. Water potential increase in sliced leaf tissue as a cause of error in vapor phase determinations of water potential. Plant Physiol. 44, 959-964 .

Baughn, J.W., 1974. Water potential in plants. Comparative measurements using the pressure chamber, psychrometer and in situ dewpoint hygrometer. Ph. d. Thesis, University of Wisconsin - Madison (USA).

Beadle, C.L., Stevenson, K.R., Neumann, H.H. & King, K.M., 1973. Diffusive resistance, transpiration and photosynthesis in single leaves of maize and sorghum in relation to leaf water potential. Can. J. Plant Sci. 53, 537-544.

Bennie, A.T.P., 1979. Die invloed van grondverdigting op die grond-plant sisteem. Ph. d. Thesis, University of the Orange Free State (South Africa).

Bidwell, R.G.S., 1974. Plant Physiology. Collier Macmillan Publishers, London.

Bower, J.W., 1978. Ecophysiological studies of three cvs of Persea americana (Mill.) emphasising photosynthesis and internal water relations. M.Sc. (Agric.) Thesis, University of Natal (South Africa).

Brown, R.W., 1972. Determination of leaf osmotic potential using thermocouple psychrometers. In Psychrometry in Water Relations Research (ed Brown, R.W. & van Haveren, B.P.), pp.88-93. Utah State University.

Burrows, F.J. & Milthorpe, F.L., 1976. Stomatal conductance in the control of gas exchange. In Water Deficits and Plant Growth Vol. IV (ed Kozlowski, T.T.), pp.103-152. Academic Press, New York.

Campbell, G.S., 1977. An Introduction to Environmental Biophysics. Springer-Verlag, New York.

Campbell, G.S. & Campbell, M.D., 1974. Evaluation of a thermocouple hygrometer for measuring leaf water potential in situ. Agron. J. 66, 24-27.

Campbell, E.C., Campbell, G.S. & Barlow, W.K., 1973. A dewpoint hygrometer for water potential measurement. Agr. Meteorol. 12, 113-121.

De Jager, J.M. & Harrison, T.D., 1979. Towards the development of an energy budget for a savanna ecosystem. Proceedings International Symposium : Dynamic changes in Savanna Ecosystems. C.S.I.R., Pretoria, 1979. (In press).

De Jager, J.M. & Kaiser, H.W., 1977. Plant and crop physiological parameters determining the environmental control of maize crop production. Crop Prod. 6, 99-103.

Denmead, O.T. & Millar, B.D., 1976. Field studies of the conductance of wheat leaves and transpiration. Agron. J. 68, 307-311.

Denmead, O.T. & Shaw, R.H., 1962. Availability of soil water to plants as affected by soil moisture content and meteorological conditions. Agron. J. 54, 385-390.

Du Pisani, A.L., 1974. An assessment of the regional net water demand for irrigation development of the Upper Berg river area based on Agroclimatological observations. Ph.d. Thesis, University of Stellenbosch (South Africa).

Fogg, D.N. & Wilkinson, N.T., 1958. The colorimetric determinination of phosphorus. Analyst 83, 406-414.

Frank, A.B., Power, J.F. & Willis, W.O., 1973. Effect of temperature and plant water stress on photosynthesis, diffusion resistance and leaf water potential in spring wheat. Agron. J. 65, 777-780.

Glauert, A.M., 1974. Practical Methods in Electron Microscopy. North-Holland Publishing Company, Amsterdam.

Hammel, J.E. & De Jager, J.M., 1980. Control of stomatal function by leaf water potential in field-grown soyabeans. (Submitted for publication).

Hansen, G.K., 1974a. Resistance to water flow in soil and plants, plant water status, stomatal resistance and transpiration of Italian ryegrass, as influenced by transpiration demand and soil water depletion. Acta Agric. Scand. 24, 83-92.

Hansen, G.K., 1974b. Resistance to water transport in soil and young wheat plants. Acta Agric. Scand. 24, 37-48.

Hayat, M.A., 1978. Introduction to Biological Scanning Electron Microscopy. University Park Press, Baltimore.

Hillel, D., 1971. Soil and Water - Physical principles and processes. Academic Press, New York.

Jameson, D.A., 1972. Thermocouple psychrometry in ecosystem research. In Psychrometry in Water Relations Research (ed Brown, R.W. & van Haveren, B.P.), pp.40. Utah State University.

Kanemasu, E.T. & Tanner, C.B., 1969. Stomatal diffusion resistance of snap beans I. Influence of leaf water potential. Plant Physiol. 44, 1547-1552.

Kanemasu, E.T., Thurtell, G.W. & Tanner, C.B., 1969. Design, calibration and field use of a stomatal diffusion porometer. Plant Physiol. 44, 881-885.

Klepper, B., 1968. Diurnal pattern of water potential in woody plants. Plant Physiol. 43, 1931-1934.

Lawlor, D.W., 1972. Growth and water use of Lolium Perenne I. Water transport. J. Appl. Ecol. 9, 79-98.

Lawlor, D.W. & Lake, J.V., 1976. Evaporation rate, leaf water potential and stomatal conductance in Lolium, Trifolium and Lysimachia in drying soil. J. Appl. Ecol. 13, 639-646.

Loveday, J., 1974. Methods for analysis of irrigated soils. C.S.I.R.O., Division of Soil. Tech. Comm. No. 54 of the Commonwealth Bureau of Soils.

Macvicar, C.N., De Villiers, J.M., Loxton, R.F., Verster, E., Lambrechts, J.J.N., Merryweather, F.R., Le Roux, J., Van Rooyen, T.H. & von M Harmse, H.J., 1977. Soil Classification - a binomial system for South Africa. A report on a research project conducted under the auspices of the Soil and Irrigation Research Institute. Department of Agricultural Technical Services (South Africa).

McCree, K.J., 1974. Changes in the stomatal response characteristics of grain sorghum produced by water stress during growth. Crop Sci. 14, 273-278.

McCree, K.J. & van Bavel, C.H.M., 1977. Calibration of leaf resistance porometers. Agron. J. 69, 724-726.

Meidner, H. & Mansfield, T.A., 1968. Physiology of Stomata. McGraw-Hill, London.

Meidner, H. & Sheriff, D.W., 1976. Water and Plants. Blackie, London.

Meyer, W.S., Walker, S. & Green, G.C., 1979. The Prediction of water use by spring wheat in South Africa. Crop Prod. 8, 185-191.

Millar, B.D. & Denmead, O.T., 1976. Water relations of wheat leaves in the field. Agron. J. 68, 303-307.

Mohsin, M.A. & Ghildyal, B.P., 1972. Design criteria of thermocouple psychrometers for water potential measurements in plants. In Psychrometry in Water Relations Research (ed Brown, R.W. & van Haveren, B.P.), pp.74-83. Utah State University.

Monteith, J.L., 1973. Principles of Environmental Physics. Edward Arnold, London.

Morrow, P.A. & Slatyer, R.O., 1971a. Leaf resistance measurements with diffusion porometers : Precautions in calibration and use. Agr. Meteorol. 8, 223-233.

Morrow, P.A. & Slatyer, R.O., 1971b. Leaf temperature effects on measurements of diffusive resistance to water vapour transfer. Plant Physoil. 47, 559-561.

Neumann, H.H., 1972. Water potential relationships in plant tissue measured by a new dewpoint hygrometer technique. Ph.d. Thesis, University of Guelph (Canada).

Neumann, H.H. & Thurtell, G.W., 1972. A peltier cooled thermocouple dewpoint hygrometer for in situ measurement of water potentials. In Psychrometry in Water Relations Research (ed Brown, R.W. & van Haveren, B.P.), pp.103-112. Utah State University.

Newman, E.I., 1969. Resistance to water flow in soil and plant II. A review of experimental evidence on the rhizosphere resistance. J. Appl. Ecol. 6, 261-272.

Oke, T.R., 1978. Boundary Layer Climates. John Wiley & Sons, New York.

Olsen, S.R., Cole, C.V., Watanabe, F.S. & Dean, L.A., 1954. Estimation of available phosphorus in soils with sodium bicarbonate. U.S.D.A. Arc. No. 939, Washington D.C.

Owen, P.C., 1952. The relation of germination of wheat to water potential. J. Expt. Botany 3, 188-203.

Peck, A.J., 1968. Theory of the Spanner psychrometer I. The thermocouple. Agr. Meteorol. 5, 433-447.

Peck, A.J., 1969. Theory of the Spanner psychrometer II. Sample effects and equilibrium. Agr. Meteorol. 6, 111-124.

Rawlins, S.L., 1964. Systematic error in leaf water potential measurements with a thermocouple psychrometer. Science 146, 644-646.

Rawlins, S.L., 1966. Theory for thermocouple psychrometers used to measure water potential in soil and plant samples. Agr. Meteorol. 3, 293-310.

Rawlins, S.L. & Dalton, F.N., 1967. Psychrometric measurement of soil water potential without precise temperature control. Soil Sci. Soc. Amer. Proc. 31, 297-301.

Rawlins, S.L., Gardner, W.R. & Dalton, F.N., 1968. In situ measurement of soil and plant leaf water potential. Soil Sci. Soc. Amer. Proc. 32, 468-470.

Reicosky, D.C., Campbell, R.B. & Doty, C.W., 1975. Diurnal fluctuation of leaf water potential of corn as influenced by soil matric potential and microclimate. Agron. J. 67, 380-385.

Richards, L.A., 1954. Diagnosis and improvement of saline and alkali soils. U.S.D.A. Agricultural Handbook No. 60. U.S. Government printing office, Washington D.C.

Richards, L.A. & Ogata, G., 1958. Thermocouple for vapour pressure measurements in biological and soil systems at high humidity. Science 128, 1089-1090.

Rutherford, R.J. & De Jager, J.M., 1975. Water status and stomatal behaviour of BP1 potatoes (Solanum Tuberosum L.) and their effect upon yield. Crop Prod. 4, 125-128.

Salisbury, F.B. & Ross, C., 1969. Plant Physiology. Wadsworth Publishing Co. Inc., California.

Savage, M.J., 1978. Water potential terms and units. Agrochemo=physica 10, 5-6.

Scholander, P.F., Hammel, H.T., Bradstreet, E.D. & Hemmingsen, E.A., 1965. Sap pressure in vascular plants. Science 148, 339-346.

Slatyer, R.O., 1967. Plant Water Relationships. Academic Press, London.

Slavik, B., 1974. Methods of Studying Plant Water Relations. Springer-Verlag, Berlin.

Steel, K.G.G. & Torrie, J.H., 1960. Principles and Procedures of Statistics - With special reference to the biological sciences. McGraw-Hill Book Co. Inc., New York.

Stoker, R. & Weatherly, P.E., 1971. The influence of the root system on the relationship between the rate of transpiration and the depression of leaf water potential. New Phytol. 70, 547-554.

Streutker, A., 1978. Tensiometer - controlled medium frequencey topsoil irrigation. A technique to improve agricultural water management. Water S.A. 4, 134-155.

Sutcliffe, J., 1979. Plants and Water. Edward Arnold, London.

Teare, T.D., Peterson, C.J. & Law, A.G., 1971. Size and frequency of leaf stomata in cultivars of Triticum Aestivum and other Triticum species. Crop Sci. 11, 496-498.

Thom, A.S., 1975. Momentum, mass and heat exchange of plant commu= nities. In Vegetation and the Atmosphere Vol. 1 (ed Monteith, J.L.), pp.57-109. Academic Press, New York.

Thomas, J.C., Brown, K.W. & Jordan, W.R., 1976. Stomatal response to leaf water potential as affected by preconditioning water stress in the field. Agron. J. 68, 706-708.

Thomas, J.R. & Weigand, C.L., 1970. Osmotic and matric suction effects on relative turgidity, temperature and growth of cotton leaves. Soil Sci. 109, 85-92.

Van Bavel, C.H., Nakayama, L.S. & Ehrler, W.L., 1965. Measuring transpiration resistance of leaves. Plant Physiol. 40, 535-540.

Van Haveren, B.P. & Brown, R.W., 1972. The properties and behaviour of water in the soil-plant-atmosphere continuum. In Psychrometry in Water Relations Research (ed Brown, R.W. & van Haveren, B.P.), pp.1-27. Utah State University.

Waring, R.H. & Cleary, B.D., 1967. Plant moisture stress : Evaluation by pressure bomb. Science 155, 1248-1254.

A P P E N D I X 1

GENERAL DIGITISING PROGRAM

```
10    ! K.L.BRISTOW
20    ! DIGITIZING PROGRAM THAT WRITES DATA DIRECTLY TO TAPE
30    ! CALLED "DIGITA"
40    !
50    OPTION BASE 1
60    SHORT V(35,24)
70    DIM A$[80],B$[10],C$[4],D$[20],E$[20]
80    Missdata=9999
90    !
100   INPUT "STATION NAME ?",A$,"MONTH ?",B$,"YEAR ?",C$,"NAME OF ELEMENT ?",D$,"
NAME OF UNITS ?",E$
110   PRINTER IS 0
120   IMAGE "STATION:"XXK,/,"MONTH:"XXK,/,"YEAR:"XXK,/,"NAME OF ELEMENT:"XXK,/,"U
NITS:"XXK
130   PRINT USING 120;A$,B$,C$,D$,E$
140   PRINT
150   PRINT
160   IMAGE 11X,"|01h0|02h0|03h0|04h0|05h0|06h0|07h0|08h0|09h0|10h0|11h0|12h0|"/,
11X,"|13h0|14h0|15h0|16h0|17h0|18h0|19h0|20h0|21h0|22h0|23h0|24h0|"
170   PRINT USING 160
180   INPUT "NO OF UNITS ON Y AXIS PER CENTIMETER ?",Units_yaxis
190   Units_yaxis=Units_yaxis*2.54
200   INPUT "YMIN ?",Ymin,"YMAX ?",Ymax
210   INPUT "NO OF DECIMAL POINTS ?(1,2)",Dec
220   IF Dec=1 THEN Dec=10
230   IF Dec=2 THEN Dec=100
240   INPUT "BEGINNING TIME FOR THE DAILY VALUES ? (2 Digits only )",Begin
250   INPUT "ENDING TIME FOR THE DAILY VALUES ? (2 Digits only )",End
260   INPUT "BEGINNING DATE ? (2 DIGITS ONLY)",Start
270   D=Start-1
280   D=D+1
290   !
300   !
310   !
320   FOR H=1 TO 24
330   V(D,H)=9999
340   NEXT H
350   !
360   GRAPHICS
370   GCLEAR
380   LOCATE 20,100,20,80
390   SCALE 1,24,Ymin,Ymax
400   AXES 1,10,1,Ymin,1,10
410   FRAME
420   FOR H=Begin TO End
430   ENTER 4;X,Y
440   BEEP
450   V(D,H)=Y*Units_yaxis
460   IF V(D,H)>Ymax THEN 730
470   IF H=Begin THEN 490
480   GOTO 510
490   MOVE H,V(D,H)
500   GOTO 520
510   DRAW H,V(D,H)
520   V(D,H)=Y*Units_yaxis*Dec
530   WAIT 100
540   NEXT H
550   !
560   PAUSE
570   !
580   INPUT "MUST DATA BE PRINTED ? (Y/N) ",Ans$
590   C$=UPC$(Ans$)
600   IF C$="Y" THEN 620
610   IF C$="N" THEN 360
620   PRINTER IS 0
630   IMAGE "DATE:"XX,ZZ,XX,"|",12(ZZZZ"|"),4X,"1"
```

```
640  PRINT USING 630;D,V(D,1),V(D,2),V(D,3),V(D,4),V(D,5),V(D,6),V(D,7),V(D,8),V
(D,9),V(D,10),V(D,11),V(D,12)
650  IMAGE "DATE:"XX,ZZ,XX,"|",12(ZZZZ"|"),4X,"2"
660  PRINT USING 650;D,V(D,13),V(D,14),V(D,15),V(D,16),V(D,17),V(D,18),V(D,19),V
(D,20),V(D,21),V(D,22),V(D,23),V(D,24)
670  !
680  !
690  !
700  INPUT "IF DIGITIZING COMPLETE TYPE END AND PRESS CONT ; OTHERWISE JUST PRES.
S CONT ",Z$
710  IF Z$=UPC$("END") THEN 760
720  GOTO 280
730  V(D,H)=Missdata
740  DRAW H,V(D,H)
750  GOTO 530
760  EXIT GRAPHICS
770  Fin=D
780  !
790  !
800  !
810  INPUT "NAME OF DATA FILE ?",File$
820  INPUT "NUMBER OF RECORDS ? (20 FOR A FULL MONTH) ",R
830  CREATE File$,R
840  ASSIGN #1 TO File$
850  READ #1,1
860  PRINT #1;A$,B$,C$,D$,E$
870  FOR D=Start TO Fin
880  PRINT #1;D
890  FOR H=1 TO 24
900  PRINT #1;V(D,H)/Dec
910  NEXT H
920  NEXT D
930  ASSIGN * TO #1
940  DISP "PROGRAM COMPLETE !"
950  END
```

APPENDIX 2

GENERAL PLOTTING PROGRAM

```
10    ! K.L.BRISTOW
20    ! GENERAL PLOTTING PROGRAM CALLED "GENPLT"
30    ! THIS PROGRAM PLOTS FUNCTIONS DEFINED BY THE USER AS WELL AS PLOTTING
40    ! POINTS THAT ARE FED IN MANUALLY
50    !
60    OPTION BASE 1
70    DIM A$[80],X$[80],Y$[80],T$[80],Title$[160]
80    SHORT X(102),Y(102)
90    Nmax=102
100   F=0
110   ! THE REQUIRED PARAMETERS FOR THE GRAPH ARE ENTERED
120       INPUT "TITLE OF GRAPH ? (e.g. Fig.1. etc)",Title$
130       INPUT "NAME OF GRAPH ? (Heading that appears in the frame)",A$
140       INPUT "HEADING FOR X-AXIS ?",X$
150       INPUT "HEADING FOR Y-AXIS ?",Y$
160       INPUT "CHARACTER SIZE FOR THE HEADING ? (NORMALLY USE 3)",Csize
170       INPUT "MIN X VALUE ?",Xmin
180       INPUT "MAX X VALUE ?",Xmax
190       INPUT "MIN Y VALUE ?",Ymin
200       INPUT "MAX Y VALUE ?",Ymax
210       INPUT "Xtic SPACING ?",Xtic
220       INPUT "Ytic SPACING ?",Ytic
230       INPUT "X INTERSECTION ?",Xint
240       INPUT "Y INTERSECTION ?",Yint
250       INPUT "MAJOR COUNT ON X AXIS ?",Xmajor
260       INPUT "MAJOR COUNT ON Y AXIS ?",Ymajor
270       INPUT "MAJOR TIC SIZE ? (NORMALLY USE 3) ",Ticsize
280       INPUT "MUST X AXIS BE LABELLED AT EACH TIC ? (Y/N) ",Ans$
290       IF Ans$="Y" THEN Tic=Xtic
300       IF Ans$="N" THEN Tic=Xtic*Xmajor
310       INPUT "MUST Y AXIS BE LABELLED AT EACH TIC ? (Y/N) ",Bns$
320       IF Bns$="Y" THEN Ticy=Ytic
330       IF Bns$="N" THEN Ticy=Ytic*Ymajor
340       !
350       PLOTTER IS 13,"GRAPHICS"
360       GRAPHICS
370       GCLEAR
380       FRAME
390       CSIZE Csize
400       LORG 5
410       MOVE 61,97
420       LABEL USING "K";A$
430       MOVE 61,2
440       IF Csize<3 THEN 460
450       CSIZE Csize-1
460       LABEL USING "K";X$
470       MOVE 2,50
480       DEG
490       LDIR 90
500       LABEL USING "K";Y$
510       LOCATE 10,110,10,90
520       SCALE Xmin,Xmax,Ymin,Ymax
530       AXES Xtic,Ytic,Xint,Yint,Xmajor,Ymajor,Ticsize
540       Yfudge=.02*(Ymax-Ymin)
550       Xfudge=.02*(Xmax-Xmin)
560       LDIR 0
570       CSIZE 2
580       !
590       ! LABELLING OF X-AXIS
600       !
610       FOR I=Xmin TO Xmax STEP ABS(Tic)
620       MOVE I,Yint-Yfudge
630       LABEL USING 640;I
640       IMAGE #,K
650       NEXT I
660       !
```

```
670         ! LABELLING OF Y-AXIS
680         !
690         FOR I=Ymin TO Ymax STEP ABS(Ticy)
700         MOVE Xint-Xfudge,I
710         LABEL USING 640;I
720         NEXT I
730         PAUSE
740         !
750         !
760     EXIT GRAPHICS
770     PRINTER IS 16
780     PRINT "This program can plot functions as well as plotting data that is in
put manually."
790     PRINT "If only the points are to be plotted without joining each point, as
 in a"
800     PRINT "scatter diagram, then type in POINT and press CONT"
810     PRINT "If you have a simple function to plot , type in FUNCTION and press
CONT ."
820     PRINT "For manual data inputs where the individual points are connected, t
ype in TRACE "
830     PRINT "and then press CONT ."
840     INPUT "FUNCTION OR TRACE OR POINT OR END OF DATA INPUT ?",Fn$
850     IF Fn$=UPC$("FUNCTION") THEN 900
860     IF Fn$=UPC$("TRACE") THEN 1400
870     IF Fn$=UPC$("POINT") THEN 1160
880     IF Fn$=UPC$("END") THEN 1960
890     PRINT LIN(5)
900     PRINT "If a function is to be plotted then you must define your function b
y typing"
910     PRINT "                              3000 DEF FN A(X)=F(X)"
920     PRINT "where F(X) is your function of the variable X (e.g. SIN(X) , (4*X^2
)-5*X^3)"
930     PRINT "and pressing STORE . After you have done this press CONT"
940     PAUSE
950     !
960     ! FUNCTIONS DEFINED BY THE USER ARE PLOTTED
970     !
980                         F=F+1
990                         Inc=(Xmax-Xmin)/(Nmax-1)
1000                        Start=Xmin-Inc
1010                        FOR I=1 TO Nmax
1020                        X(I)=Start+I*Inc
1030                        Y(I)=FNA((X(I)))
1040                        NEXT I
1050                        GRAPHICS
1060                        MOVE X(1),Y(1)
1070                        FOR I=2 TO Nmax
1080                        DRAW X(I),Y(I)
1090                        NEXT I
1100                        LORG 1
1110                        LABEL USING "K";"(",F,")"
1120                        PAUSE
1130                        EXIT GRAPHICS
1140                        GOTO 840
1150 !
1160 ! DATA POINTS ARE PLOTTED
1170 !
1180 EXIT GRAPHICS
1190 INPUT "NUMBER OF DATA POINTS TO BE PLOTTED ?",N
1200 FOR I=1 TO N
1210 DISP "Enter the coordinates for point # ";I;"(X,Y,CONT)";
1220 INPUT "",X(I),Y(I)
1230 PRINT USING Image1;I,X(I),Y(I)
1240 IF I=N THEN BEEP
1250 NEXT I
1260 INPUT "MUST ANY CORRECTIONS BE MADE TO DATA POINTS ? (Y/N) ",Ans$
```

```
1270 IF Ans$=UPC$("N") THEN 1300
1280 IF Ans$=UPC$("Y") THEN GOSUB Correction
1290 GOTO 1260
1300 GRAPHICS
1310 LORG 5
1320 FOR I=1 TO N
1330 MOVE X(I),Y(I)
1340 LABEL USING "K";"x"
1350 NEXT I
1360 PAUSE
1370 EXIT GRAPHICS
1380 GOTO 840
1390 !
1400 ! DATA TO SHOW TRENDS IS NOW ENTERED AND PLOTTED ON THE SAME AXES
1410 !
1420          EXIT GRAPHICS
1430          Label$="xo+*#$&@"
1440          INPUT "NO. OF DATA SETS TO BE PLOTTED ON THE SAME AXES ? MAX=8",No
1450          Data=1
1460          PRINTER IS 16
1470          L$=Label$[Data,Data]
1480          DISP "Enter the distinguishing title for plot #";Data;
1490          INPUT "",T$(Data)
1500          DISP "Enter the no of data points for data set #";Data;
1510          INPUT "",N
1520          N=INT(N)
1530          PRINT "DATA SET #";Data
1540          PRINT
1550          FOR I=1 TO N
1560          DISP "Enter the coordinates for point # ";I;"(X,Y,CONT)";
1570          INPUT "",X(I),Y(I)
1580          PRINT USING Image1;I,X(I),Y(I)
1590          IF I=N THEN BEEP
1600          NEXT I
1610          PRINT LIN(1)
1620          INPUT "MUST ANY CORRECTIONS BE MADE TO DATA POINTS ? (Y/N) ",Ans$
1630          C$=UPC$(Ans$)
1640          IF C$="N" THEN 1670
1650          IF C$="Y" THEN GOSUB Correction
1660          GOTO 1620
1670          GRAPHICS
1680          LORG 5
1690          MOVE X(1),Y(1)
1700          FOR I=2 TO N
1710          DRAW X(I),Y(I)
1720          NEXT I
1730          FOR I=1 TO N
1740          MOVE X(I),Y(I)
1750          LABEL USING "A";L$
1760          NEXT I
1770          IF Data=No THEN 840
1780          Data=Data+1
1790          PAUSE
1800          EXIT GRAPHICS
1810          GOTO 1460
1820 !
1830 Correction:!
1840          PRINT "Make any alterations to data points by typing in the coordi
nate with the correct"
1850          PRINT "value e.g. type X(2)=2.5 and press EXECUTE , type Y(4)=3.6
and press EXECUTE"
1860          PRINT "When all points are corrected press CONT"
1870          PAUSE
1880          FOR I=1 TO N
1890          PRINT USING Image1;I,X(I),Y(I)
1900          IF I=N THEN BEEP
```

```
1910          NEXT I
1920          RETURN
1930 !
1940 Image1:IMAGE "POINT # "DDDD":",5X,"X="K,5X,"Y="K
1950 !
1960 DUMP GRAPHICS
1970 !
1980 ! ROUTINE TO IDENTIFY THE VARIOUS CURVES THAT ARE PLOTTED
1990 !
2000 PRINTER IS 0
2010 PRINT LIN(2)
2020 PRINT Title$
2030 PRINT LIN(5)
2040 PRINT "IDENTIFICATION OF THE CURVES "
2050 PRINT
2060 FOR Data=1 TO No
2070 PRINT Label$[Data,Data];"--------";Label$[Data,Data];SPA(3);T$(Data)
2080 NEXT Data
2090 END
3000 DEF FNA(X)=SIN(X)
```

A P P E N D I X 3

THE PROGRAM USED TO ESTIMATE EVAPOTRANSPIRATION - MAKES USE OF A REITERATIVE TECHNIQUE TO BALANCE THE ENERGY BUDGET EQUATION

```
10   ! K.L.BRISTOW
20   ! PROGRAM THAT USES A REITERATIVE METHOD TO ESTIMATE SENSIBLE AND LATENT
30   ! HEAT FLUXES OF THE SURFACE ENERGY BUDGET.
40   ! NET RADIATION AND SOIL HEAT FLUX WERE RECORDED DIRECTLY BY MEANS OF
50   ! SOIL HEAT FLUX PLATES AND A NET RADIOMETER RESPECTIVELY.
60   ! THE EVAPORATIVE AND CONVECTIVE TERMS ARE ESTIMATED FROM WIND SPEED
70   ! AND WET- AND DRY-BULB TEMPERATURES.
80   ! NOTE: CARE MUST BE TAKEN TO USE THE CORRECT FORMAT WHEN RECALLING
90   ! DATA FROM MAGNETIC TAPE.
100  !
110  ! THE PROGRAM IS CALLED "EVAP-3"
120  !
130  OPTION BASE 1
140  DIM A$[30],B$[30],C$[30],D$[30],E$[30]
150  DIM A2$[30],B2$[30],C2$[30],D2$[30],E2$[30]
160  DIM A3$[30],B3$[30]
170  SHORT Rn(31,24),G(31,24)
180  SHORT T1(24),T2(24),T3(24),T4(24),T5(24),T6(24)
190  SHORT U1(24),U2(24),U3(24)
200  SHORT R1(24),R2(24),S1(24),S2(24),U(24),Rn2(24),G2(24),C(24),Le(24),Leq(24)
,Lep(24)
210  SHORT E(24),E1(24),E2(24),E3(24),E4(24),E0(24),E01(24),E02(24),Rho(24),Diff
(24),Ri(24),F(24),Delta(24),Ra(24)
220  !
230  ! ROUTINE TO READ NET RADIATION DATA STORED ON TAPE
240  !
250  INPUT "FILE NAME (NET RADIATION) ?",Rn$
260  INPUT "LAST DAY ON FILE ? (e.g. 31)",Last
270  ASSIGN #1 TO Rn$
280  READ #1,1
290  READ #1;A$,B$,C$,D$,E$
300  FOR D=1 TO Last
310  FOR H=1 TO 24
320  READ #1;Rn(D,H)
330  Rn(D,H)=Rn(D,H)*18.35      ! CALIBRATION FACTOR USED IN THIS STUDY IS 18.35
340  NEXT H
350  NEXT D
360  !
370  ! ROUTINE TO READ SOIL HEAT FLUX DATA STORED ON TAPE
380  !
390  INPUT "FILE NAME (SOIL HEAT FLUX) ?",Shf$
400  ASSIGN #2 TO Shf$
410  READ #2,1
420  READ #2;A2$,B2$,C2$,D2$,E2$
430  READ #2;D
440  FOR H=6 TO 20
450  READ #2;G(D,H)
460  NEXT H
470  IF TYP(2)=3 THEN 510
480  IF D=31 THEN 510
490  GOTO 430
500  !
510  ! ROUTINE TO READ TEMPERATURE AND WIND DATA STORED ON TAPE
520  !
530  INPUT "FILE NAME (TEMPERATURE AND WIND DATA) ?",Tw$
540  ASSIGN #3 TO Tw$
550  READ #3,1
560  READ #3;A3$,B3$
570  INPUT "JULIAN DAY FOR WHICH REITERATION IS REQUIRED ?",Julian
580  READ #3;Day
590  READ #3;H
600  H=H/100
610  READ #3;T1(H)          !DRY-BULB TEMP.  REF LEVEL 2
620  READ #3;T2(H)          !WET-BULB TEMP.  REF LEVEL 2
630  READ #3;T3(H)          !DRY-BULB TEMP.  REF LEVEL 1
640  READ #3;T4(H)          !WET-BULB TEMP.  REF LEVEL 1
```

```
650  READ #3;T5(H)          !DRY-BULB TEMP.  CANOPY SURFACE
660  READ #3;T6(H)          !WET-BULB TEMP.  CANOPY SURFACE
670  READ #3;U1(H)          !WIND SPEED - REF LEVEL 1
680  READ #3;U2(H)          !WIND SPEED - REF LEVEL 2
690  READ #3;U3(H)          !WIND SPEED - REF LEVEL 3
700  IF H=24 THEN 720
710  GOTO 590
720  IF Day=Julian THEN 750
730  GOTO 580
740  !
750  ! INPUT DATA REQUIRED FOR REITERATIVE PROCESS
760  !
770  INPUT "DAY OF MONTH FOR WHICH REITERATION IS CARRIED OUT ?",D
780  INPUT "REFERENCE LEVEL AT WHICH WIND AND TEMP. IS MEASURED ? (1 or 2)",Wref
790  INPUT "CROP HEIGHT ?",Croph
800  INPUT "A-PAN EVAPORATION FOR THE DAY ?",Apan
810  INPUT "BEGINNING OF TIME PERIOD FOR WHICH TO CALCULATE Le etc. ? (e.g 07) "
,Begin
820  INPUT "END OF TIME PERIOD ? (e.g. 18)",End
830  D1=.63*Croph
840  Zo=.13*Croph
850  IF Wref=1 THEN Z=D1+Zo+.5
860  IF Wref=2 THEN Z=2
870  !
880  ! PREPARATION OF PRINTOUT FORMAT
890  !
900  PRINTER IS 0
910  Etot=0
920  PRINT "_____
_____"
930  PRINT
940  PRINT USING "K";D," ";B2$," ";C$
950  PRINT
960  PRINT USING "K";"CROP HEIGHT: ";Croph," m."
970  PRINT USING "K";"REFERENCE LEVEL: ";Z," m."
980  PRINT
990  IMAGE "TIME    Rn    G     C     Le    Leq    Lep    F    To    TM   Tair
  B  E(mm/h)"
1000 PRINT USING 990
1010 PRINT
1020 !
1030 ! REITERATIVE PROCESS BEGINS
1040 !
1050 FOR H=Begin TO End
1060 !
1070 !
1080 S1(H)=T5(H)
1090 S2(H)=T6(H)
1100 IF Wref=1 THEN 1120
1110 IF Wref=2 THEN 1160
1120 R1(H)=T3(H)
1130 R2(H)=T4(H)
1140 U(H)=U1(H)+.3
1150 GOTO 1200
1160 R1(H)=T1(H)
1170 R2(H)=T2(H)
1180 U(H)=U2(H)+.3
1190 !
1200 ! CALCULATE VAPOUR PRESSURE FOR REFERENCE LEVEL
1210 !
1220 E1(H)=6.11*EXP(5347.61*(1/273.16-1/(273.16+R2(H))))
1230 E2(H)=E1(H)-.66*(R1(H)-R2(H))
1240 E3(H)=6.11*EXP(5347.61*(1/273.16-1/(273.16+R1(H))))
1250 E4(H)=E3(H)-E2(H)
1260 IF E2(H)<0 THEN E2(H)=0
1270 !
```

```
1280 ! CALCULATE RELATIVE HUMIDITY FOR SURFACE LEVEL
1290 !
1300 E02(H)=6.11*EXP(5347.61*(1/273.16-1/(273.16+S1(H))))
1310 E01(H)=6.11*EXP(5347.61*(1/273.16-1/(273.16+S2(H))))
1320 E0(H)=E01(H)-.66*(S1(H)-S2(H))
1330 IF E0(H)<0 THEN E0(H)=0
1340 Rho(H)=E0(H)/E02(H)*100
1350 IF Rho(H)<0 THEN Rho(H)=0
1360 !
1370 ! CALCULATE EQUILIBRIUM EVAPORATION Leq(H)
1380 !
1390 Delta(H)=E02(H)/(273.16+S1(H))^2*(6790.5-5.02808*(273.16+S1(H))+4916.8*10^(
-.0304*(273.16+S1(H)))*(273.16+S1(H))^2+174209*10^(-1302.88/(273.16+S1(H))))
1400 Leq(H)=(Rn(D,H)-G(D,H))*Delta(H)/(Delta(H)+.66)
1410 !
1420 ! CALCULATE POTENTIAL EVAPORATION Lep(H)
1430 !
1440 Ra(H)=LOG((Z-D1)/Zo)^2/(.41^2*U(H))
1450 Lep(H)=((Rn(D,H)-G(D,H))*Delta(H)+1.2*1010*E4(H)/Ra(H))/(Delta(H)+.66)
1460 !
1470 ! SET THE INITIAL To VALUE AND MAX AND MIN LEVELS
1480 !
1490 To=20
1500 Big=100
1510 Small=-100
1520 !
1530 ! COMPUTE THE STABILITY FACTOR
1540 !
1550 Ri(H)=9.81/((R1(H)+S1(H))/2+273.16)*(R1(H)-S1(H))*(Z-D1)/U(H)^2
1560 IF Ri(H)>0 THEN 1580
1570 IF Ri(H)<0 THEN 1600
1580 F(H)=(1-5*Ri(H))^2
1590 GOTO 1620
1600 F(H)=(1-16*Ri(H))^(3/4)
1610 !
1620 ! COMPUTE Rn , G , C , LE AND APPLY THE CORRECTION FACTOR TO C AND LE
1630 !
1640 Rn2(H)=-Rn(D,H)
1650 G2(H)=G(D,H)
1660 Log=LOG((Z-D1)/Zo)^2
1670 C(H)=F(H)*1.2*1010*.41*.41*U(H)*(To-R1(H))/Log
1680 Vap=6.11*EXP(5347.61*(1/273.16-1/(273.16+To)))*Rho(H)/100-E2(H)
1690 Le(H)=F(H)*1.2*1010*.41*.41*U(H)*Vap/(Log*.66)
1700 Diff(H)=Rn2(H)+G2(H)+Le(H)+C(H)
1710 IF ABS(Diff(H))<1 THEN Correct
1720 IF Diff(H)<0 THEN Small
1730 IF Diff(H)>0 THEN Big
1740 Correct:!
1750 !
1760 ! EXPRESS LE AS EVAPORATION IN mm. AND PRINT OUT REQUIRED DATA
1770 !
1780 IF Le(H)>0 THEN 1810
1790 IF Le(H)<0 THEN E(H)=0
1800 GOTO 1820
1810 E(H)=3600/2454000*Le(H)
1820 IMAGE ZZ,3X,MDDDD,1X,MDDD,2X,MDDDD,2X,MDDDD,2X,MDDDD,2X,MDDDD,1X,MD.DD,1X,M
DD.D,1X,MDD.D,1X,MDD.D,1X,MD.D,1X,MDD.DD
1830 PRINT USING 1820;H,Rn2(H),G2(H),C(H),Le(H),Leq(H),Lep(H),F(H),To,S1(H),R1(H
),C(H)/Le(H),E(H)
1840 Etot=Etot+E(H)
1850 GOTO 1970
1860 !
1870 Big:! ADJUST THE To VALUE WHICH IS TOO BIG
1880     Big=To
1890     To=To-(Big-Small)/2
1900     GOTO 1640
```

```
1910 !
1920 Small:! ADJUST THE To VALUE WHICH IS TOO SMALL
1930    Small=To
1940    To=To+(Big-Small)/2
1950    GOTO 1640
1960 !
1970 NEXT H
1980 !
1990 PRINT
2000 IMAGE 47X,"DAILY EVAPORATION (mm) ET= ",X,DD.DD
2010 PRINT USING 2000;Etot
2020 IMAGE 47X,"A-PAN EVAPORATION (mm) Ep= ",X,DD.DD
2030 PRINT USING 2020;Apan
2040 IMAGE 68X,"ET/Ep =",DD.DD
2050 PRINT USING 2040;Etot/Apan
2060 !
2070 ! ALLOWS ONE TO CONTINUE WITH THE NEXT DAY
2080 !
2090 INPUT "DO YOU WANT ANOTHER DAY ? (Y/N)",Ans$
2100 IF Ans$="N" THEN 2120
2110 IF Ans$="Y" THEN 570
2120 DISP "PROGRAM COMPLETE"
2130 END
```